


For Reference

NOT TO BE TAKEN FROM THIS ROOM

Ex LIBRIS
UNIVERSITATIS
ALBERTAENSIS





Digitized by the Internet Archive
in 2022 with funding from
University of Alberta Library

<https://archive.org/details/Lutener1976>

THE UNIVERSITY OF ALBERTA

RELEASE FORM

NAME OF AUTHORSTUART BOYD LUTENER.....
TITLE OF THESISTHERMOLYSIS OF VINYLOXIRANE.....
.....
.....
DEGREE FOR WHICH THESIS WAS PRESENTEDPh.D.
YEAR THIS DEGREE GRANTED1976.....

Permission is hereby granted to THE UNIVERSITY OF
ALBERTA LIBRARY to reproduce single copies of this
thesis and to lend or sell such copies for private,
scholarly or scientific research purposes only.

The author reserves other publication rights, and
neither the thesis nor extensive extracts from it may
be printed or otherwise reproduced without the author's
written permission.

THE UNIVERSITY OF ALBERTA

THERMOLYSIS OF VINYLOXIRANE

BY



STUART BOYD LUTENER

A THESIS

SUBMITTED TO THE FACULTY OF GRADUATE STUDIES AND RESEARCH
IN PARTIAL FULFILMENT OF THE REQUIREMENTS FOR THE DEGREE

OF

DOCTOR OF PHILOSOPHY

DEPARTMENT OF CHEMISTRY

EDMONTON, ALBERTA

SPRING 1976

THE UNIVERSITY OF ALBERTA

FACULTY OF GRADUATE STUDIES AND RESEARCH

The undersigned certify that they have read, and recommend to the Faculty of Graduate Studies and Research for acceptance, a thesis entitled

"THERMOLYSIS OF VINYLOXIRANE"

submitted by STUART BOYD LUTENER in partial fulfilment of the requirements for the degree of Doctor of Philosophy.

A B S T R A C T

The thermolysis of 2-vinyloxirane has been studied in the gas phase over the range 292 - 312°C ($E_a = 47.8$ kcal.mole⁻¹, log A = 14.1) and found to give rise to 2,3-dihydrofuran, 3-butenal, (E) and (Z)-2-butenal together with carbon monoxide and propene.

Chiral 2-vinyloxirane has been synthesized, optically pure, from D-mannitol. The racemization of 2-vinyloxirane has been studied in the gas phase over the temperature range 240 - 275°C ($E_a = 44.2$ kcal.mole⁻¹, log A = 13.5).

cis and trans-3-Deuterio-2-vinyloxirane have been synthesized by a stereoselective route utilizing as a key step the disiamylborane/protonolysis reduction of an alkyne to an alkene. 2-Vinyloxirane-3,3-d₂ has been synthesized by a route utilizing the lithium aluminum deuteride reduction of an ester as the method of introduction of deuterium.

The kinetic deuterium isotope effect on the overall decomposition ($\delta\Delta G^\ddagger$ 140 - 220 cal. mole⁻¹ per deuterium) of 2-vinyloxirane has been studied at 307.4°C. A slow cis-trans isomerization of the 3-deuterio-2-vinyloxiranes has been detected during thermolysis.

A study of the racemization of 2-vinyloxirane-3,3-d₂ (obtained by a partial asymmetric hydroboration) showed

no significant isotope effect on the rate of racemization.

The facile racemization of the 2-vinyloxirane system, and the formation of 2,3-dihydrofuran, have been interpreted in terms of a reversible electrocyclic carbon-carbon ring opening to a planar carbonyl-ylide.

The slow, relative to thermolysis, cis-trans isomerization of the 3-deuterio-2-vinyloxiranes has been interpreted in terms of two possible mechanisms: (A) that it arises as a result of an isomerization of a carbonyl-ylide intermediate, and (B) the preferred interpretation, is that it is a consequence of a carbon-oxygen biradical intermediate formed on the reaction coordinate for the thermolysis to butenals.

It has been suggested, from a study of the deuterium distribution in the butenals, that 3-butenal and/or its dienol tautomer are the primary products of carbon-oxygen bond cleavage of the oxirane ring.

A C K N O W L E D G E M E N T S

The author would like to express his sincere gratitude to Professor Robert J. Crawford, who conceived this research problem, for his invaluable guidance and counselling during the course of this work.

The author also wishes to thank Dr. R. D. Cockroft, whose preliminary experiments within our research group stimulated a detailed study of the vinyloxirane system.

The author wishes to thank the staff of the spectroscopy laboratories for their valuable contributions.

The support of the technical staff of the Department of Chemistry was greatly appreciated.

The author is indebted to Mrs. Mary Waters for her typing expertise.

The author would also like to thank his wife for her patience and understanding during the course of this work.

Finally the author wishes to thank the Department of Chemistry and the University of Alberta for their financial support.

T A B L E O F C O N T E N T S

Page

HISTORICAL

A. Isomerization of cyclopropanes.....	1
B. Isomerization of oxiranes.....	5
<u>OBJECTIVE</u>	12

RESULTS

A. Syntheses.....	14
B. Thermolysis of 2-vinyloxirane.....	22
C. Racemization of 2-vinyloxirane.....	35
D. Thermolysis of deuterated 2-vinyloxiranes	
(i) Isotope effect on overall decomposition rate.	41
(ii) Isotope effect on the rate of racemization	43
(iii) Deuterium location in the thermolysis products.....	45
(iv) Product distributions.....	59
(v) Control experiment.....	77

DISCUSSION

A. Product Studies.....	78
B. Kinetic Studies.....	89

EXPERIMENTAL

A. Air bath system for thermolysis studies.....	108
B. Oil bath system for racemization studies.....	111

	<u>Page</u>
C. Preparations.....	112
<u>REFERENCES</u>	134
VITA.....	139
APPENDIX A.....	140
APPENDIX B.....	189

L I S T O F T A B L E S

<u>TABLE</u>		<u>PAGE</u>
I	First-order rate constants for the thermolysis of 2-vinyloxirane	33
II	First-order rate constants for the racemization of 2-vinyloxirane	38
III	Observed rate constants for the thermolysis of deuterated 2-vinyloxiranes at 307.4°C	42
IV	Deuterium isotope effects on the thermolysis of 2-vinyloxiranes	44
V	Observed rate constants for the racemization of $\sim\sim$ 30 and $\sim\sim$ 31 at 240.0°C	46
VI	Rate constants for the formation of 2,3-dihydrofuran	73
VII	Rate constants for the formation of 2,3-dihydrofuran at 307.4°C	76
VIII	The deuterium distribution in the 3-butenal produced from thermolyses of $\sim\sim$ 21, $\sim\sim$ 13 and $\sim\sim$ 20 at 307.4°C	82
IX	The deuterium distribution in the 2-butenals produced from thermolyses of $\sim\sim$ 21, $\sim\sim$ 13 and $\sim\sim$ 20 at 307.4°C	85
X	Arrhenius activation parameters for the reactions of the 2-vinyloxirane system	90
XI	Rate constants and relative rates for the thermal reactions of the 2-vinyloxirane system	91
XII	Deuterium isotope effects on the thermal reactions of 2-vinyloxirane	92
XIII	Calculated rates of formation of butenals in the 2-vinyloxirane system at 307.4°C	97
XIV	Isotope effects for reactions having non-linear activated complexes	98

<u>TABLE</u>		<u>PAGE</u>
XV	Infrared frequencies used to calculate the secondary deuterium kinetic isotope effect for oxirane ring opening <u>via</u> carbon-oxygen bond cleavage	100
XVI	The partitioning of a carbon-oxygen biradical intermediate from 2-vinyl-oxirane	105

L I S T O F F I G U R E S

<u>FIGURE</u>		<u>PAGE</u>
1	The 100 MHz p.m.r. spectrum of 2-vinyloxirane (12) ~~	15
2.	The 100 MHz p.m.r. spectrum of <u>cis</u> -3-deuterio- 2-vinyloxirane (13) ~~	18
3.	The 100 MHz p.m.r. spectrum of <u>trans</u> -3-deuterio- 2-vinyloxirane (20) ~~	18
4.	The 100 MHz p.m.r. spectrum of 2-vinyloxirane- 3,3- <u>d</u> ₂ (21) ~~	18
5.	GC trace of the thermolysis products of 12 ~~	23
6.	The 100 MHz p.m.r. spectrum of 2,3-dihydro- furan from 12 ~~	25
7.	The 100 MHz p.m.r. spectrum of (<u>E</u>) and (<u>Z</u>)- 2-butenals from 12 ~~	25
8.	The 100 MHz p.m.r. spectrum of 3-butenal from 12 ~~	25
9.	A typical rate plot for the thermolysis of 12 ~~	29
10.	Plot of log k <u>versus</u> 1/T for the thermolysis of 12 ~~	34
11.	A typical rate plot for the racemization of 2-vinyloxirane	36
12.	Plot of log k <u>versus</u> 1/T for the racemiza- tion of 2-vinyloxirane	40
13.	The 100 MHz p.m.r. spectrum of the dihydro- furan from 21 ~~	48
14.	The 100 MHz p.m.r. spectrum of the 3-butenal from 21 ~~	48

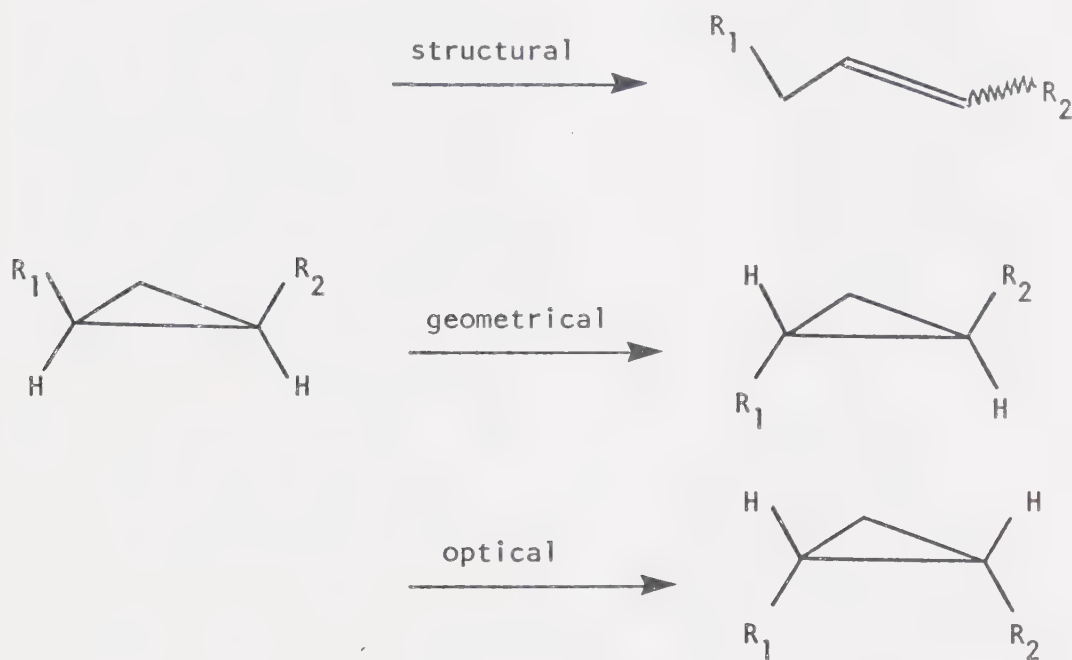
<u>FIGURE</u>		<u>PAGE</u>
15	The 100 MHz p.m.r. spectrum of the 2-butenals from <u>21</u> ~~	48
16	The 13.81 MHz d.m.r. spectrum of 3-butenal from <u>21</u> ~~	50
17	The 13.81 MHz d.m.r. spectrum of 2-butenal from <u>21</u> ~~	50
18	The 100 MHz p.m.r. spectrum of dihydrofuran from <u>13</u> ~~	52
19	The 100 MHz p.m.r. spectrum of 3-butenal from <u>13</u> ~~	52
20	The 100 MHz p.m.r. spectrum of 2-butenal from <u>13</u> ~~	52
21	The 13.81 MHz d.m.r. spectrum of 3-butenal from <u>13</u> ~~	54
22.	The 13.81 MHz d.m.r. spectrum of 2-butenal from <u>13</u> ~~	54
23.	The 100 MHz p.m.r. spectrum of <u>13</u> recovered from a partial thermolysis	54
24.	The 100 MHz p.m.r. spectrum of dihydrofuran from <u>20</u> ~~	57
25.	The 100 MHz p.m.r. spectrum of 3-butenal from <u>20</u> ~~	57
26.	The 100 MHz p.m.r. spectrum of 2-butenal from <u>20</u> ~~	57
27.	The 100 MHz p.m.r. spectrum of <u>20</u> recovered from a partial thermolysis	58
28.	The 13.81 MHz d.m.r. spectrum of 3-butenal from <u>20</u> ~~	58
29.	The 13.81 MHz d.m.r. spectrum of 2-butenal from <u>20</u> ~~	58

<u>FIGURE</u>		<u>PAGE</u>
30	Product distribution for the thermolysis of $\underline{12}$ at 307.4°	62
31	Product distribution for the thermolysis of $\underline{13}$ at 307.4°	63
32	Product distribution for the thermolysis of $\underline{21}$ at 307.4°	64
33	Product distribution for the thermolysis of $\underline{12}$ at 307.4° in the presence of a trace of air	66
34.	Product distribution for the thermolysis of $\underline{21}$ at 307.4° in the presence of a trace of air	67
35.	Comparison of relative product distributions from the thermolysis of $\underline{12}$ with a change in condition of the reaction vessel	69
36.	Typical rate plot for the formation of 2,3-dihydrofuran	72
37.	Plot of $\log k$ <u>versus</u> $1/T$ for the formation of 2,3-dihydrofuran	74
38.	Trace of the high-resolution mass spectrum of the $M + 1$ peak of 2-butenals isolated from the control experiment	77
39.	Reaction co-ordinate wherein the biradical is a post-transition state intermediate	102
40.	Schematic diagram of the apparatus used for thermolyses	109

H I S T O R I C A L

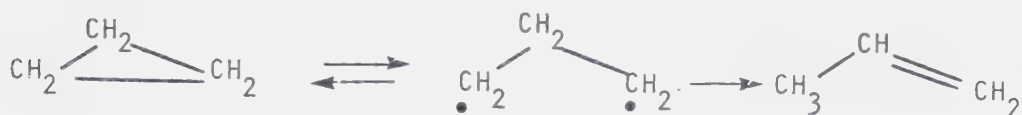
A. Isomerization of cyclopropanes

The thermal isomerization of strained cyclic systems has been extensively studied in an effort to elucidate the mechanisms of bond-cleavage processes. The thermolysis of cyclopropane and its substituted derivatives has been the focus of considerable attention and has resulted in the identification of the occurrence of structural, geometrical and optical isomerization processes.

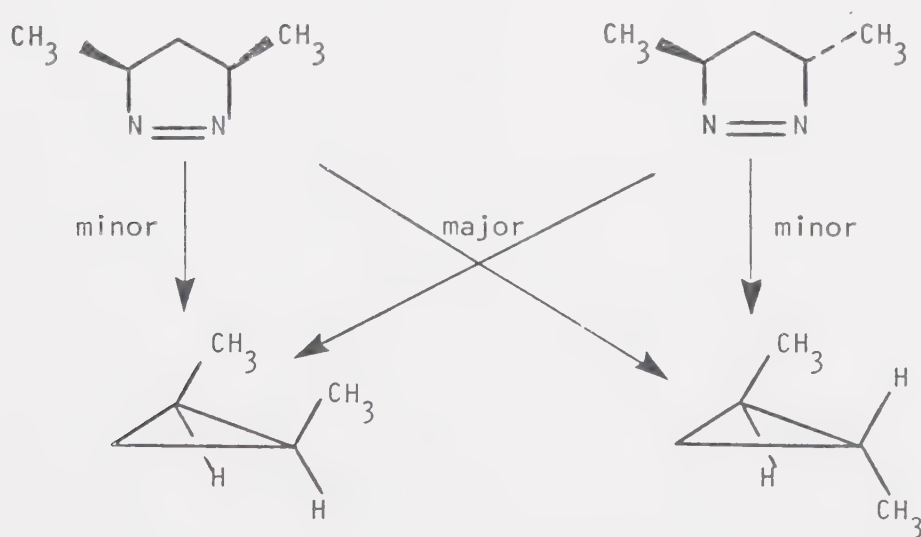


The trimethylene biradical, first proposed (1) as an intermediate in the structural isomerization of cyclopropane to propylene, has more recently been applied (2) as a general concept to explain the structural and

geometrical isomerizations of substituted cyclopropanes. A hydrogen shift in the trimethylene intermediate (TMM) can formally account for the olefin formation and internal rotation of TMM can account for geometrical isomerization. The perplexing question of the mode of formation



of TMM has been a subject of much controversy: is it produced as an intermediate of random stereochemistry, or is there a degree of stereochemical integrity retained during its formation? The first evidence for a planar trimethylene intermediate which suffered a preferred conrotatory reclosure was provided by Crawford and Mishra (3) in the thermolysis of cis and trans-3,5-dimethyl-1-pyrazoline.

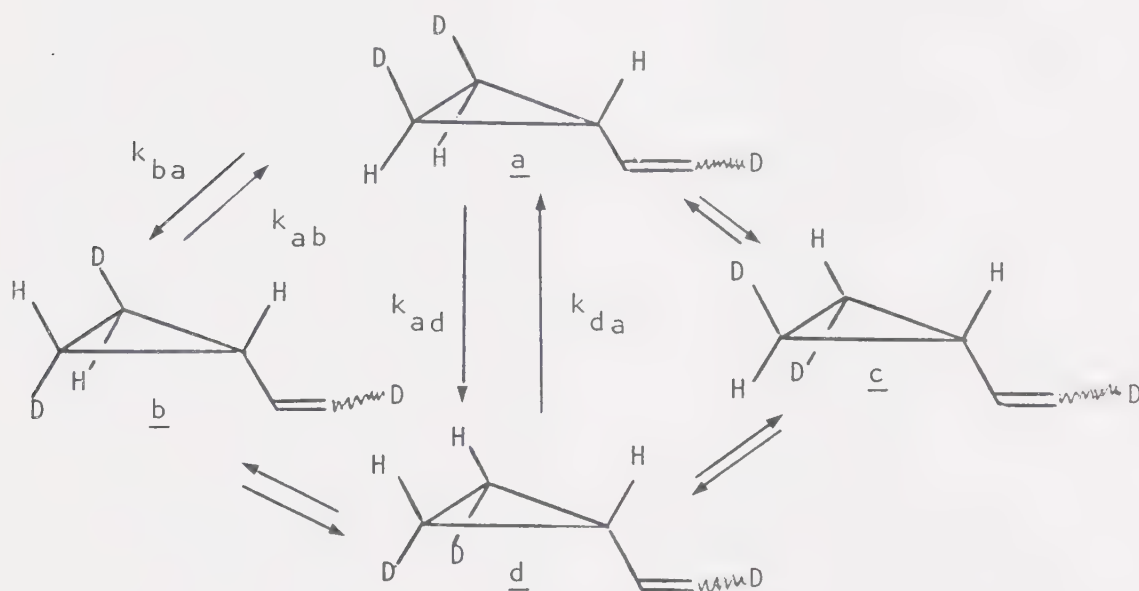


On the basis of quantum mechanical calculations Hoffman (4) has suggested that TMM should have a planar geometry with the terminal hydrogens and the three ring carbons in a common plane, and should be formed and re-cyclized by synchronous conrotations of the terminal methylene groups. Until recently, a definitive experimental verification of the theoretical prediction of the mode of cyclopropane stereoisomerization has not been forthcoming. In a series of elegant studies, Berson (5,6) has demonstrated the operation of a synchronous double methylene rotation process in the chiral 1,2-dideuteriocyclopropane and chiral 1-phenyl-2-deuteriocyclopropane systems.

The thermal decomposition of vinylcyclopropane has been found (7) to give rise to mainly cyclopentene together with small amounts of 1,4-pentadiene and (E) and (Z)-1,3-pentadienes. The formation of the products has been interpreted by the intermediacy of a biradical, but the possibility of a concerted path to cyclopentene has also been considered (8). Willcott and Cargle (9) showed that the thermolysis of cis-2-deuterio-vinylcyclopropane led to complete cis-trans equilibration of the deuterium label at least five times faster than the structural isomerization to cyclopentene. They suggested that a random biradical was responsible for the cis-trans equilibration. Since the starting material was achiral

the stereochemical nature of the biradical intermediate was not clearly defined.

In a later study (10) these authors observed that the thermolysis of cis-1,2-dideuterio-trans-3-vinylcyclopropane gave trans-2,3-dideuterio-1-vinylcyclopropane at twice the rate of formation of cis-2,3-dideuterio-cis-1-vinylcyclopropane. Their experimental result was consistent with a mechanism in which the stereochemistry was lost simultaneously at two centres.



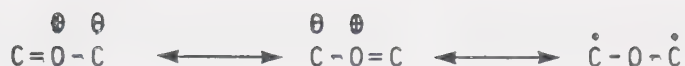
It should be noted that it was assumed that only the most substituted bond broke, an assumption shown to be invalid for the stereoisomerization of chiral 1-phenylcyclopropane-2-d (6). From a study of the racemization of trans-1,2-divinylcyclopropane, Arai and Crawford (11) concluded

that the ring opening was not a concerted electrocyclic process. Baldwin (12) has suggested that a one-centre epimerization may be a viable mechanism for the thermal rearrangement of 1,2-dialkenylcyclopropanes.

B. Isomerization of oxiranes

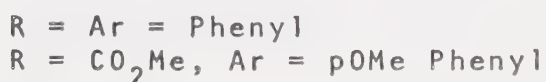
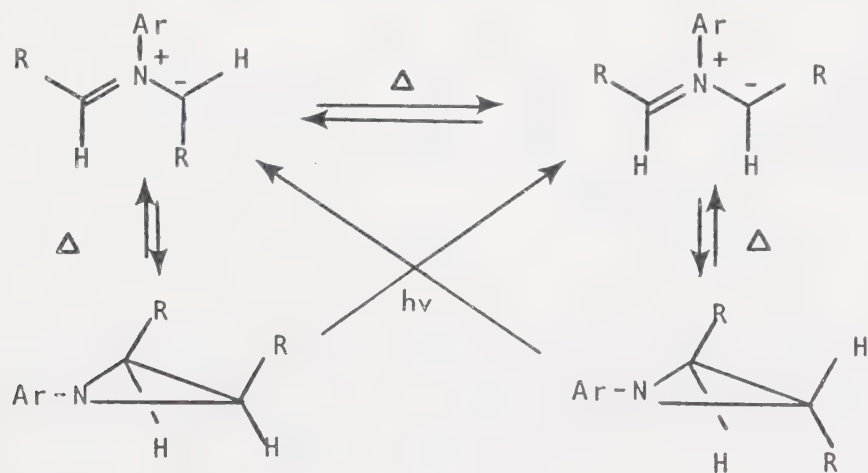
Oxiranes provide an interesting system for the study of both carbon-carbon and carbon-oxygen bond cleavage processes. Although the thermolysis of simple oxiranes is complicated by surface catalysis, a recent study of 2,2,3,3-tetramethyloxirane has minimized this drawback (13). The mechanism has been discussed in terms of a pair of initially formed biradicals produced by the fission of a carbon-carbon or carbon-oxygen bond, which can either rearrange or decompose to produce the observed products. Flowers (14) has shown that a competitive, but slower, cis-trans isomerization accompanies the thermal decomposition of cis and trans-2,3-dimethyloxirane. He suggested that the rotation about the carbon-oxygen bond in a biradical intermediate, at a rate slow relative to product formation, may account for the cis-trans isomerization.

Recent theoretical calculations (15) have shown that the open form of a variety of three-membered ring systems is essentially a linear combination of the structures:

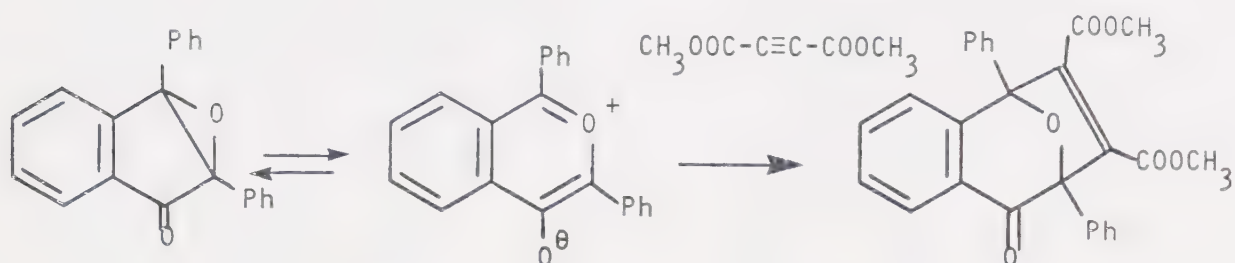


The ring open form of oxiranes is a 4π electron system since the lone pair electrons on the oxygen mix with the p-orbitals on the terminal carbons. The highest occupied molecular orbital of this system is antisymmetric and resembles the allyl anion (4), and thus orbital symmetry considerations (16) suggest it would exhibit synchronous conrotatory closure. The above theoretical predictions were also applied to the aziridine system, which is isoelectronic with the oxirane system.

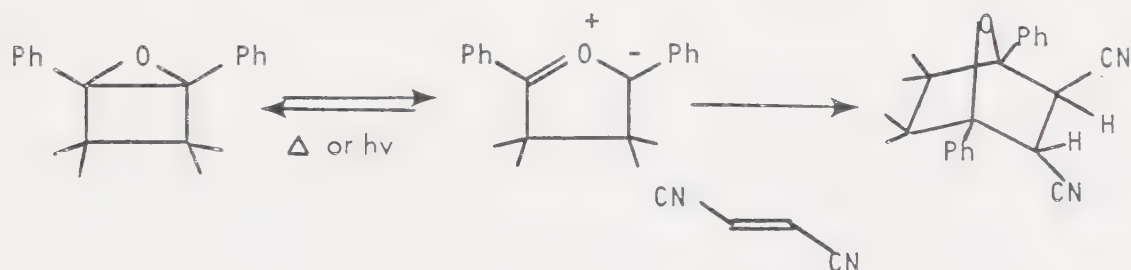
Huisgen (17) has convincingly demonstrated the stereospecific thermal conrotatory and photochemical disrotatory processes in trisubstituted aziridine systems. In the absence of dipolarophiles a thermal equilibration was observed, and accounted for by rotation in the azomethine ylid.



Ullman and Milks (18) provided early evidence for a reversible ring opening in an oxirane system. Thermal treatment of the oxirane at 80 - 100° gave a red solution which faded on cooling and regenerated the starting material unchanged. Treatment of the red solution with dimethyl acetylenedicarboxylate produced a 1:1 adduct.



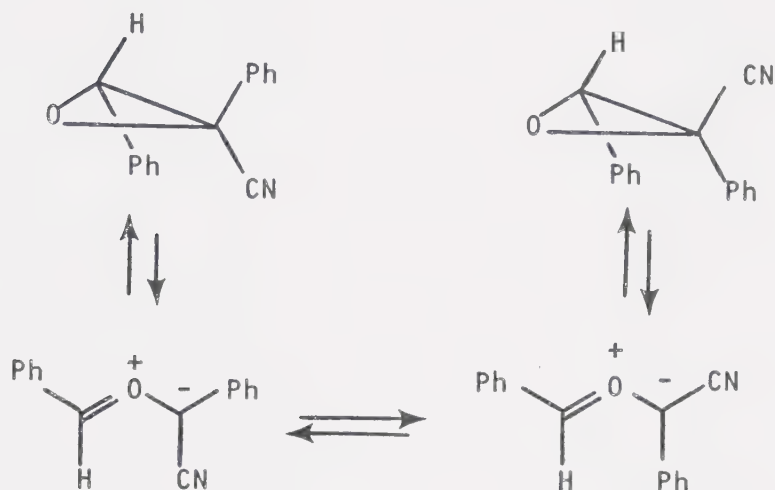
Arnold and Karnischky (19) reported that the thermal or photochemical treatment of a 5-oxabicyclo[2.1.0]pentane system produced a colored species capable of undergoing a 1,3-dipolar cycloaddition.



The stereospecific ring opening and reclosure of cis and trans-2,3-diphenyloxirane with the production of a colored intermediate was observed during low temperature photolysis by Griffin et al. (20). It was noted however that

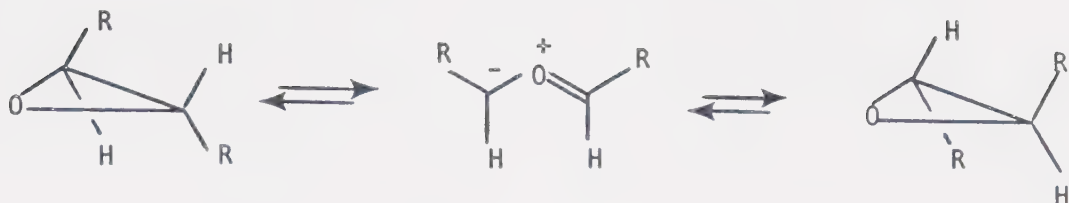
2-phenyloxirane, under the same conditions, failed to give rise to a colored intermediate.

Huisgen (21) has demonstrated the thermal stereospecific conrotatory carbonyl ylide \longrightarrow oxirane interconversion in the 1,2-diphenyl-2-cyano-oxirane system. In the absence of a dipolarophile, a thermal equilibration was observed to produce an 83:17 ratio in favor of the trans-diphenyl isomer.



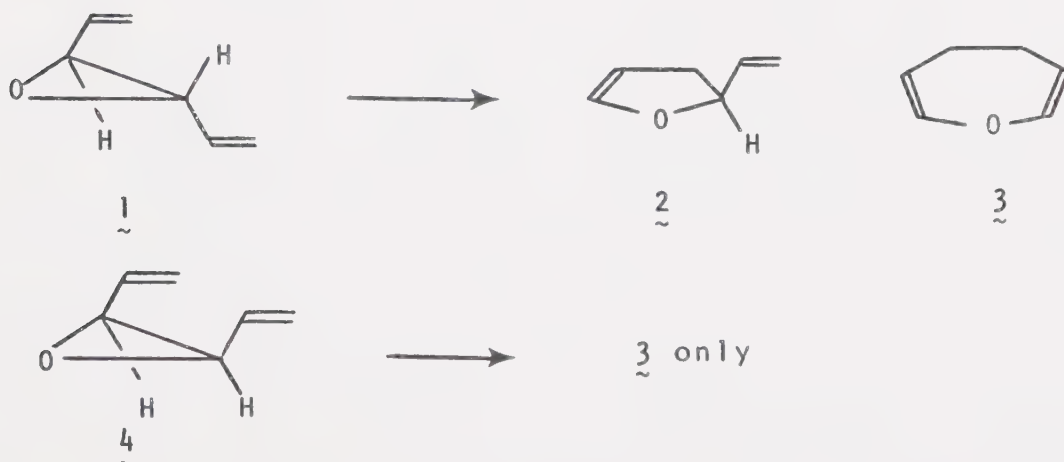
It should be noted at this point that systems designed to test carbonyl ylide formation have used highly substituted oxiranes, where carbon-carbon bond cleavage is thus favored over competitive carbon-oxygen bond cleavage.

The racemization of oxiranes provides an extremely sensitive test for the reversible carbonyl ylide formation



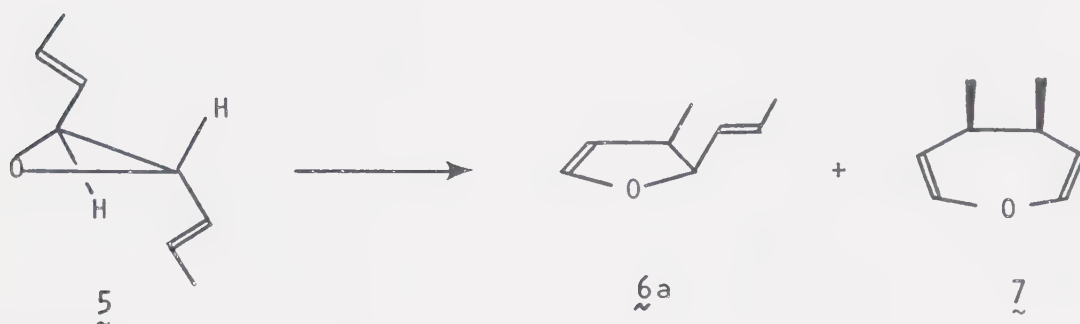
The racemization and cis-trans isomerization of 2,3-diaryl-oxirane has recently been studied by Macdonald and Crawford (22). It was observed that trans-1-phenyl-2-p-tolyloxirane racemizes, at 207°, 220 times faster than it undergoes trans-cis isomerization. A reversible conrotatory ring opening was invoked to explain this observation, but the mode of trans-cis isomerization could not clearly be defined.

Vogel (23) has shown that the thermolysis of trans-2,3-divinyloxirane (1) gives rise to 2-vinyl-2,3-dihydrofuran (2) and 4,5-dihydro-oxepin (3). The cis-oxirane (4) was found to isomerize readily above 50° to produce only 3.

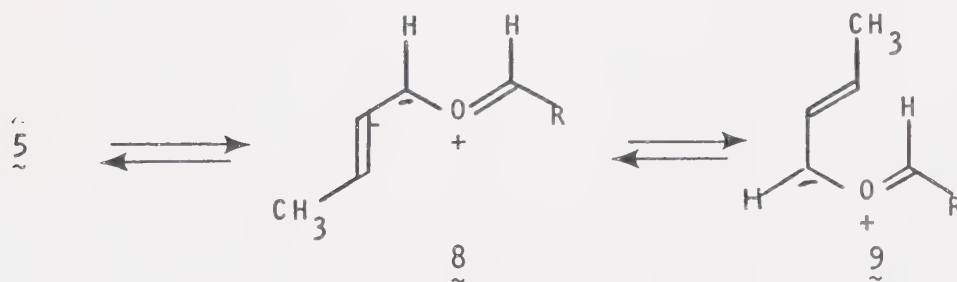


Carbon-carbon bond cleavage to a biradical was invoked to explain these observations, together with a concerted Cope rearrangement for the conversion $\underline{4} \longrightarrow \underline{3}$.

Recent attention has been focussed on the stereochemical aspects of the 2,3-divinyloxirane rearrangement. Chuche (24) has shown that the thermolysis of trans-(E,E)-2,3-dipropenyloxirane ($\underline{5}$) gave only $\underline{6a}$ and $\underline{7}$.

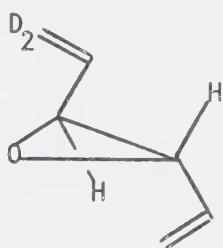


The mechanistic course of the reaction was explained by the formation of the carbonyl ylide $\underline{8}$ which underwent an internal rotation to produce ylide $\underline{9}$.

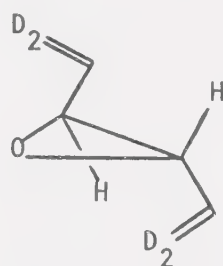


It was suggested that a five centre (6π) disrotatory closure of 9 produced 6, and a three centre (4π) conrotatory closure generated cis-oxirane which rapidly suffered a Cope rearrangement to 7.

Recent work in our laboratory (25a) has established the facile racemization of (+)-trans-2,3-divinyloxirane and a slower but competitive rearrangement to racemic 2-vinyl-2,3-dihydrofuran. The formation of a carbonyl ylide was invoked to explain the racemization and the formation of the products. The racemic nature of the dihydrofuran produced allowed the exclusion of a concerted sigmatropic migration as a viable mechanism for its formation. The thermolysis of the terminally-deuterated trans-2,3-divinyloxiranes 10 and 11 has also recently been studied in our laboratory (25b).



10



(-) 11

Isotope effects were examined and the suggestion was made that both the dihydrofuran and dihydrooxepin products are produced from a common intermediate.

O B J E C T I V E

Theoretical calculations have suggested that the carbon-carbon bond in the oxirane ring system should thermally undergo a preferred conrotatory mode of opening and recyclization. The stereospecific detection and interception of this ring-open form has been convincingly demonstrated for oxirane systems containing substituents capable of considerable electron delocalization. The intermediacy of a carbonyl ylide has been suggested as a rational mechanism for the isomerization of disubstituted ethylenic and phenylethylenic oxirane systems.

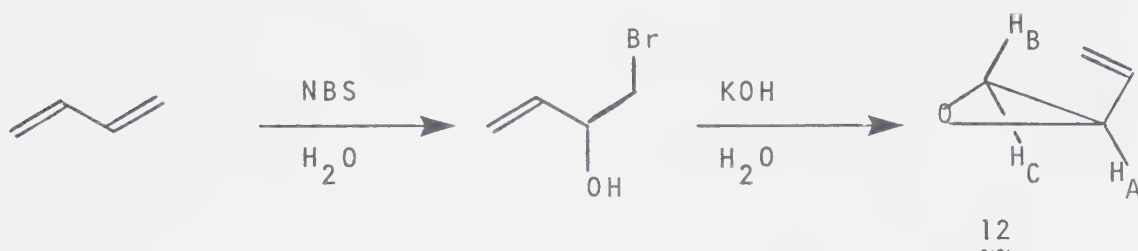
A common factor of the oxirane systems selected for study has been the assumption that carbon-carbon bond cleavage proceeds with the exclusion of competitive carbon-oxygen bond cleavage. It would thus be of considerable interest to examine the isomerization of an oxirane system wherein carbon-carbon and carbon-oxygen bond cleavage processes would be expected to be competitive processes. The 2-vinyloxirane system was thus selected for study, although the thermal isomerization had not previously been reported. By the utilization of deuterium substitution a minimal perturbation of the system would be expected, and a useful mechanistic probe into the thermal isomerization would be provided. The thermolysis of chiral 2-vinyloxirane should provide a sen-

sitive test for the possibility of a reversible bond cleavage process.

R E S U L T S

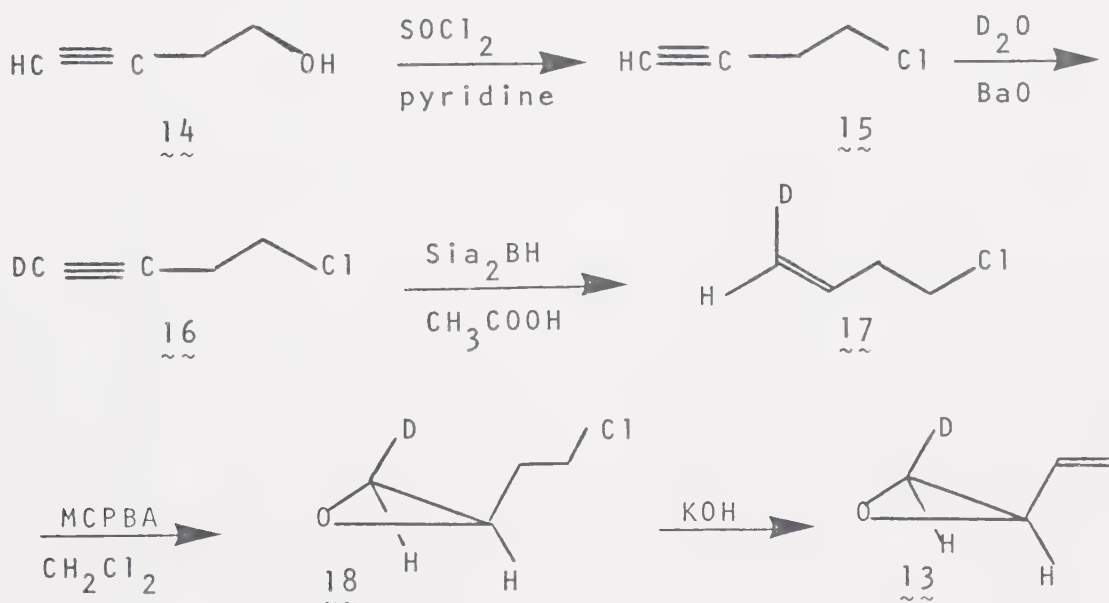
A. Synthesis

2-Vinyloxirane (12) was prepared by the base catalyzed cyclization of 1-bromo-3-buten-2-ol. The latter was obtained from butadiene by treatment with N-bromosuccinimide in the presence of water. The n.m.r. spectrum

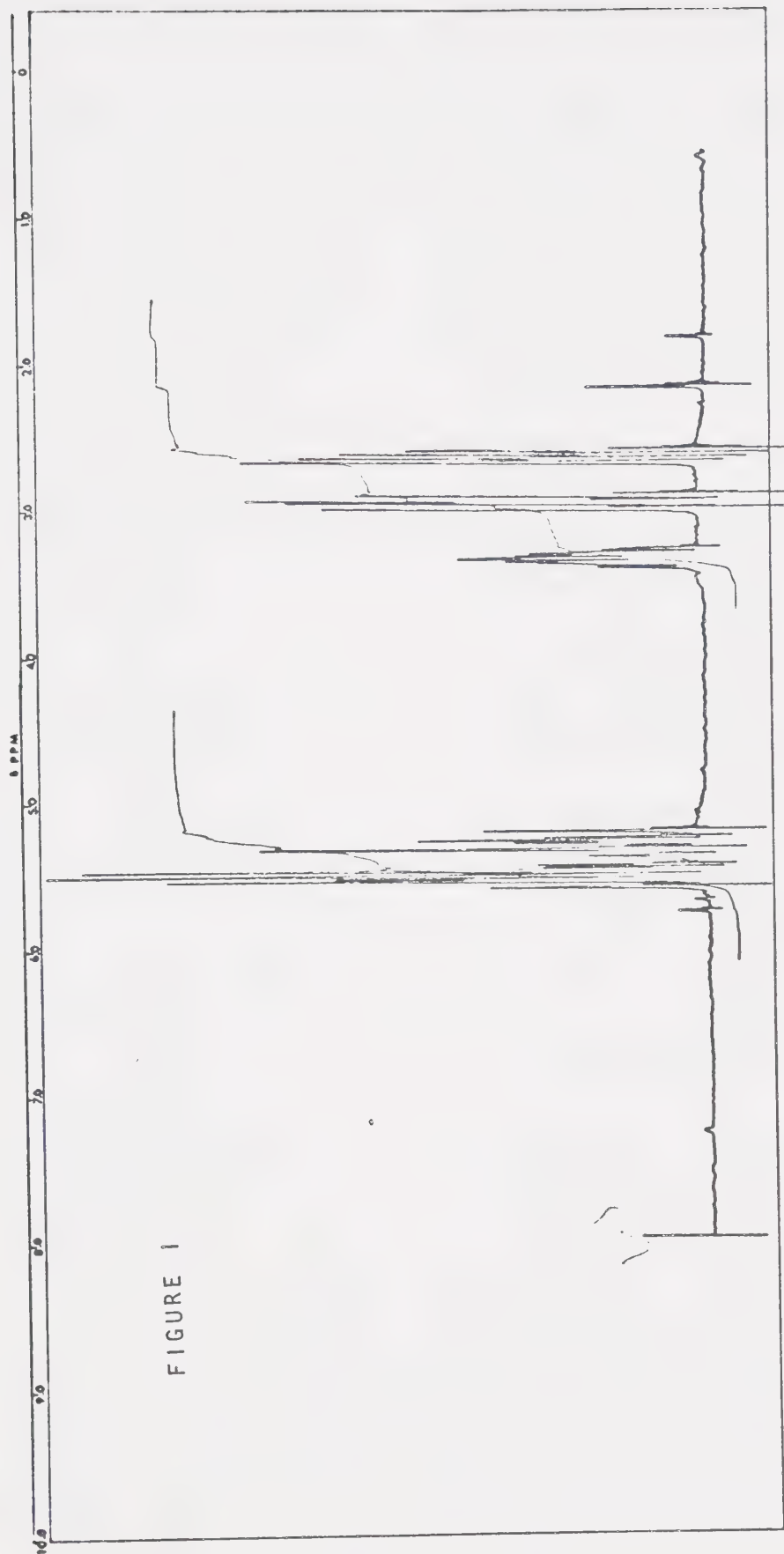


of 12 is shown in Figure 1. H_A δ 3.35, H_B δ 2.63 and H_C δ 2.95.

The cis-3-deuterio-2-vinyloxirane (13) was prepared as outlined in Scheme 1. 3-Butyn-1-ol (14) was obtained

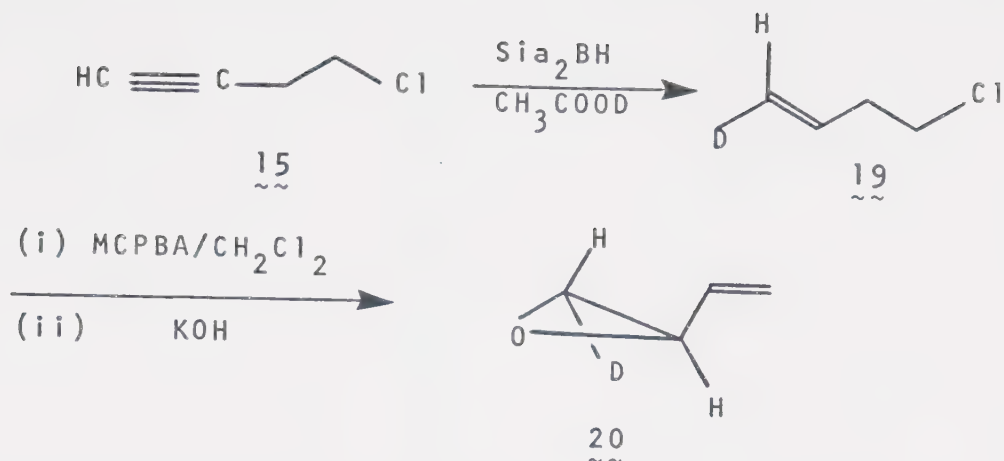


SCHEME 1



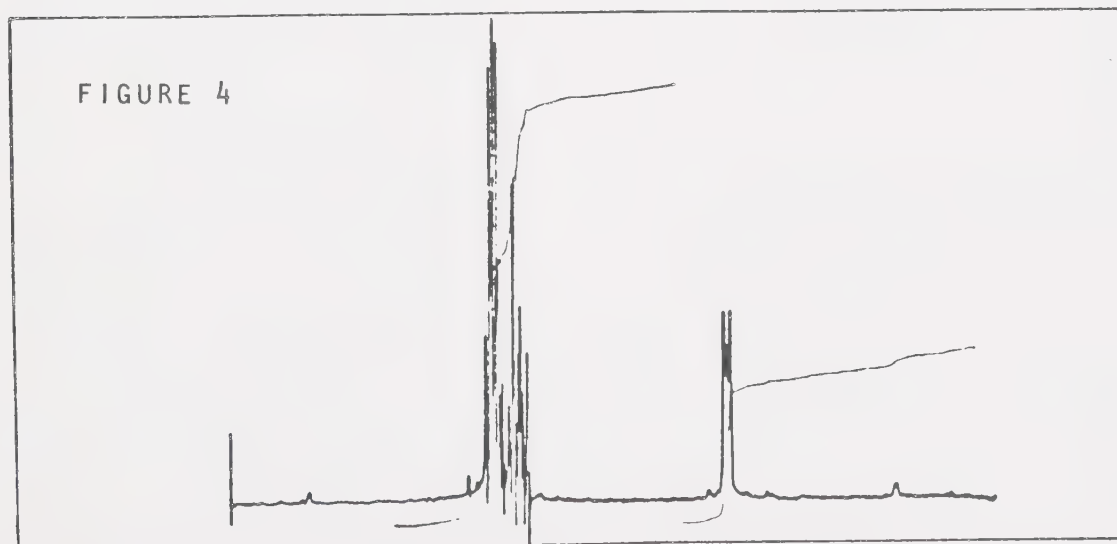
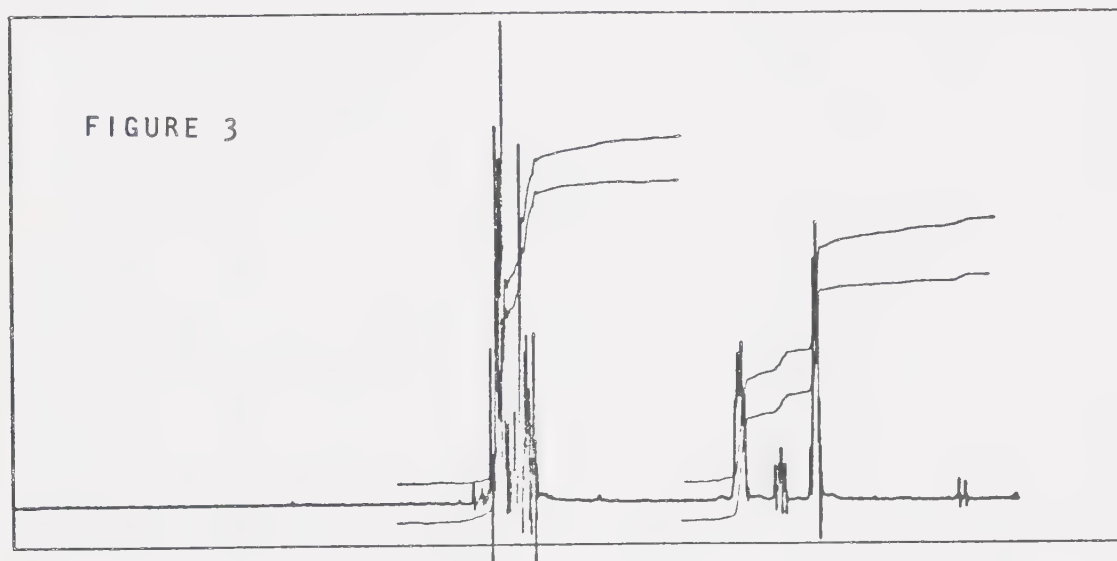
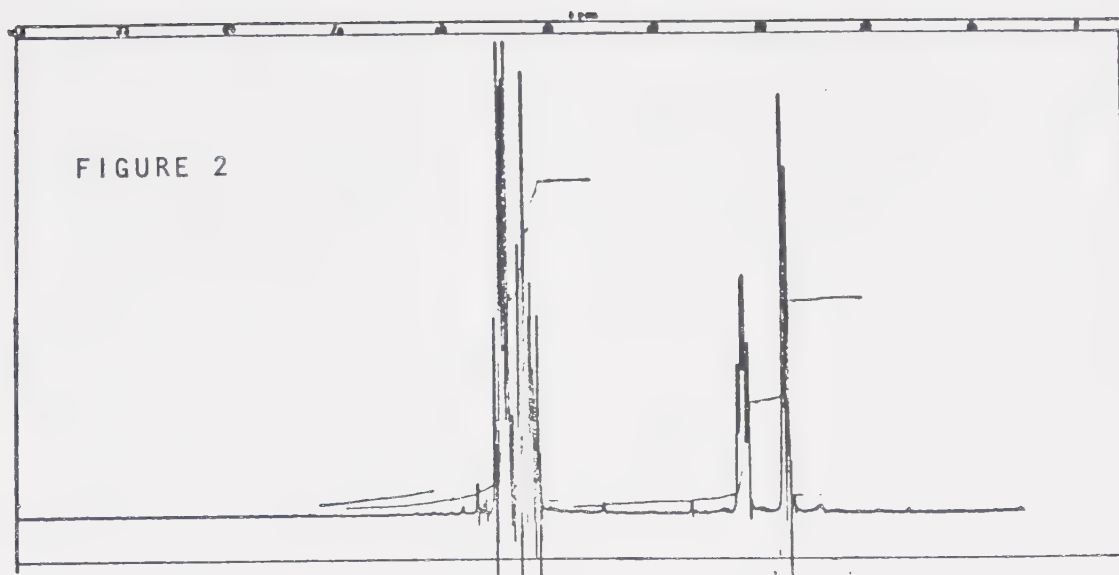
by the action of sodium acetylide on ethylene oxide according to the procedure of Schulte and Reiss (26). Treatment of 14 with thionyl chloride and pyridine according to the procedure of Roberts (27) furnished 4-chloro-1-butyne (15) which was subjected to barium oxide catalyzed deuterium exchange to produce 16. The stereospecific reduction of 16 to (Z)-4-chloro-1-butene-1-d (17) was effected by the disiamylborane/protonolysis procedure of Brown (28). The epoxidation of 17 with meta-chloroperbenzoic acid in methylene chloride produced the oxirane (18) which on treatment with powdered potassium hydroxide according to the procedure of Reppe (29) furnished the desired cis-3-deuterio-2-vinyloxirane (13). The n.m.r. spectrum of 13 is shown in Figure 2. The deuterium content of 13 could not be determined by mass spectrometry because of the extreme ease of fragmentation even at low ionization potentials. It was estimated to be 96.8% cis-d₁ by n.m.r. integration.

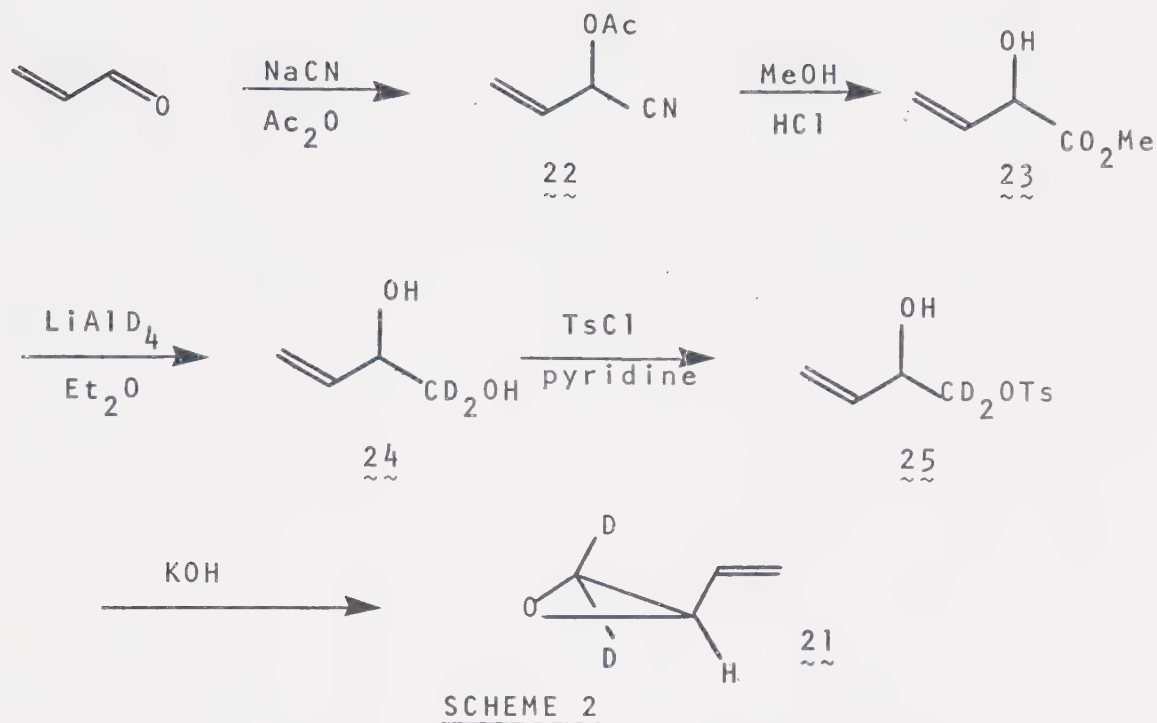
The trans-3-deuterio-2-vinyloxirane was prepared by modification of the sequence outlined in scheme 1. Treatment of 15 with disiamylborane followed by deuterolysis with deuterioacetic acid produced (E)-4-chloro-1-butene-1-d (19). The deuterium content of 19 was not as high as expected, possibly due to the presence of water in the deuterioacetic acid.



The trans-3-deuterio-2-vinyloxirane (20) was obtained from 19 by the same procedure outlined in scheme 1 for the conversion of 17 to 13. The n.m.r. spectrum of 20 is shown in Figure 3. The deuterium content was calculated as 81.4% trans-d₁ from integration of the n.m.r. spectrum.

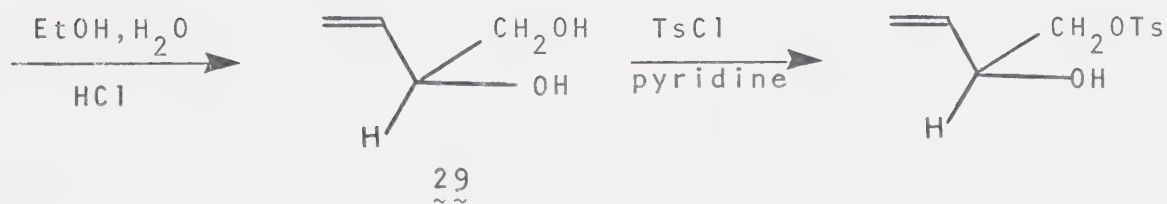
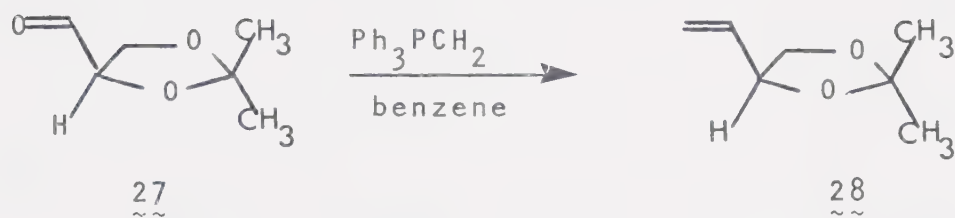
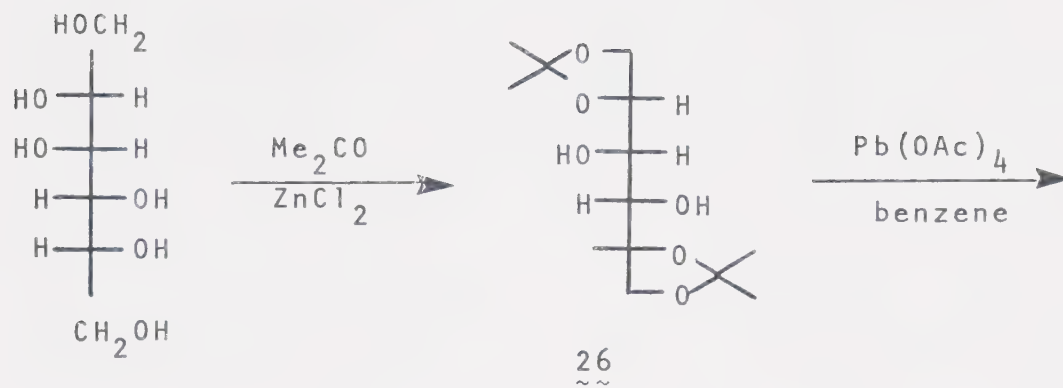
The 2-vinyloxirane-3,3-d₂ (21) was prepared as outlined in scheme 2. Acrolein was condensed with sodium cyanide in the presence of acetic anhydride according to the procedure of Chedron (30) to give 22. The acid-catalyzed methanolysis of 22 gave methyl 2-hydroxy-3-butenate (23), which was reduced to 3-buten-1,2-diol-1,1-d₂ (24) by lithium aluminum deuteride in ether.





The treatment of 24 with one equivalent of *p*-toluenesulfonyl chloride in pyridine gave the monotosylate (25) which on heating with powdered potassium hydroxide produced the desired 2-vinyloxirane-3,3-d₂ (21). The n.m.r. spectrum of 21 is shown in Figure 4. The deuterium content was calculated to be 98.5% from integration of the n.m.r. spectrum.

Chiral 2-vinyloxirane was prepared from an optically pure precursor as outlined in scheme 3. Commercial *D*-mannitol was converted to the 1,2-5,6-diisopropylidene derivative (26) by treatment with zinc chloride in acetone following the improved procedure of Tipson (31).



SCHEME 3

The lead tetra-acetate oxidation of 26 according to the procedure of Baer (32) gave isopropylidene-D-glyceraldehyde (27). This substance readily polymerized in the presence of water and was preferably used immediately for the next step. The treatment of 27 with methylene triphenylphosphorane under salt-free conditions according to the procedure of Schlosser (33) gave the dioxolane 28, which was then hydrolyzed to (-)-(S)-3-buten-1,2-diol (29) with hydrochloric acid in ethanol. The diol (29) was converted to (+)-(S)-2-vinyloxirane (30) as previously described for the conversion of 24 to 21. The optical rotation of the (+)-(S)-2-vinyloxirane thus prepared was:

$$[\alpha]_{589}^{25} + 8.306, \quad [\alpha]_{365}^{25} + 45.883 \quad (6.959 \text{ g/100 ml, 2-propanol}).$$

On the assumption that no racemization occurred in the sequence 29 to 30 then this measured rotation corresponds to an optical purity of at least 95%.

Several unsuccessful synthetic routes to chiral 2-vinyloxirane-3,3-d₂ were investigated, but were abandoned in favor of a partial asymmetric destruction. The treatment of 21 with di-3-pinanylborane by an adaption of the procedure of Brown (34) gave (-)-(R)-2-vinyloxirane 3,3-d₂ (31).

$[\alpha]_{589}^{25} = 0.977$, $[\alpha]_{365}^{25} = 5.752$ (3.686 g/100 ml, 2-propanol).

B. Thermolysis of 2-vinyloxirane

The thermal decomposition of 2-vinyloxirane was carried out in a 1000 ml Pyrex flask situated in a well thermostated air bath as described in detail in the experimental section. The reaction was found to proceed at a convenient rate at temperatures around 300°. The components of the reaction mixture were cleanly separated by gas chromatography on a 10 ft 1/8 in i.d. column of 10% β - β' -oxydipropionitrile on 80-100 mesh high-performance chromosorb WAW/DMCS. A typical gas chromatogram is shown in Figure 5.

A qualitative analysis of the products was performed by allowing the reaction to proceed to approximately 50% completion and subsequently trapping the products by liquid nitrogen cooling. Non-condensable product was identified by high resolution mass spectrometry, the only product found being carbon monoxide. In the same manner propene (not condensable at -78°) was also identified. The condensable products were separated by preparative GC on ODPN at 40° and identified by mass spectrometry and comparison of their n.m.r. spectra with those of authentic compounds. The thermal decomposition of 2-vinyloxirane was thus shown to produce the products illustrated in scheme 4.

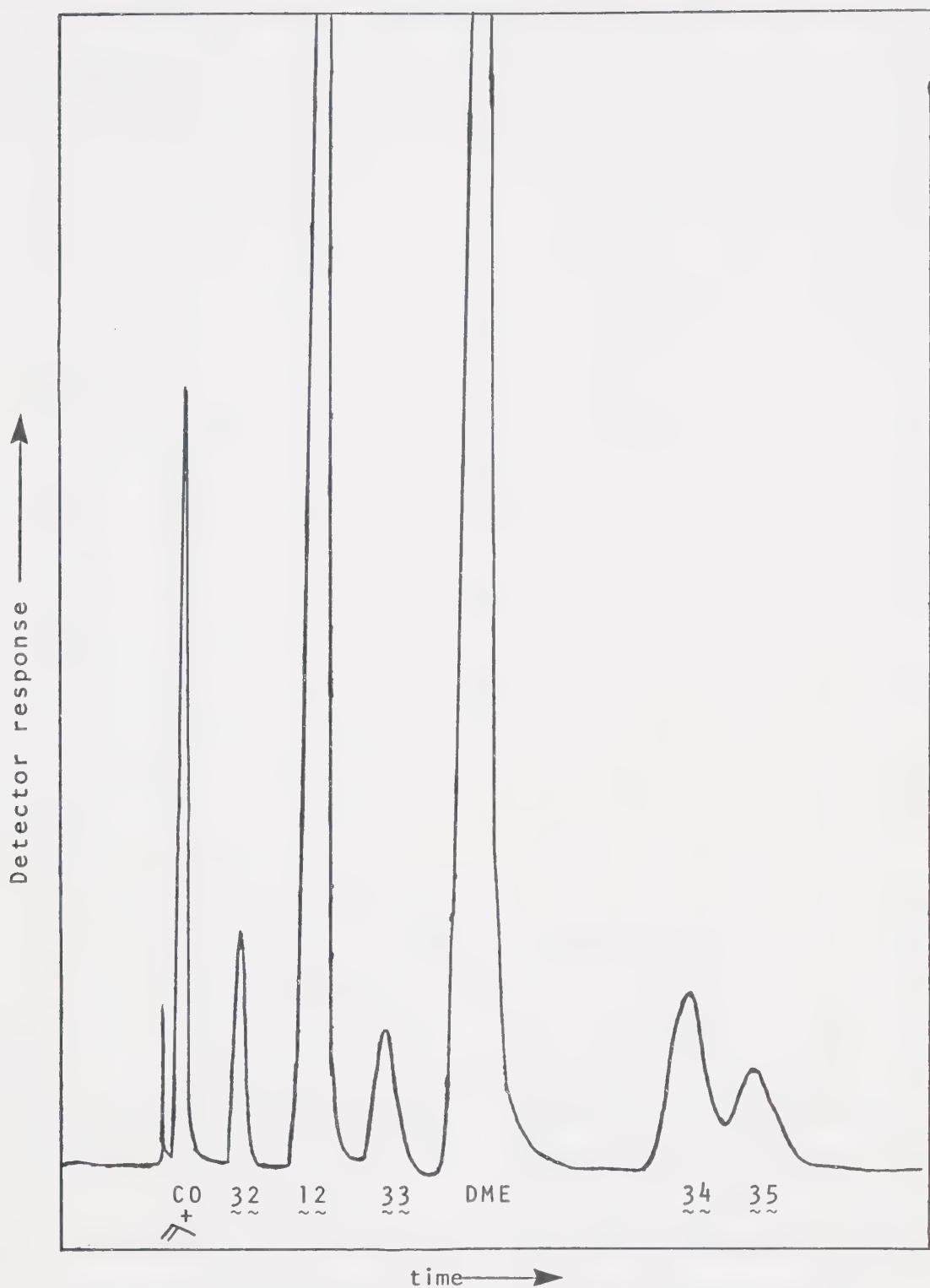
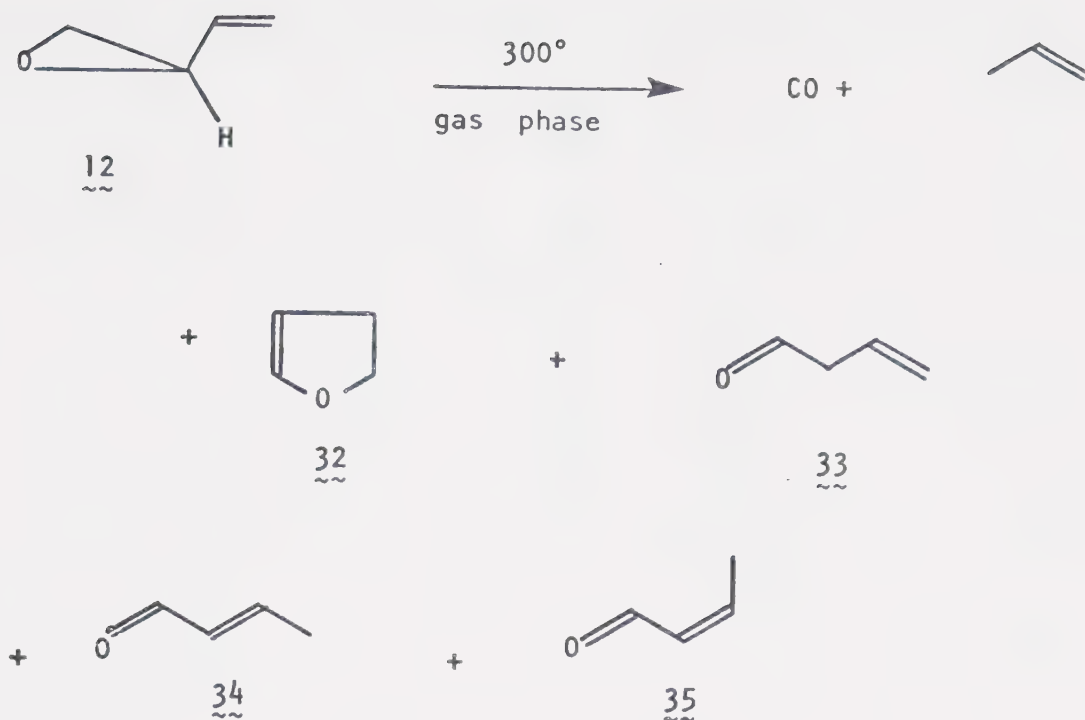


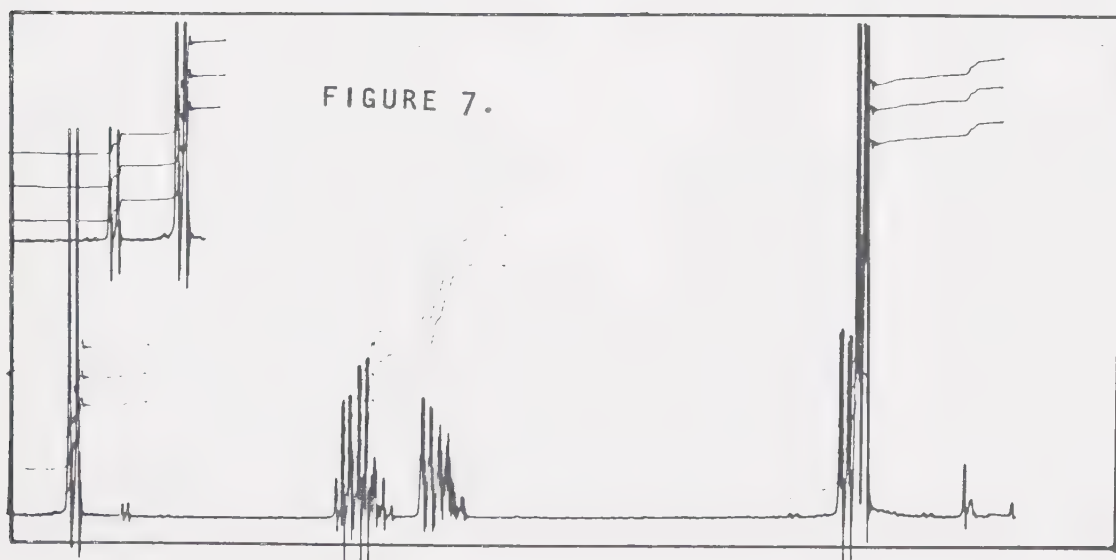
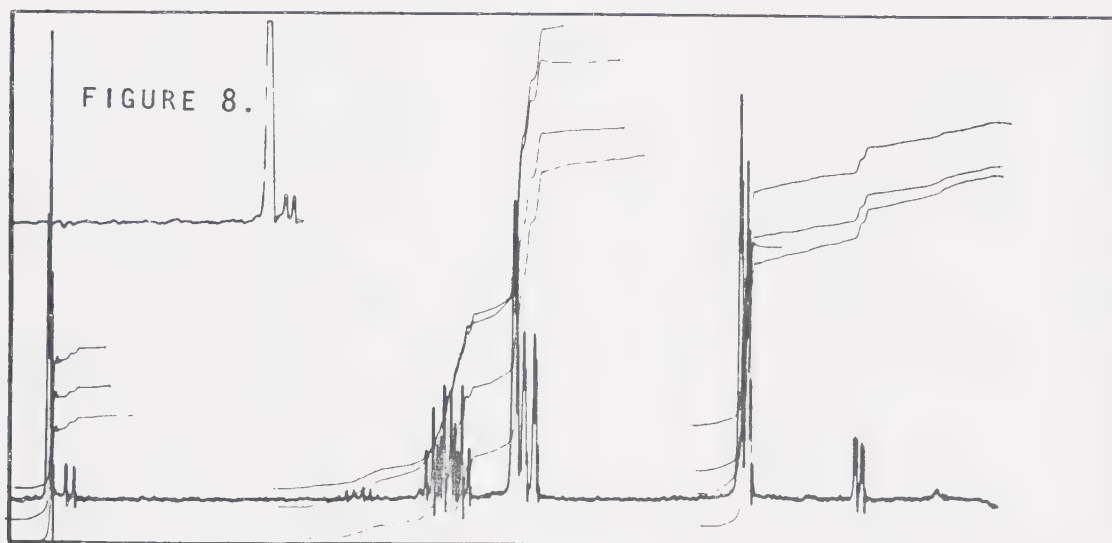
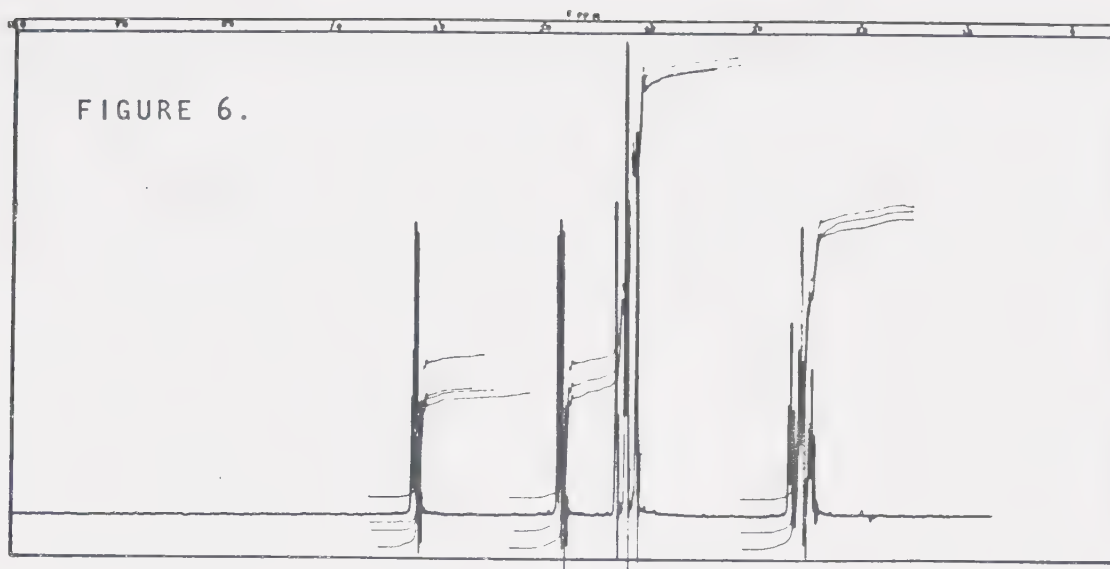
FIGURE 5. Gas chromatogram of the products from the thermolysis of 2-vinylloxirane (12) at 307.4° obtained on the 10 ft ODPN column at 30°.



SCHEME 4

The 100 MHz n.m.r. spectrum of the 2,3-dihydrofuran isolated from the thermolysis is shown in Figure 6. The n.m.r. spectrum was in agreement with that previously published (35).

The (E) and (Z)-2-butenal isomers could not be separated by preparative GC and the 100 MHz spectrum of the mixture obtained is shown in Figure 7. The signals attributed to 34 and 35 are readily discernable and are in good agreement with the values previously reported (36). The methyl groups of 34 and 35 appear as doublets of doublets centred at δ 2.03 and 2.17 (reported δ 1.93 and 2.10) respectively. The aldehyde protons resonate as doublets centred 9.42 and 10.04 δ (reported δ 9.40 and 10.6) respectively. The β -vinyl protons resonate as a



multiplet centred in the δ 6.8 region (reported δ 6.85 and 6.64 for $\underline{\underline{34}}$ and $\underline{\underline{35}}$ respectively), and the α -vinyl protons resonate as a multiplet centred in the δ 6 region (reported δ 5.99 and 5.81 for $\underline{\underline{34}}$ and $\underline{\underline{35}}$ respectively). The slight discrepancy of the values observed and those reported was attributed to a combination of concentration and temperature effects as well as instrument calibration.

The 100 MHz n.m.r. spectrum of the 3-butenal isolated from the thermolysis is shown in Figure 8. This is the first time that the n.m.r. spectrum of 3-butenal of relatively high purity has been obtained. Earlier attempts at GC purification of 3-butenal in this laboratory have resulted in almost 50% isomerization to (E) and (Z)-2-butenal. Inspection of Figure 8 shows that the 3-butenal contains about 10% (E)-2-butenal as evidenced by the methyl resonances at δ 2.03 and the aldehyde doublet at δ 9.42. The doublet possessing further fine splitting centred at δ 3.1 (2H) was assigned to the methylene group deshielded by adjacent vinyl and carbonyl functions. The multiplet centred in the δ 5.2 region (2H) was assigned to the terminal vinyl protons, and that centred in the 5.9 region (1H) to the lone vinyl proton. The aldehyde proton appeared as a triplet (1H) centred at δ 9.62.

Quantitative rate experiments were conducted in the static Pyrex vacuum system over the range 292 to 312°

with a temperature control of better than $\pm 0.1^\circ$. 1,2-Dimethoxyethane was chosen as an internal standard as it had a convenient GC retention time between that of 3-butenal and the 2-butenals and was shown to be thermally stable under the reaction conditions.

Reactant samples were prepared by degassing a mixture of dry 2-vinyloxirane (140 mg) and freshly purified anhydrous 1,2-dimethoxyethane (130 mg), which was then expanded into the evacuated reaction vessel from the heated (100°) inlet system.

The decomposition was followed by periodically expanding an aliquot to the vacuum line and analyzing the product on the GC system that was connected directly to the vacuum line. The product composition was determined by electronic integration of the thermal conductivity detector response which was assumed to be equal for each of the components. The relative detector response was, however, inconsequential to the rate study since the ratio of oxirane/standard was used directly to follow the disappearance of the 2-vinyloxirane. Reproducible results were obtained only after the reaction vessel had been "aged" by treatment with light hydrocarbon (Skelly B) at 350° followed by two treatments with hexamethyldisilazane at 300° . Traces of oxygen rapidly destroyed the surface condition of the reaction vessel as noted in a related study (13). This resulted in an accelerated decomposition

of the oxirane with a concomitant increase in the proportion of 3-butenal produced early in the reaction.

The rate constant of a first-order gas phase reaction of the type



is given by the equation

$$\log C_t = \log C_o - \left(\frac{k}{2.303} \right) t$$

where k is the first-order rate constant, C_t is the concentration of A at time t and C_o is the initial concentration of A. If the rate of decomposition of 2-vinyloxirane follows first-order kinetics then a plot of $\log(\text{oxirane/standard})$ versus time should be a straight line of slope $-k/2.303$. Linear first-order plots were obtained as indicated in Figure 9 which shows a typical plot of $\log(\text{epoxide/standard})$ versus time for a kinetic run at 307.40° . The decomposition was thus shown to follow first order kinetics, and the rate constant together with the associated error limits was determined by application of the method of least squares (37).

In this instance, the time values are assumed to be correct, and all errors are assumed to reside in the recorded values of $\log(\text{epoxide/standard})$, each of which is given equal weighting. In place of the equation form

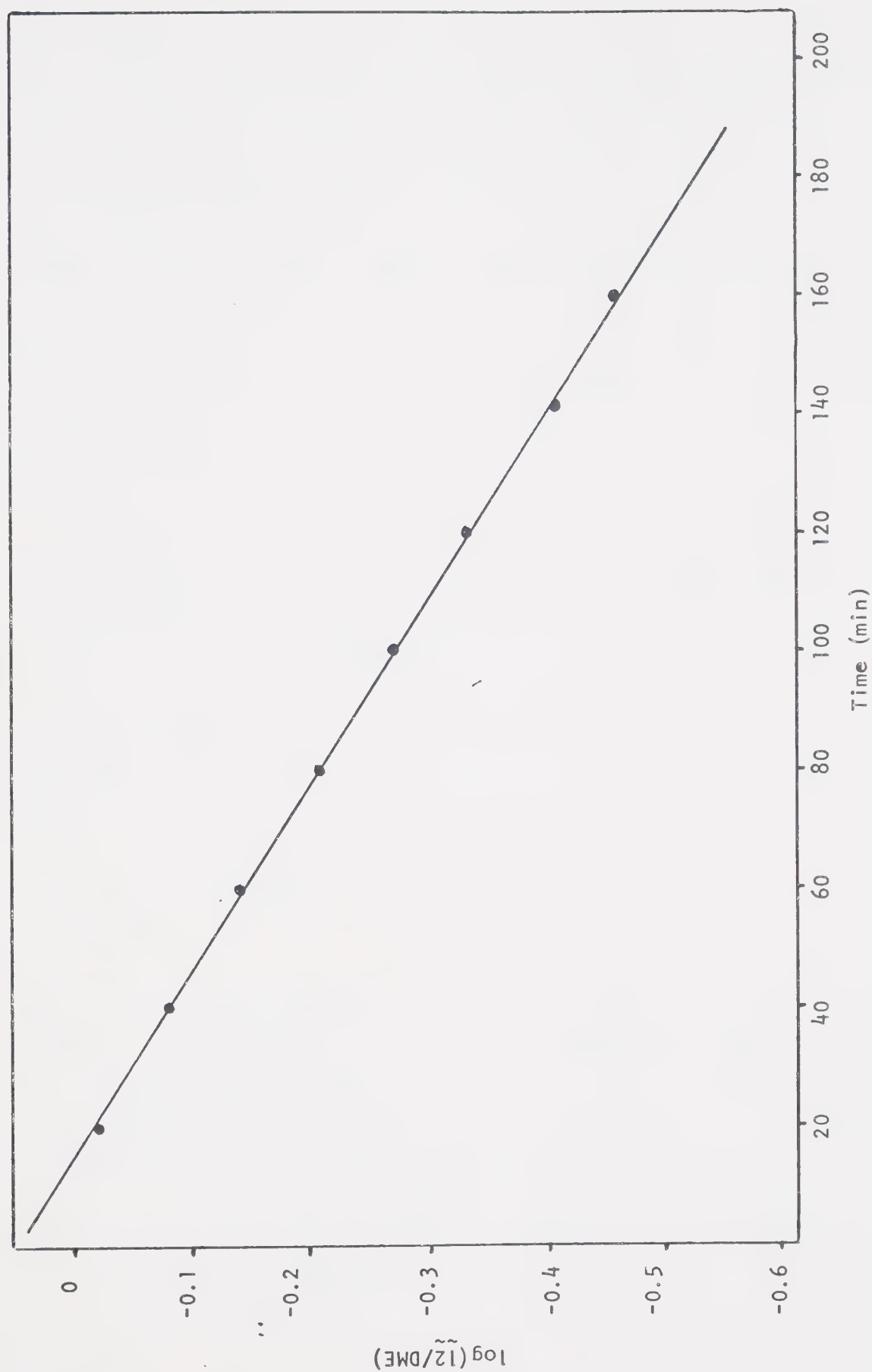


FIGURE 9: Plot of $\log(I_2/DME)$ versus time for the thermolysis of 2-vinyloxirane at 307.4°C

$y = a + bx$, it is simpler to convert to the form $Y = bX$. For fitting to the equation in this form the following relationships are used:

$$\sum Y^2 = \sum y^2 - n(\bar{y})^2, \quad \sum X^2 = \sum x^2 - n(\bar{x})^2, \quad \sum XY = \sum xy - n\bar{x}\bar{y}$$

The term b in the least squares equation is given by

$$b = \frac{\sum XY}{\sum X^2}$$

The least squares line passes through the point \bar{x}, \bar{y} , and the term, a , is therefore given by

$$a = \bar{y} - b\bar{x}$$

An estimate of the standard error of the term b is given by:

$$\text{s.e.}(b) = \sqrt{\frac{\sum Y^2 - b \sum XY}{(n-2) \sum X^2}}$$

The term, $n-2$, represents the number of degrees of freedom which in the case of a straight line fit is two less than the total number of data points.

An estimate of the standard error of the term a is given by:

$$\text{s.e.}(a) = \sqrt{\left(\sum Y^2 - b \sum XY\right) \left(\frac{1/n + (\bar{x})^2 / \sum X^2}{n-2}\right)}$$

The association of particular confidence limits with an estimated mean value implies a prediction of the reliability of this estimate as judged from both the spread of the data and the number of data in the sample from which the mean has been estimated. A commonly accepted practice is to quote the term "Probable Error" which is given for a least squares analysis as:

$$\text{Probable Error (slope)} = 0.6745 \times \text{Standard Deviation (slope)}$$

The "probable error" is that magnitude of deviation whose probability of being exceeded is one-half, i.e. it corresponds to a 50% confidence limit. The usefulness of the standard deviation as a predictor decreases considerably as the sample size decreases, but some compensation for errors involved in predicting from small samples is provided by the use of a table of "t" values. Thus the confidence limits of b and a are given by

$$\pm t \times \text{s.e.}(b)$$

and

$$\pm t \times \text{s.e.}(a)$$

where the value of "t" is chosen from a table of "t" values for a particular confidence level, a commonly chosen level being 90%.

A program was written for the Hewlett-Packard Model

65 programmable pocket calculator to perform a least squares analysis and calculate the associated errors, and this is detailed in the Appendix.

The rate constants for the thermal decomposition of 2-vinyloxirane at various temperatures are shown in Table I, the individual values of the rate constants are given in the Appendix.

The effect of the temperature on the rate constant is given by the Arrhenius equation:

$$k = Ae^{-E_a/RT}$$

where E_a is the activation energy and A is the frequency factor. This can be expressed in a logarithmic form as:

$$\log k = \log A - \frac{E_a}{2.303R} \times \left(\frac{1}{T}\right)$$

Thus a plot of $\log k$ versus $(1/T)$ should give a straight line of slope $-E_a/2.303R$ and an intercept corresponding to $\log A$. The activation parameters were determined by a least squares analysis in which the rate constants were not rounded off for computational purposes. The values of the activation parameters together with their 90% confidence limits were determined to be:

$$E_a = 47.8 \pm 1.0 \text{ Kcal.mole}^{-1}$$

$$\log A = 14.1 \pm 0.4$$

TABLE I

First-order rate constants for the thermal decomposition
of 2-vinyloxirane

Temperature (°C)	Number of runs	$10^5 k \text{ (sec}^{-1}\text{)}$	
		\pm probable error	at 90% confidence
292.70	4	4.18 ± 0.13	4.18 ± 0.22
297.52	7	6.15 ± 0.21	6.15 ± 0.23
302.16	6	8.38 ± 0.26	8.38 ± 0.31
307.40	8	12.42 ± 0.15	12.42 ± 0.15
312.50	8	17.68 ± 0.29	17.68 ± 0.29

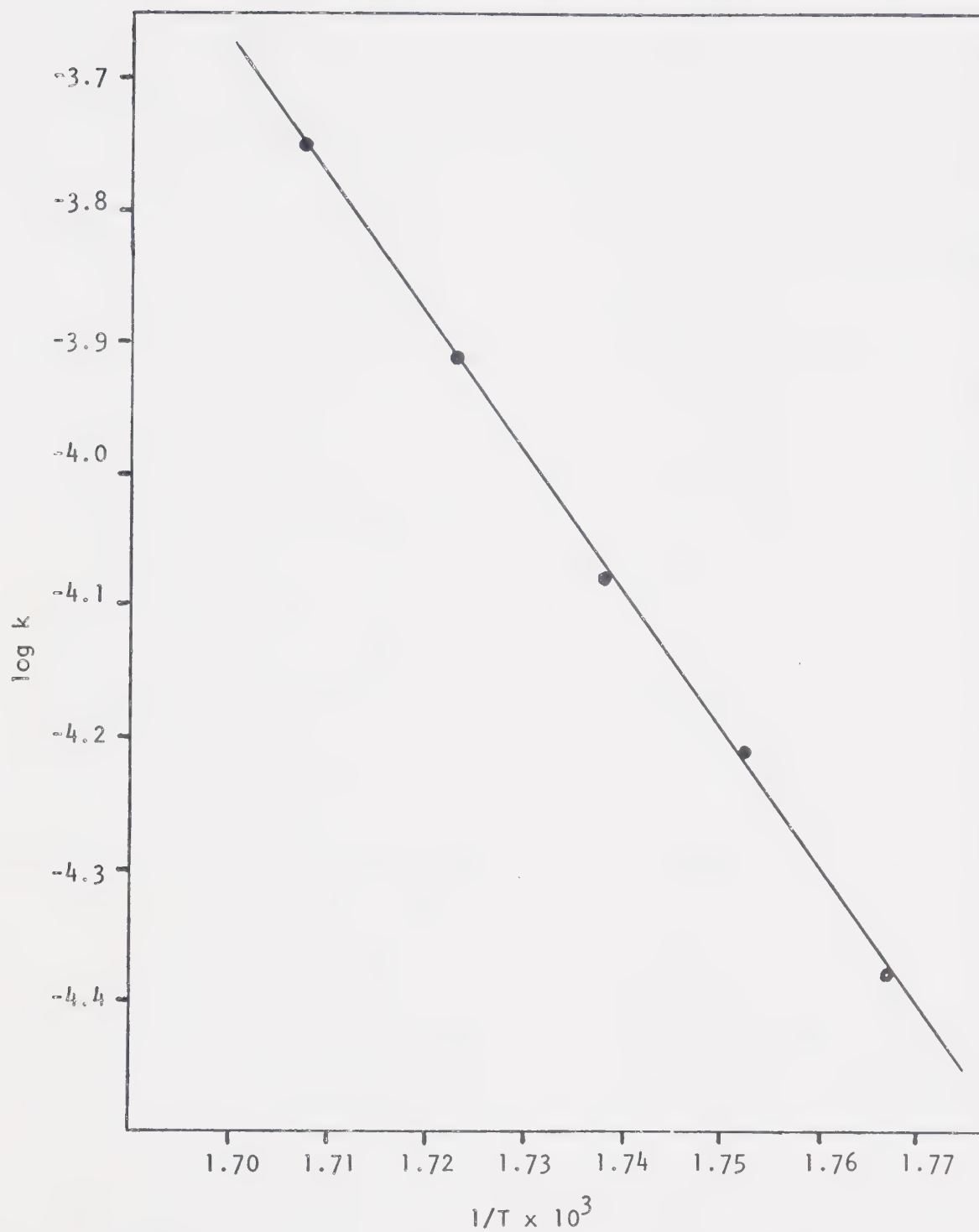


FIGURE 10. Plot of $\log k$ versus $1/T$ for the thermolysis of 2-vinyloxirane

A graphical plot of $\log k$ versus $(1/T)$ is shown in Figure 10.

C. Racemization of 2-vinyloxirane

To further delineate the mechanisms of the thermal isomerization of 2-vinyloxirane, a study of the racemization of chiral 2-vinyloxirane was undertaken.

A preliminary experiment was conducted by heating a sample of chiral 2-vinyloxirane at 292.70° in the static Pyrex system for one half-life of the thermal decomposition. The products were trapped with liquid nitrogen and the 2-vinyloxirane was separated by preparative GC on ODPN at 40° . The optical rotation of a solution of the recovered 2-vinyloxirane in 2-propanol was measured at each wavelength available on the Perkin Elmer Model 241 polarimeter. At each wavelength the optical rotation was found to be zero. Thus the racemization process is considerably faster than that for the thermal decomposition.

The racemization process was then studied in the static Pyrex vacuum system over the range 255° to 275° . The sample (1 gram) was degassed, transferred to a breakseal and introduced to the reaction vessel from the heated (100°) inlet system. Recovery of residual sample showed that approximately 0.8 g had been introduced, to give an initial pressure of about 0.5 atm in the reaction vessel. Aliquots (~ 70 mg) were recovered periodically, analyzed by GC and

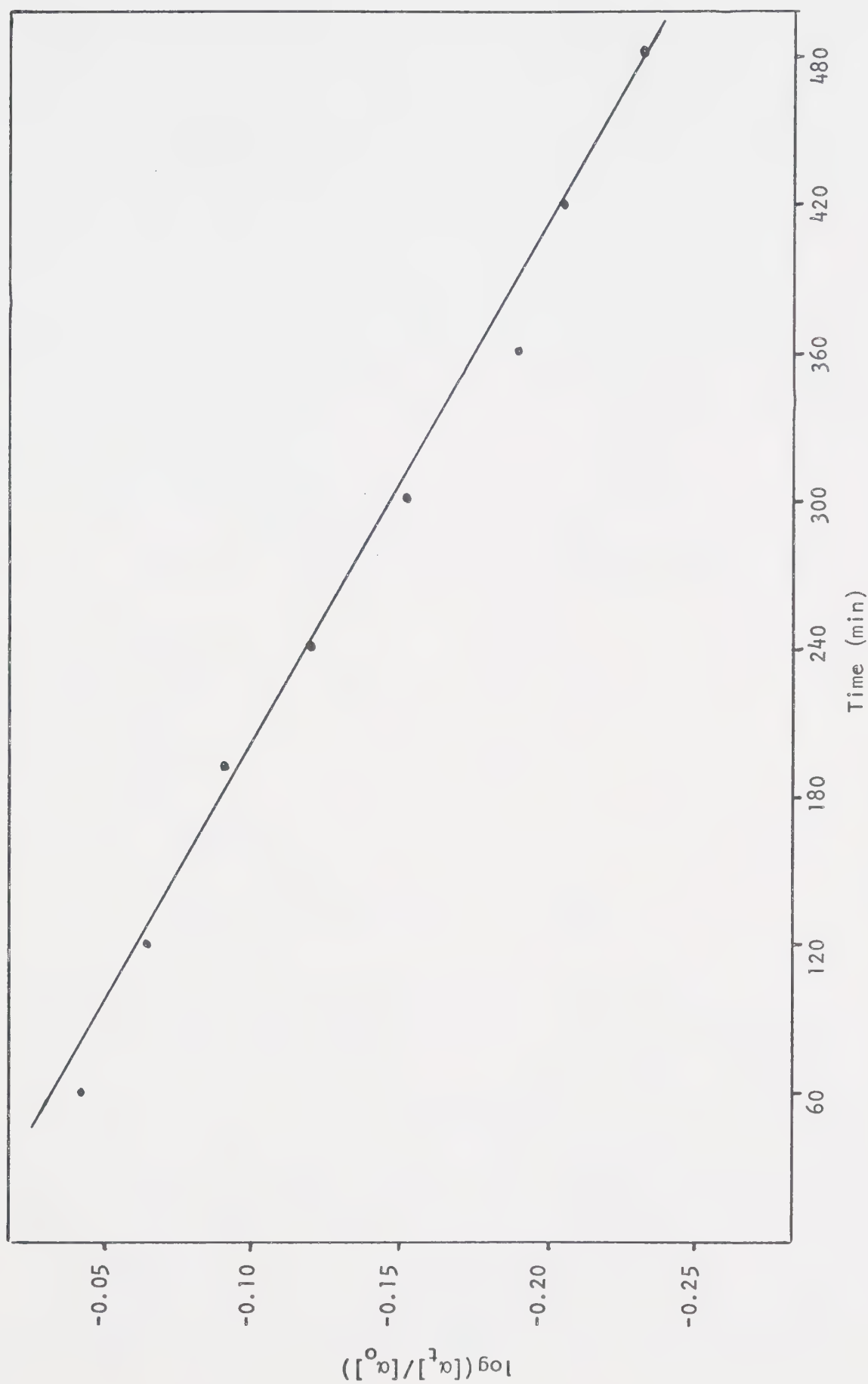


FIGURE 11: Plot of $\log([\alpha]_t/[\alpha]_0)$ for the racemization of 2-vinyloxirane at 255.0°

the optical rotation determined of a solution in 2-propanol in a thermostated 1 dm cell. The specific rotations were calculated with a correction applied for the percentage thermal decomposition that had occurred.

The rate constant (k_{obs}^{α}) was determined from the data in the following manner. For a first-order gas phase reaction of the type $A \longrightarrow \text{products}$, it is known that

$$\log \left(\frac{[\alpha]_t - [\alpha]_{\infty}}{[\alpha]_0 - [\alpha]_{\infty}} \right) = \frac{-kt}{2.303} \quad \text{where}$$

$[\alpha]_0$ = specific rotation at time = 0

$[\alpha]_t$ = specific rotation at time = t

$[\alpha]_{\infty}$ = specific rotation at more than 10 half lives

k = first order rate constant k_{obs}^{α} .

Since $[\alpha]_{\infty}$ was previously shown to be zero a plot of $\log ([\alpha]_t / [\alpha]_0)$ versus time should give a straight line of slope equal to $-k/2.303$. A typical plot is shown in Figure 11. The rate constants were evaluated by a least-squares analysis and together with the associated error limits are given in Table II. The rate constant for the interconversion of the two enantiomers (k_1) is related to the observed rate constant (k_{obs}^{α}) by the relationship

TABLE II

First order rate constants for the racemization of
2-vinyloxirane (sec⁻¹)

Run #	Temp. (°C)	$10^5 k_{\text{obs}}$ + probable	$10^5 k_1$ error	$10^5 k_1$ at 90% confidence level
1	265.0	3.96 ± 0.05	1.98 ± 0.03	1.98 ± 0.08
2	265.0	3.92 ± 0.05	1.96 ± 0.03	1.96 ± 0.07
3	275.0	8.22 ± 0.06	4.11 ± 0.03	4.11 ± 0.09
4	255.0	1.77 ± 0.02	0.855 ± 0.01	0.885 ± 0.03

$$2k_1 = k_{\text{obs}}^{\alpha}$$

The Arrhenius activation parameters for the racemization process were determined from the relationship

$$\log k = \log A - E_a/2.303RT$$

by plotting $\log k_{\text{obs}}$ versus $(1/T)$, as shown in Figure 12.

The values of $\log A$ and E_a were determined by a least-squares analysis as

	<u>\pm Probable Error</u>	<u>At the 90% confidence level</u>
$\log A$	13.5 ± 0.27	13.5 ± 0.7
E_a (Kcal.mole ⁻¹)	44.2 ± 0.7	44.2 ± 1.6

The complete kinetic data from which the rate constants and the activation parameters were determined is given in the Appendix.

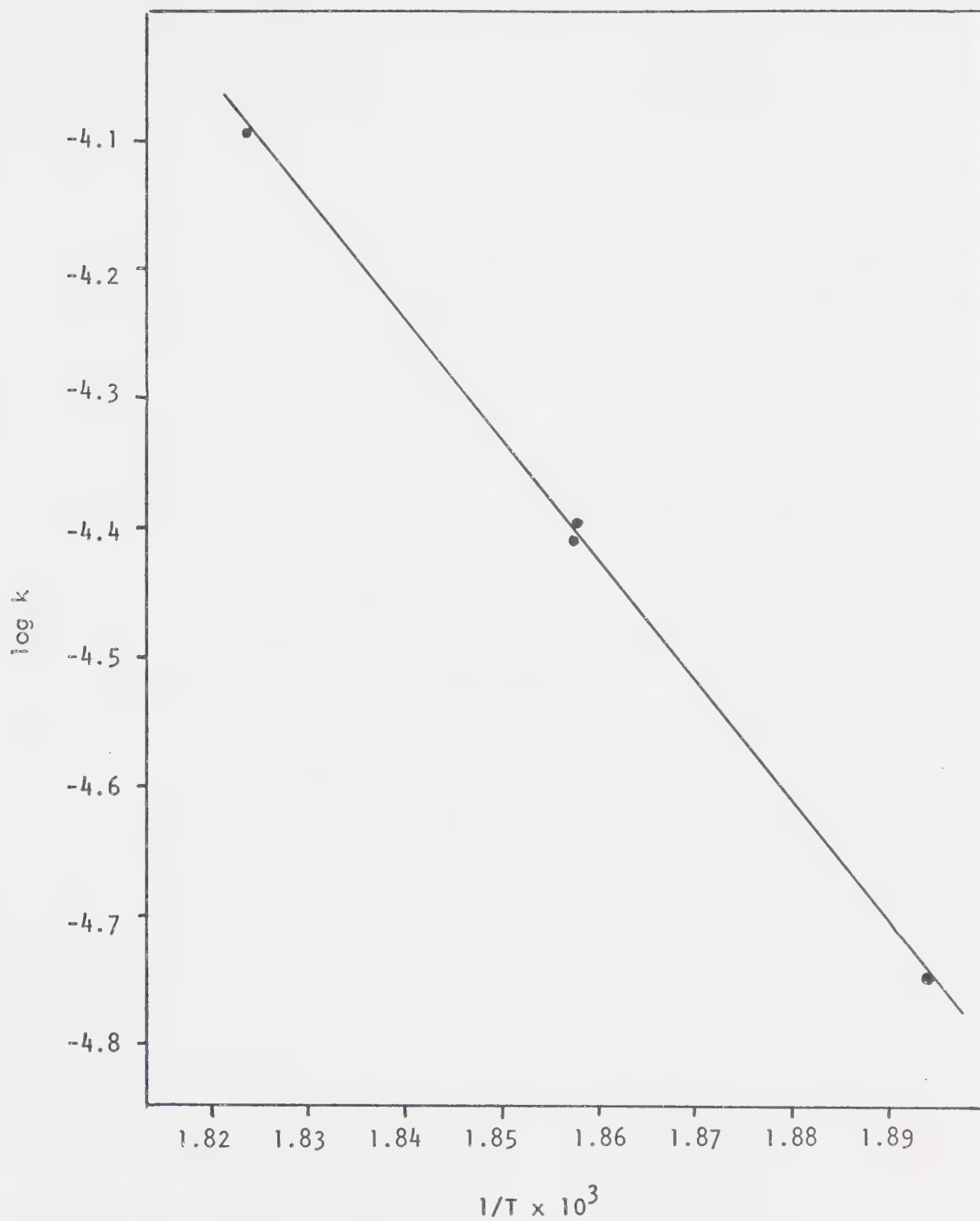
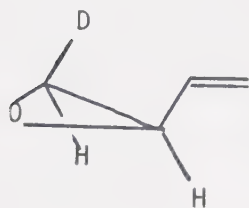


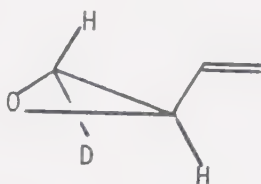
FIGURE 12: Plot of $\log k$ versus $1/T$ for the racemization of 2-vinyloxirane

D. Thermolysis of deuterated 2-vinyloxiranes

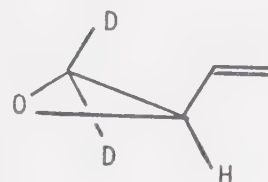
The racemization study indicated that a rapid reversible ring cleavage process was accompanying the thermal decomposition of 2-vinyloxirane. It was anticipated that the presence of deuterium on the oxirane ring would influence the overall kinetics of the rearrangement process and also provide a sensitive probe into the mode of formation of the products. Thus the compounds cis-3-deuterio-2-vinyloxirane (13), trans-3-deuterio-2-vinyloxirane (20) and 2-vinyloxirane-3,3-d₂ (21) were synthesized and their thermolyses investigated.



13



20



21

(i) Isotope effect on the overall decomposition rate

The thermolyses of 2-vinyloxirane (12) and the deuterated 2-vinyloxiranes were conducted in the static Pyrex system at 307.40°C as previously described. For each run a plot of log (epoxide/standard) versus time gave a good straight line and the rate constant was determined by a least squares analysis. The observed rate constants together with the associated error limits are given in Table III; individual rate data are detailed in the Appendix.

TABLE III

Observed rate constants* for the decomposition of deuterated 2-vinyloxiranes at 307.40°C

Compound	Number of Runs	Observed rate constant \pm probable error	$10^4 k(\text{sec}^{-1})$ at 90% confidence level
<u>12</u> ~~	8	1.24 ± 0.01	1.24 ± 0.01
<u>13</u> ~~	3	1.06 ± 0.01	1.06 ± 0.03
<u>20</u> ~~	3	1.07 ± 0.01	1.07 ± 0.02
<u>21</u> ~~	3	0.98 ± 0.01	0.98 ± 0.02

* Not corrected for isotopic purity.

The observed rate constants were corrected for the isotopic purity of the oxirane as determined by n.m.r.

where

$\frac{1}{3}$	96.8% \underline{d}_1	3.2% \underline{d}_0
$\frac{2}{0}$	81.4% \underline{d}_1	18.6% \underline{d}_0
$\frac{2}{1}$	98.5% \underline{d}_2	1.5% \underline{d}_0

The corrections were made by using the equation

$$k_D(\text{corrected}) = \frac{k_{\text{observed}} - k_{\underline{d}_0} \times \text{mol. fraction } \underline{d}_0}{\text{mol. fraction } \underline{d}}$$

The corrected rate constants and the calculated values of k_H/K_D are given in Table IV.

(ii) Isotope effect on the racemization rate

The deuterium isotope effect on the rate of the racemization process was investigated by comparing the rate of racemization of (+)-(S)-2-vinyloxirane with that of chiral 2-vinyloxirane-3,3- \underline{d}_2 . The study was conducted by heating concurrently samples of the oxiranes (0.3 g) in breakseals (~75 ml volume) in the well-thermostated oil bath at 240.0° (controlled to better than $\pm 0.1^\circ$ for the duration of the thermolysis). The products were separated by preparative GC and the specific rotation of the recovered oxirane measured in 2-propanol at

TABLE IV

Deuterium isotope effects on the thermolysis of 2-vinyloxiranes

Compound	$10^4 k$ corrected (sec^{-1})	k_H/k_D (at 90% confidence level)	$\delta\Delta G^\ddagger/n$ (cal mole^{-1}) [*]
13 ~~	1.06	1.17 ± 0.03	$+185 \pm 25$
20 ~~	1.03	1.21 ± 0.02	$+219 \pm 19$
21 ~~	0.97	1.28 ± 0.02	$+141 \pm 10$

^{*} where n is the number of deuterium atoms per molecule

both 436 nm and 365 nm. The first-order rate constant for the racemization process was calculated from the relationship

$$k_{\text{obs}}^{\alpha} = \frac{-2.303}{t} \log \frac{[\alpha]_t}{[\alpha]_0}$$

where $k_{\text{obs}}^{\alpha} = 2k$ (racemization)

$[\alpha]_t$ = specific rotation at time t (sec)

$[\alpha]_0$ = specific rotation at $t = 0$

The mean values of k_{obs}^{α} for (+)-(S)-2-vinyloxirane (30) and (-)-(R)-2-vinyloxirane-3,3-d₂ (31) are given in Table V. The complete kinetic data are detailed in the Appendix. Thus the value of $k_{\text{H}}/k_{\text{D}}$ was calculated to be 1.01 ± 0.07 at the 90% confidence level.

(iii) Deuterium location in the thermolysis products

Samples of the oxiranes (0.3 g) were thermolyzed in the static Pyrex air-bath system at 307.40°. The products were trapped with liquid nitrogen cooling and then separated by preparative GC on the 6 ft ODPN column at 40°. The location of the deuterium in the products was determined by comparison of the 100 MHz n.m.r. spectra with those of the products from non-deuterated 2-vinyloxirane. The application of deuterium

TABLE V

Observed rate constants for the racemization of 30 and 31 at 240.0°C

Compound	Number of runs	$10^6 k_{\text{obs}}^{\alpha} \text{ (sec}^{-1}\text{) at 90\% confidence level}$
<u>30</u>	6	4.02 ± 0.14
<u>31</u>	3	3.99 ± 0.15

magnetic resonance spectroscopy (d.m.r.) proved to be a useful adjunct to the conventional 100 MHz n.m.r. for the location of deuterium in a molecule. The 13.81 MHz proton decoupled d.m.r. spectra were measured in dilute solution in carbon tetrachloride with deuteriochloroform as an internal reference.

The 100 MHz n.m.r. spectra of the thermolysis products from 2-vinyloxirane-3,3- d_2 are shown in Figures 13, 14 and 15. A comparison of the dihydrofuran produced (Fig. 13) with the corresponding non-deuterated product (Fig. 6) shows two salient features: the absence of the C2 triplet (δ 4.2) and the simplification of the C3 multiplet (δ 2.6). These observations are consistent with the location of both deuterium atoms at C2.

The 100 MHz spectrum of the 3-butenal produced (Fig. 14) displays the presence of a small amount of (E)-3-butenal as evidenced by the doublet δ 2.02. The absence of the C1 aldehyde signal (δ 9.8) is consistent with exclusively deuterium located in the aldehyde group. The considerable decrease in the C2 methylene signal (δ 3.1) is consistent with a deuterium migration to C2. The two vinyl signals in the δ 5.9 and δ 5.2 regions in the approximate ratio 1:2 suggests that deuterium is absent from C3 and C4. These conclusions are confirmed by an inspection of the corresponding d.m.r. spectrum (Fig. 16).

FIGURE 13

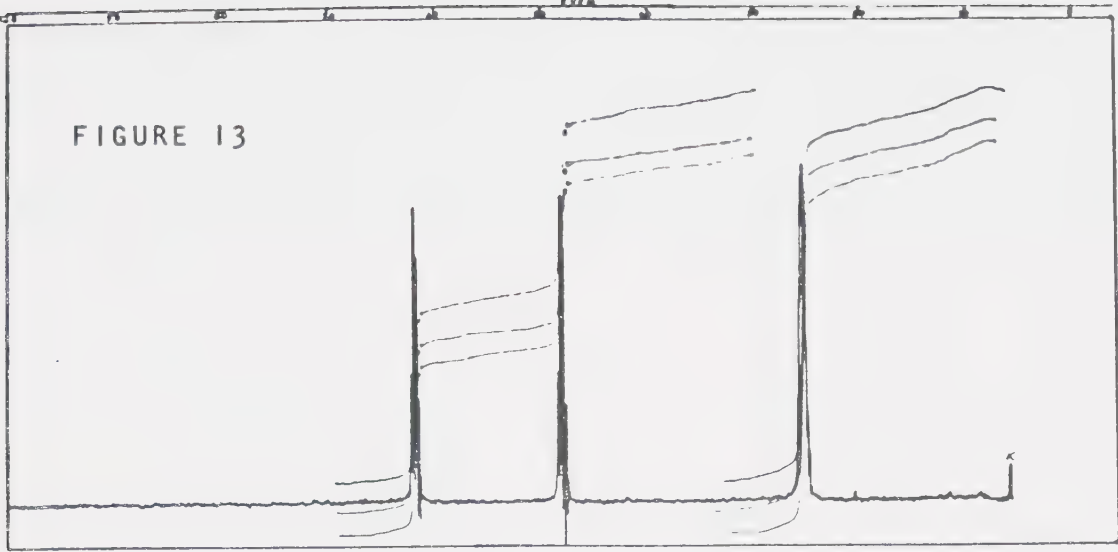


FIGURE 14

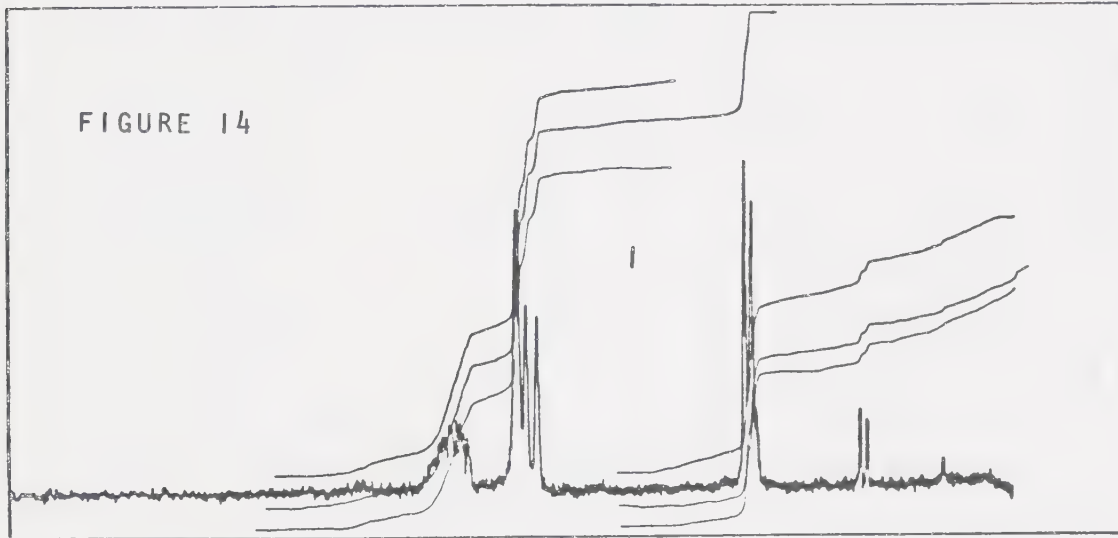
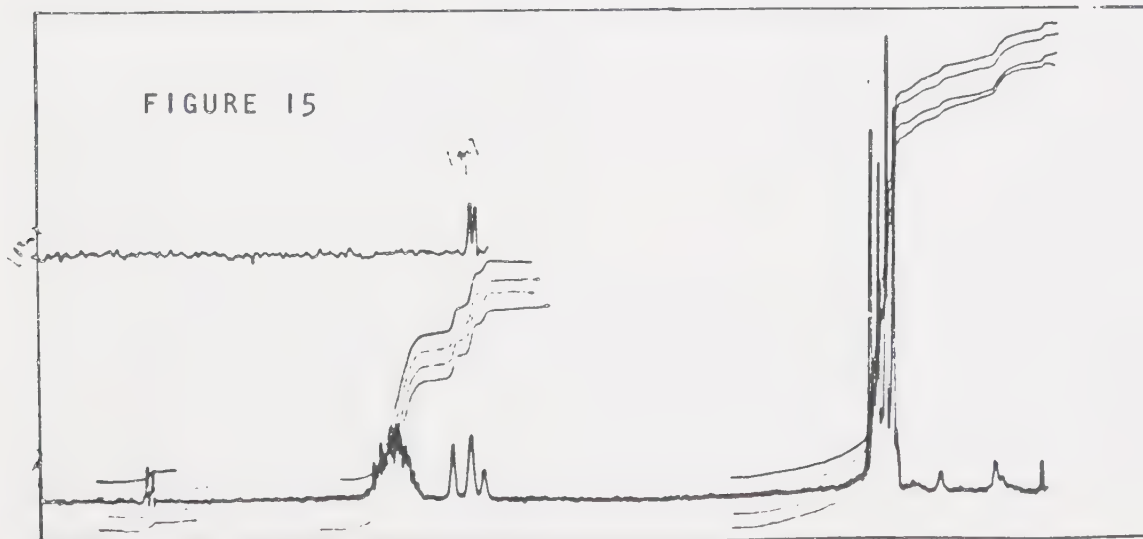


FIGURE 15



The spectrum displays only two distinct deuterium signals: 2.3 ppm downfield (C1-D) and 4.2 ppm upfield (C2-D), from the reference deuteriochloroform, in the ratio 57:43. Thus there is no evidence for the presence of deuterium at C3 or C4.

A comparison of the (E) and (Z)-2-butenals (Fig. 15) with the corresponding non-deuterated products (Fig. 7) indicates that exclusively deuterium is located in the C1 aldehyde group, as evidenced by the absence of the aldehyde signals at δ 9.42 and 10.04. A reduction in intensity of both the C2 olefinic and C4 methyl signals is apparent which suggests the presence of deuterium at both positions. These conclusions are confirmed by an examination of the corresponding d.m.r. spectrum (Fig. 17), which displays three distinct signals for each 2-butenal isomer. The signals 2.16 ppm downfield, 1.24 ppm and 5.301 ppm upfield in the ratio 52:27:21 were tentatively assigned to the (E)-2-butenal. The signals 2.76 ppm downfield, 1.38 ppm and 5.16 ppm upfield in the ratio 51:26:23 were tentatively assigned to the (Z)-2-butenal.

The 100 MHz spectrum of the recovered 2-vinyloxirane-3,3-d₂ was judged unchanged by comparison with the starting material. Thus the deuterium distribution in the products can be summarized as:

FIGURE 16.

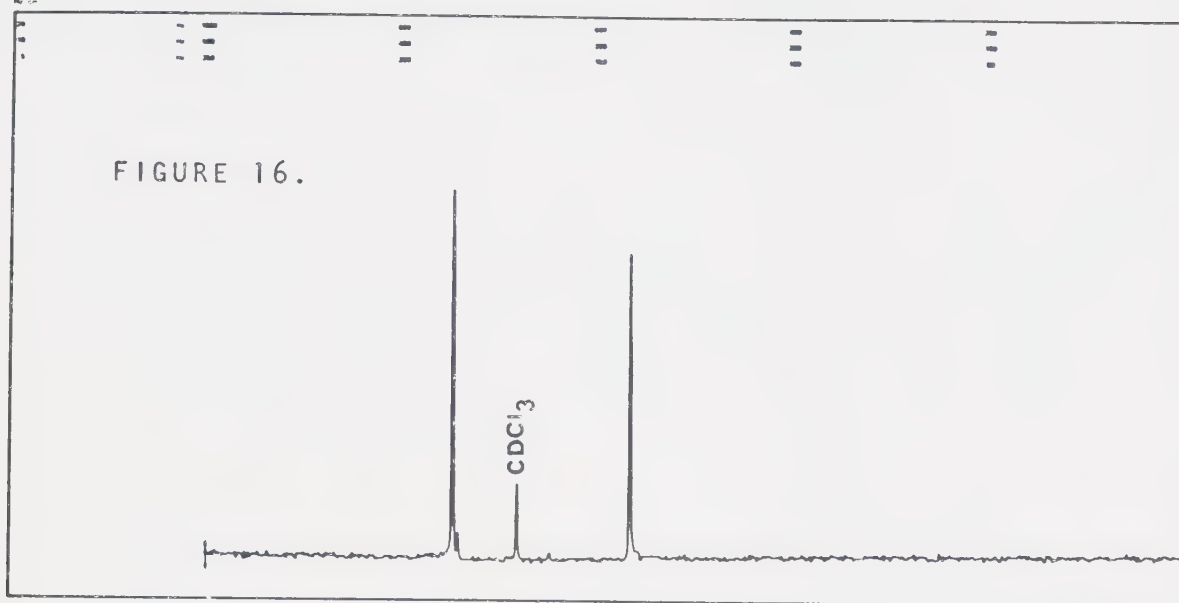
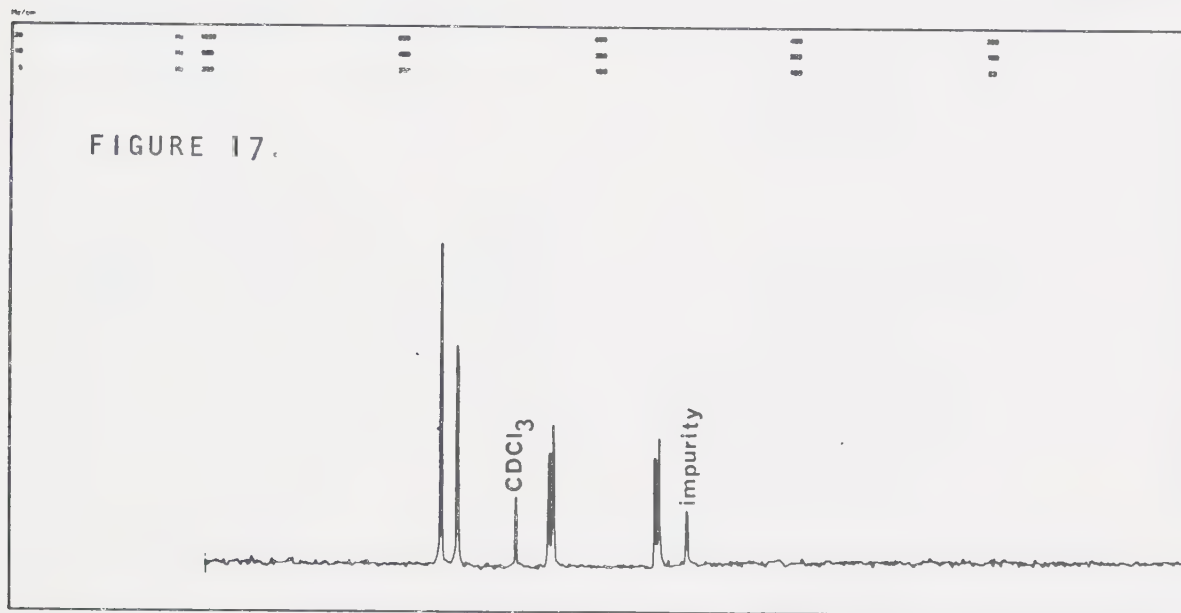
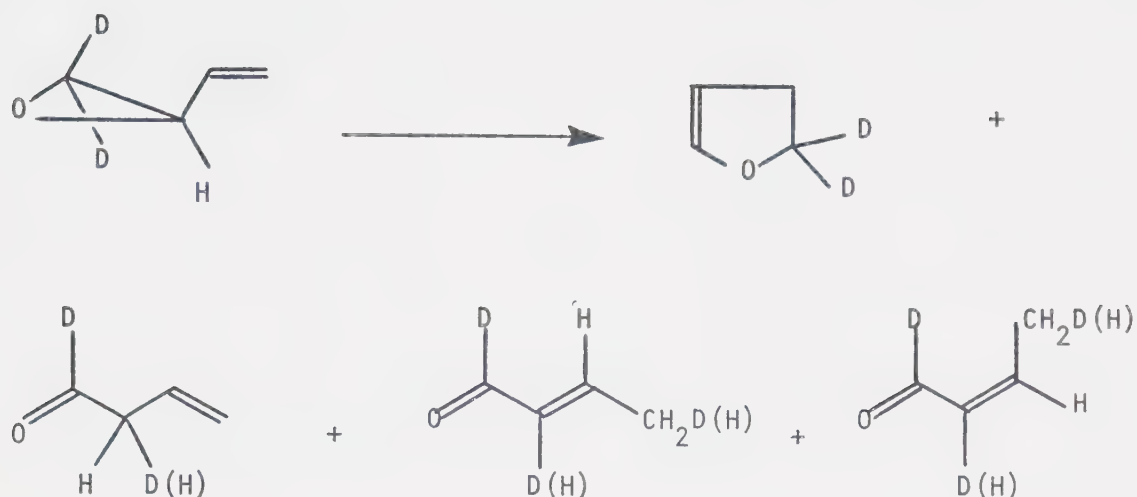


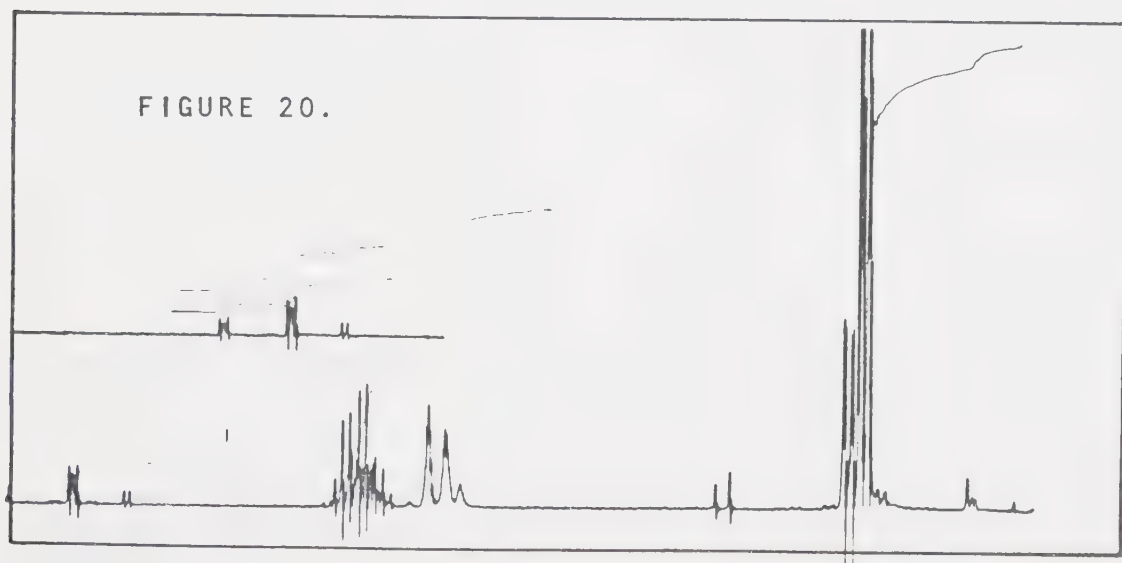
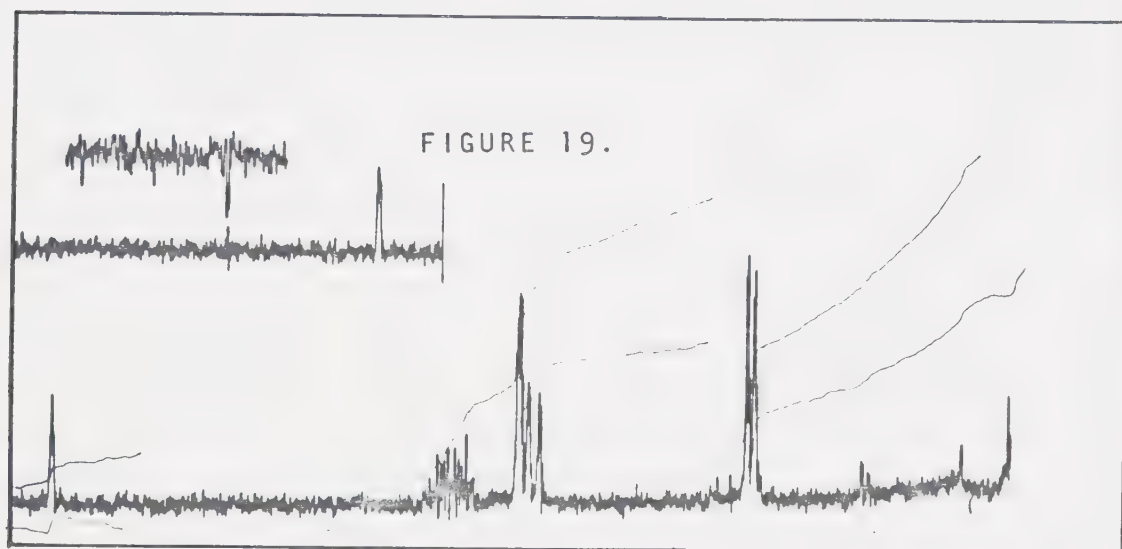
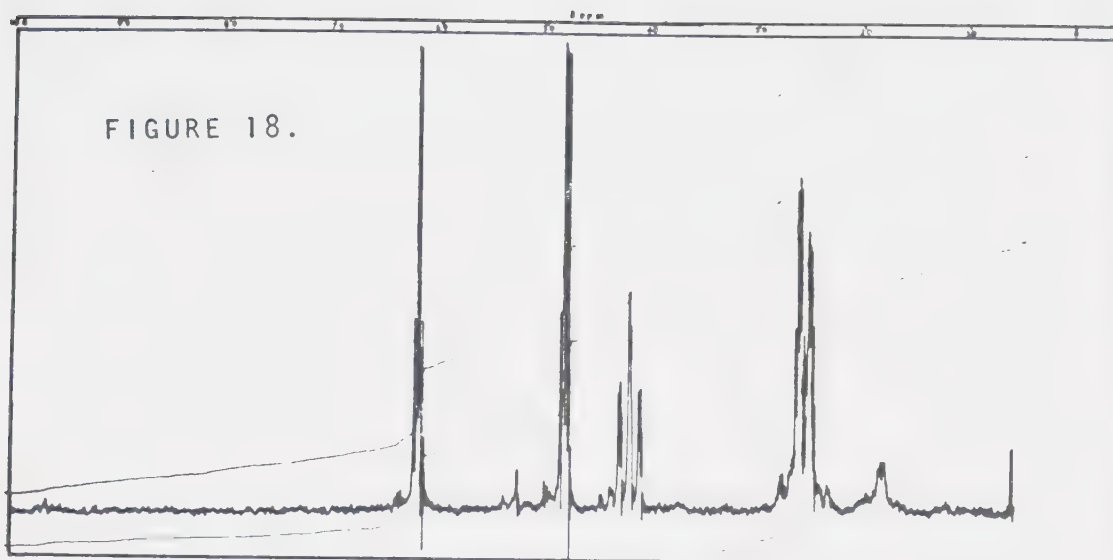
FIGURE 17.





The 100 MHz n.m.r. spectra of the thermolysis products from *cis*-3-deuterio-2-vinyloxirane are given in Figures 18, 19 and 20. An inspection of the spectrum of the dihydrofuran produced (Fig. 18) displays an approximately 50% decrease in the intensity of the C2 triplet (δ 4.2) together with fine splitting introduced into both the C2 and C3 signals. These observations are consistent with the location of deuterium at C2.

The spectrum of the 3-butenal produced (Fig. 19) displays a considerable decrease in intensity of the C1 aldehyde signal (δ 9.8) and a small decrease in intensity of the C2 methylene signal (δ 3.1) when compared to the corresponding non-deuterated product. These observations suggest the distribution of deuterium



between C1 and C2, a conclusion which is confirmed by an inspection of the corresponding d.m.r. spectrum (Fig. 21). The spectrum displays only two distinct deuterium signals: 2.44 ppm downfield and 4.14 ppm upfield in the ratio 69:31 respectively. Thus there is no evidence for the presence of deuterium at C3 or C4.

A comparison of the spectrum of the (E) and (Z)-2-butenals (Fig. 20) with the corresponding non-deuterated products indicates a considerable reduction in the intensities of the C1 aldehyde signals. A small reduction in the intensities of the C2 olefinic and C4 methyl signals is also apparent. These observations are consistent with a deuterium distribution between C1, C2 and C4. This is confirmed by an examination of the corresponding d.m.r. spectrum (Fig. 22) which displays three signals, in the ratio 83:10:7, corresponding to positions C1, C2 and C4 respectively. The lack of signals for (Z)-2-butenal in the d.m.r. spectrum was disconcerting, but a check of the 100 MHz n.m.r. spectrum showed that the (Z)-2-butenal originally present had isomerized to (E)-2-butenal.

An inspection of the 100 MHz n.m.r. spectrum of the recovered oxirane (Fig. 23) shows the presence of a new signal (δ 2.63) consistent with a small amount of cis to trans isomerization, and that equilibrium had not been attained.

FIGURE 21.

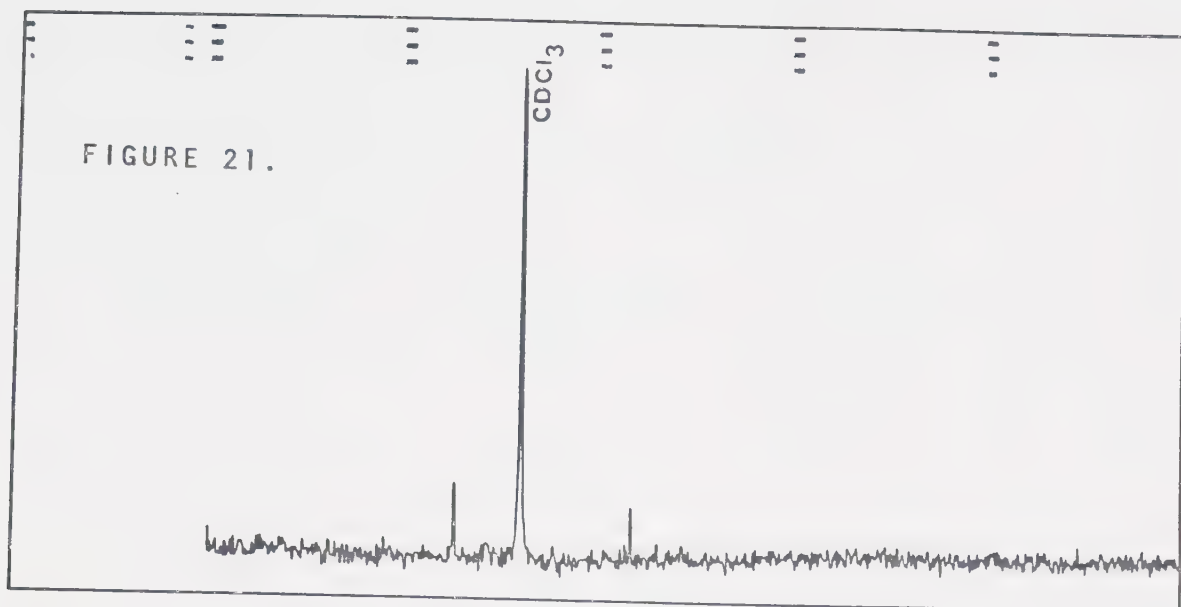


FIGURE 22.

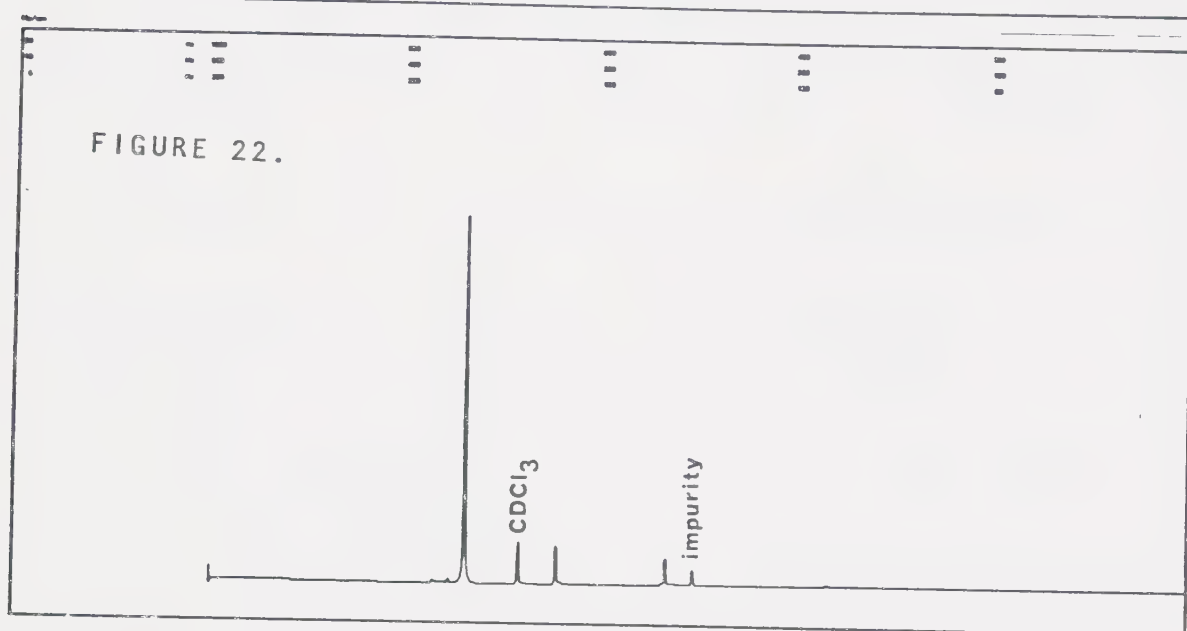
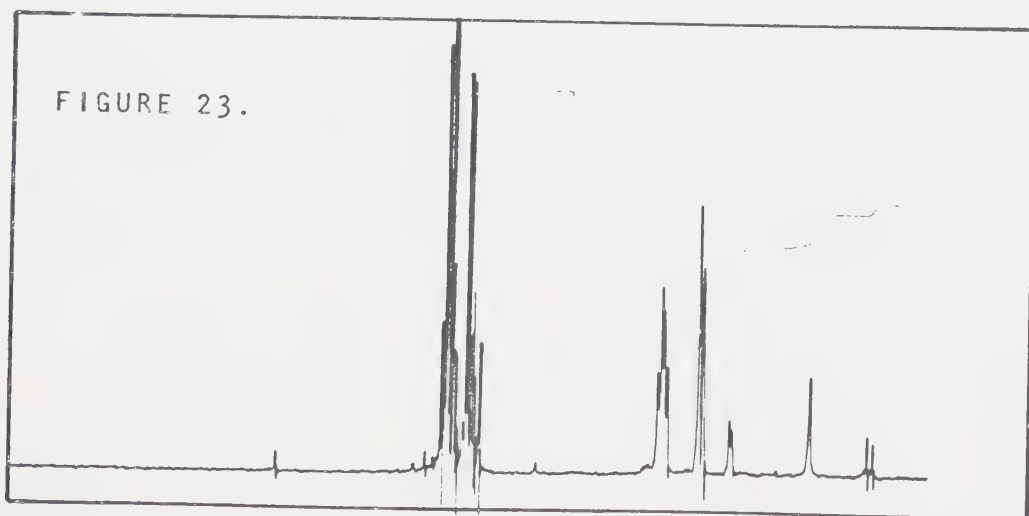
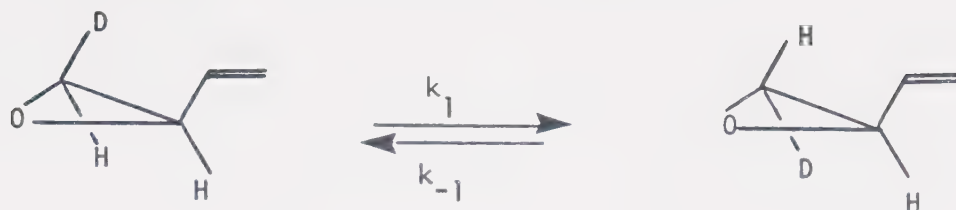


FIGURE 23.



For the isomerization of cis to trans:



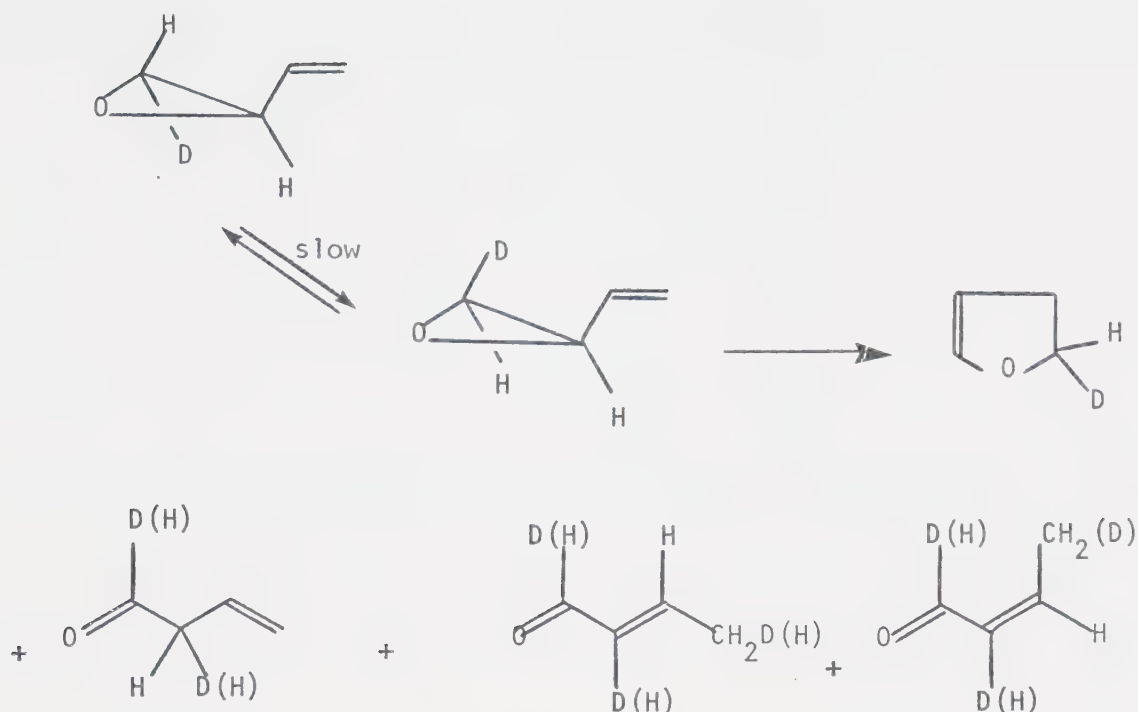
the rate constant k_1 is given by

$$k_1 = \frac{1}{2t} \ln(C_e / C_e - C_t)$$

where C_e is the equilibrium concentration of trans isomer

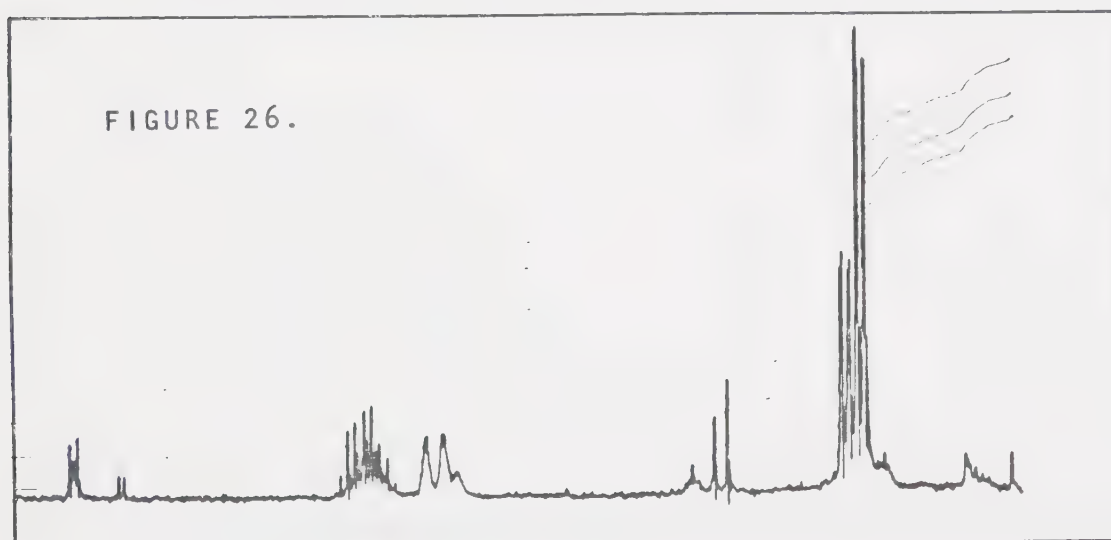
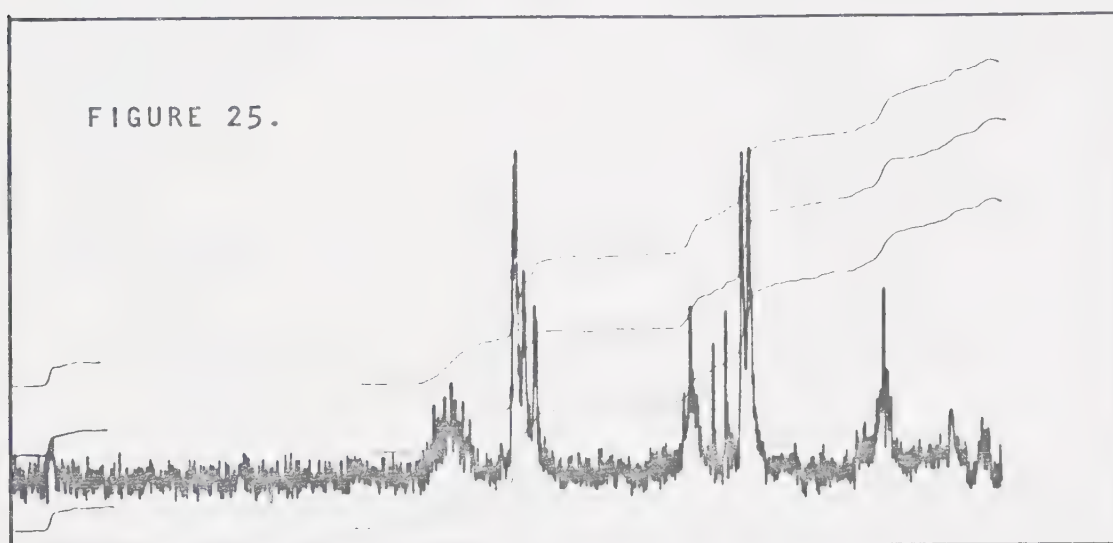
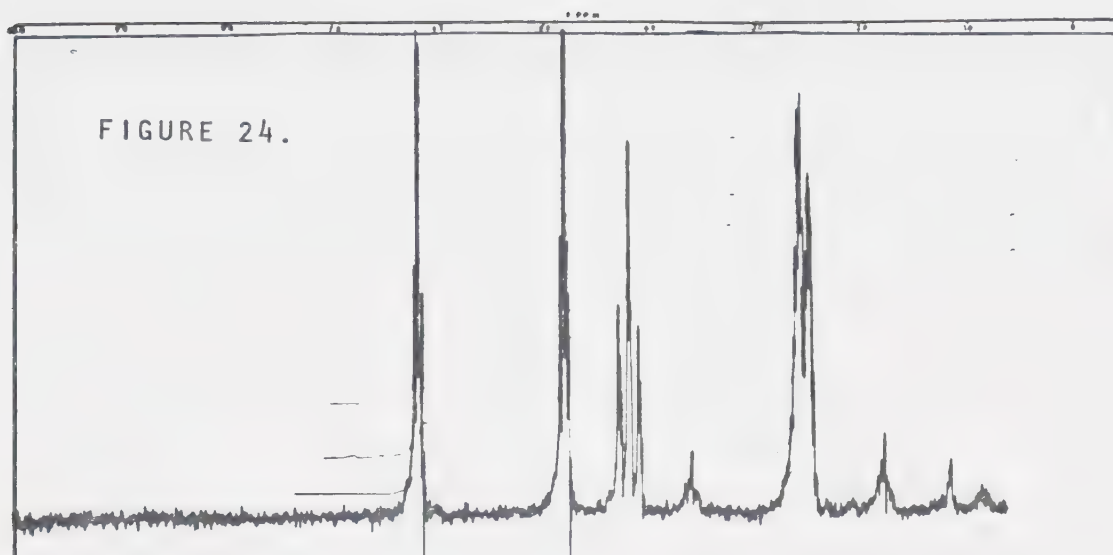
C_t is the concentration of trans isomer at time t .

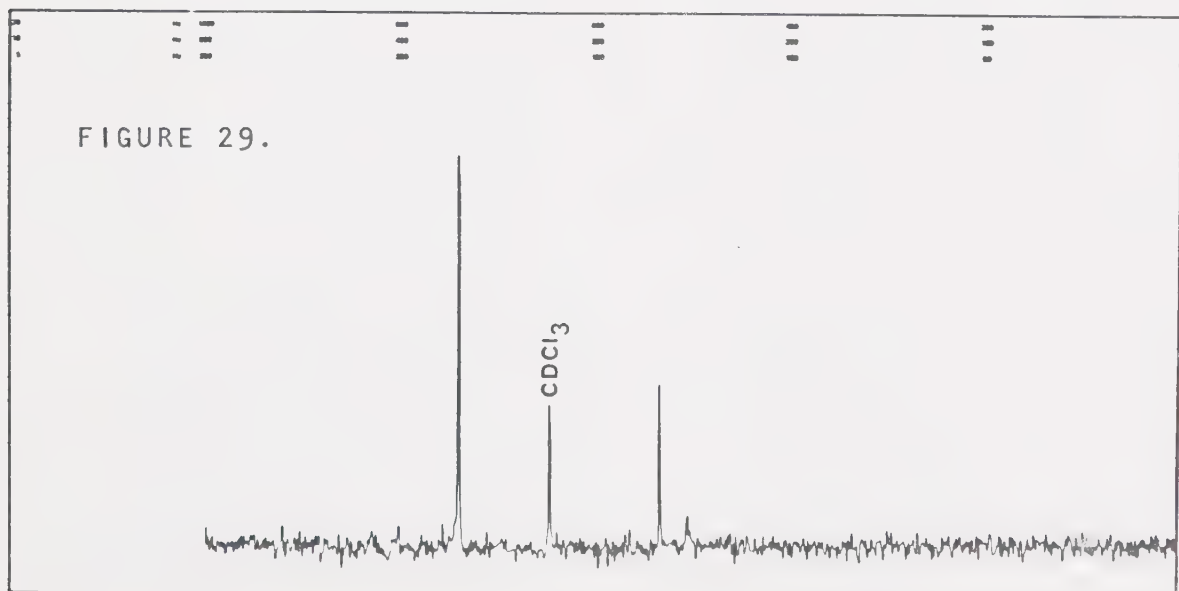
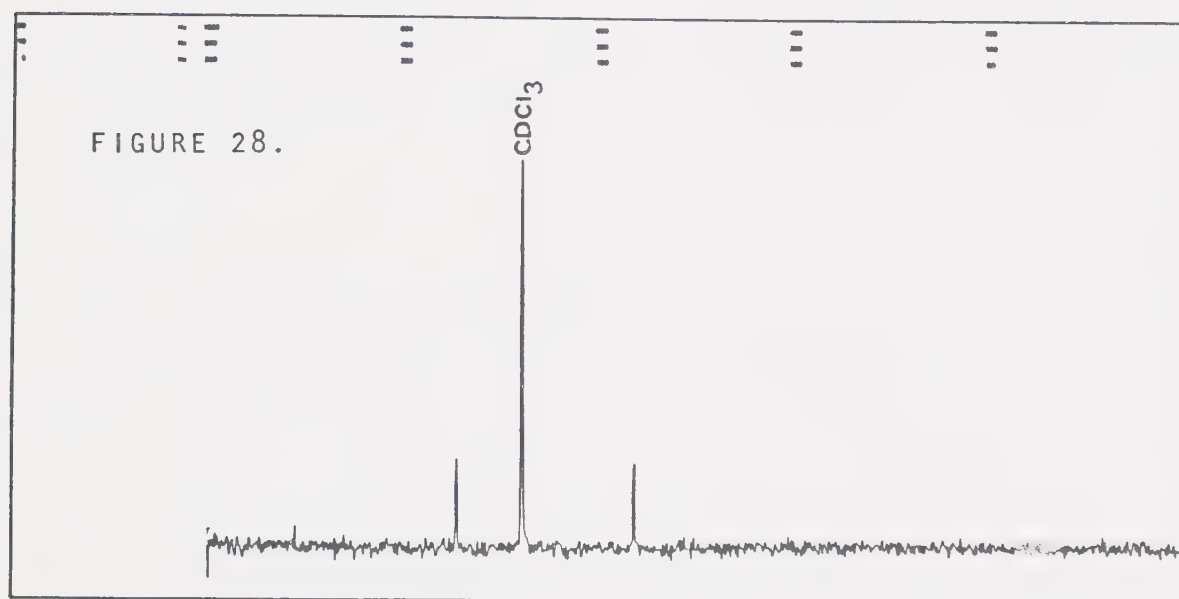
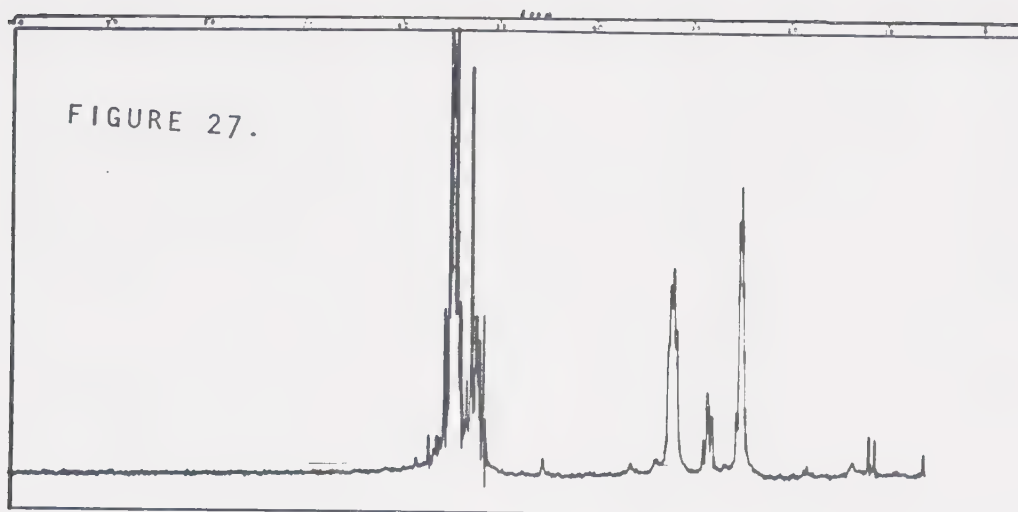
For the recovered sample at $t = 190$ min the percentage of trans isomer was determined as 17% by integration of the n.m.r. spectrum. Substitution of these values into the above equation gives $k_1 = 1.8 \times 10^{-5} \text{ sec}^{-1}$ for the rate of isomerization of cis to trans, and thus the decomposition is proceeding at approximately seven times the rate of isomerization. Thus the deuterium distribution in the thermolysis of cis-3-deuterio-2-vinyloxirane can be summarized as:



The 100 MHz n.m.r. spectra of the thermolysis products of *trans*-3-deuterio-2-vinyloxirane are shown in Figures 24, 25 and 26. The spectrum of the dihydrofuran produced (Fig. 24) compared well with that for the corresponding product from the *cis*-oxirane (Fig. 18), indicating deuterium location at C2. The d.m.r. spectrum (Fig. 28) of the 3-butenal indicated a deuterium distribution between C1 and C2 in the ratio 47:53. The integration of the corresponding p.m.r. spectrum (Fig. 25) gave the ratio as 69:31.

The spectrum of the (*E*) and (*Z*)-2-butenals (Fig. 26) again indicates a distribution of deuterium between C1, C2 and C4, which is confirmed by an inspection of the corresponding d.m.r. spectrum (Fig. 29) as a ratio 68:18:14.





The 100 MHz n.m.r. spectrum of the recovered oxirane (Fig. 27) displays an increase in the intensity of the δ 2.95 signal, an observation consistent with a small amount of trans to cis isomerization of deuterium. The trans:cis ratio was established as 84:16 by n.m.r. integration of the spectrum of the oxirane recovered from a 190 min thermolysis at 307.4°C. The rate constant was calculated as previously described for the cis to trans isomerization and gave a value of $k = 1.7 \times 10^{-5} \text{ sec}^{-1}$.

(iv) Product distributions

The product distribution with time was determined for the vinyloxiranes 12, 13 and 21 in the static Pyrex system at 307.4°C. The relative product percentages were measured by electronic integration of the thermal conductivity detector response. The detector response factors were assumed to be the same for each product.

The condition of the reaction vessel was observed to have a considerable influence on the product distribution. It was noted earlier that traces of air in the system detracted from the reproducibility of the kinetic data and caused a fast initial decomposition of the oxirane. The product distributions obtained from thermolyses in the well-conditioned reaction vessel will

be considered first, and then the marked changes introduced by the presence of air in the system will be exemplified.

The product distributions with time, in the well-conditioned system, for $\underline{12}$, $\underline{13}$ and $\underline{21}$ are shown in Figures 30, 31 and 32 respectively. The salient features of the thermal decomposition are apparent from an inspection of Figure 30. The major course of the reaction is ultimately a fragmentation to carbon monoxide and propene. An induction period for this fragmentation is apparent, which suggests that it is a result of secondary processes. The relative proportions of the isomeric butenals reach a maximum and slowly decrease thereafter. This is consistent with the thermal instability of these compounds under the reaction conditions. The 2,3-dihydrofuran is formed slowly and at a regular rate. It has already been noted that after ten half-lives the dihydrofuran is the major product produced apart from the fragmentation products.

The influence of deuterium substitution is apparent from a comparison with Figures 31 and 32. The most notable feature is the marked decrease in the rate of fragmentation to propene and carbon monoxide produced by successive deuterium substitution of the oxirane ring. The initial rates of formation of the butenals

KEY FOR FIGURES 30-34

- Propene and carbon monoxide
- 2,3-Dihydrofuran
- 3-Butenal
- △ (E)-2-Butenal
- ▼ (Z)-2-Butenal

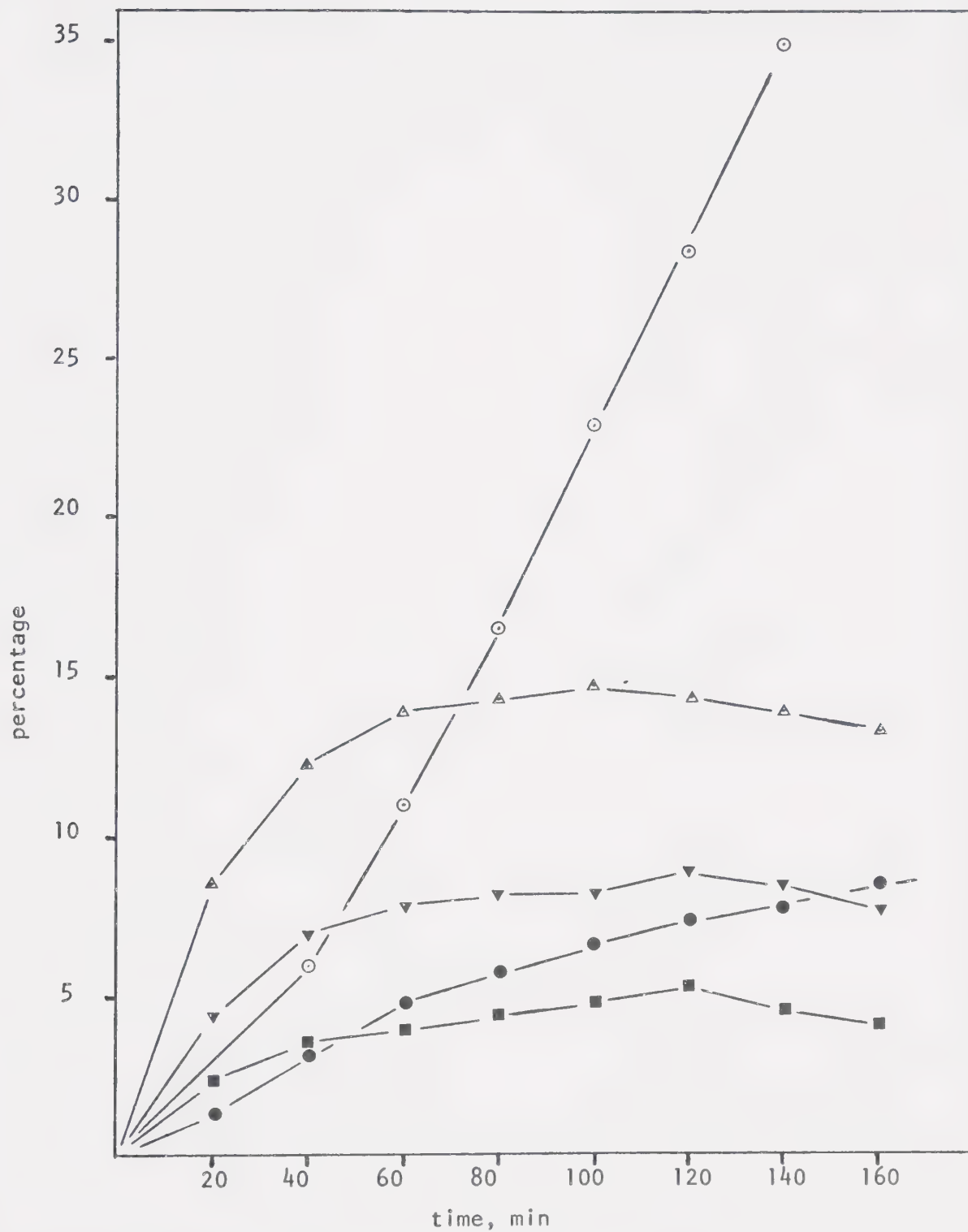


FIGURE 30. Product distribution for the thermolysis of 12 at 307.4°C in the well-conditioned system.

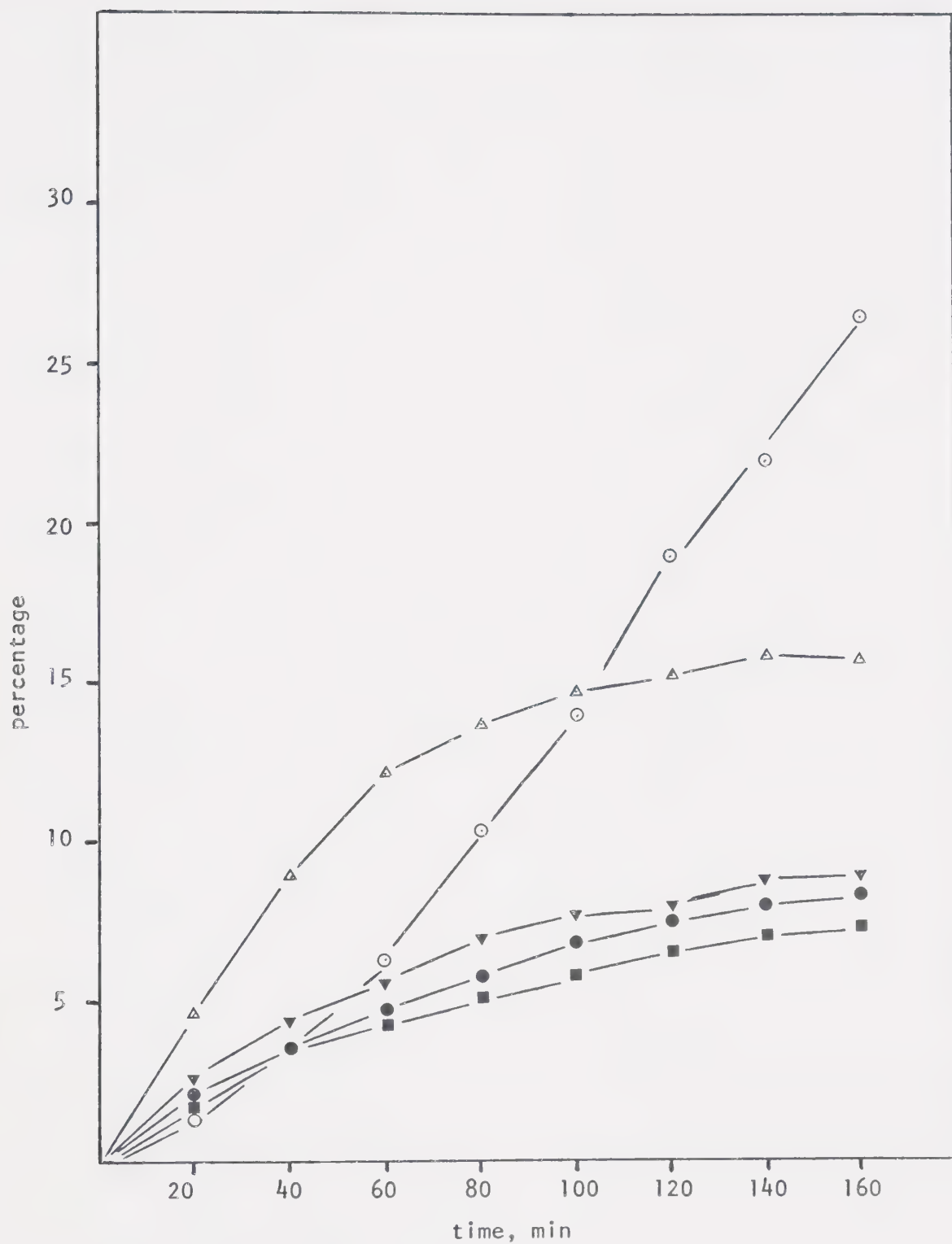


FIGURE 31. Product distribution for the thermolysis of 13 at 307.4°C in the well-conditioned system.

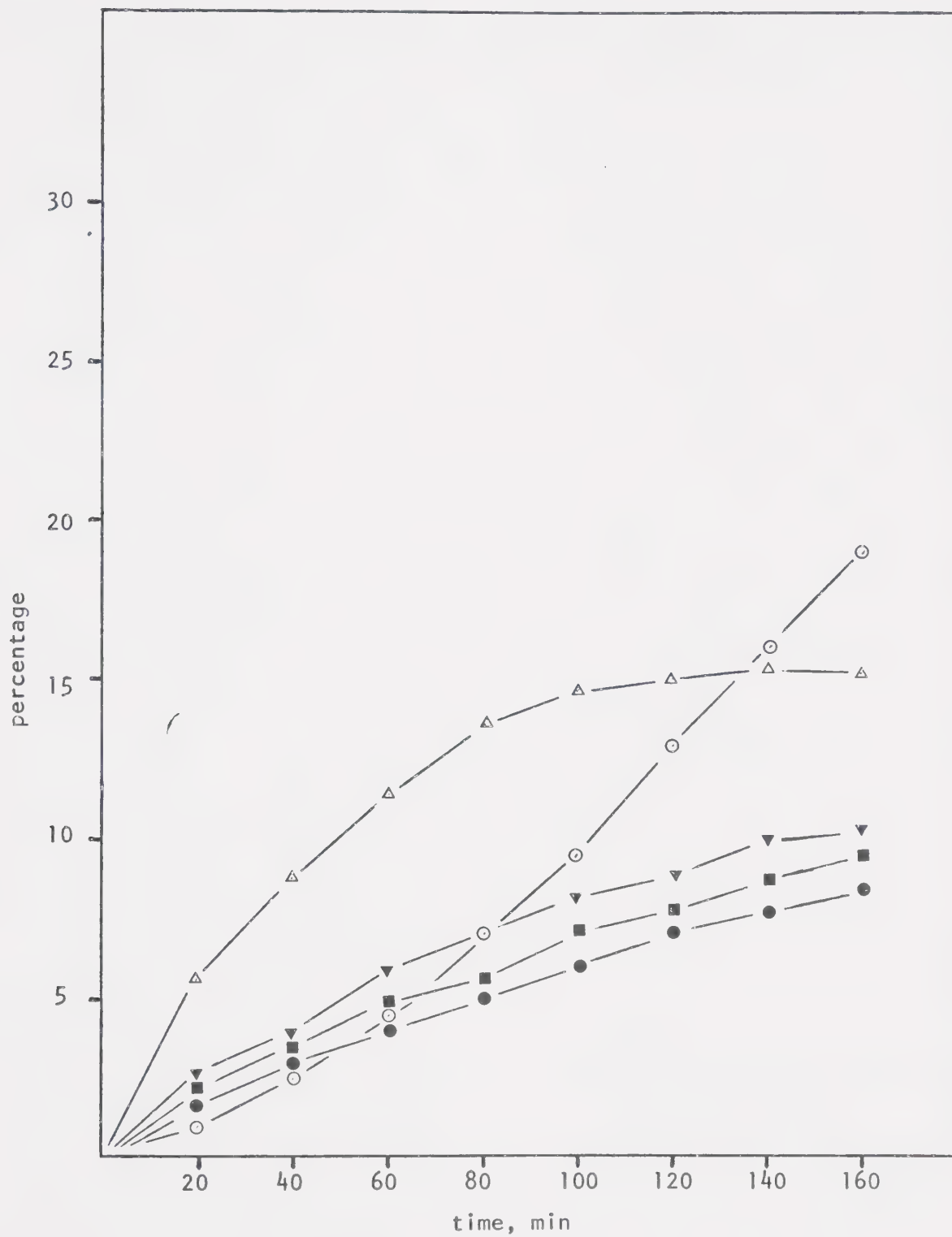


FIGURE 32. Product distribution for the thermolysis of 21 at 307.4°C in the well-conditioned system.

appear to be slightly reduced, and their thermal stability increased. It appears that there is little effect on the dihydrofuran formation by the deuterated oxiranes.

The presence of a trace of air in the system has a marked effect on the thermal decomposition as can be seen from an inspection of Figures 33 and 34. The striking feature is the complete reversal of the relative proportions of the isomeric butenals. The initial rates of formation of 3-butenal and (Z)-2-butenal are increased considerably, and apparently the 3-butenal is initially the major product of the reaction. Figure 35 shows a comparison of the thermolysis of 2-vinyloxirane with the change in condition of the reaction vessel. It can be seen from an inspection of Figure 35 that the major feature is an appreciable increase in the proportion of isomeric butenals. A smaller effect is noticeable on the extent of fragmentation but there is very little difference in the relative percentage of 2,3-dihydrofuran produced.

From the results of the product composition studies it was felt that the formation of 2,3-dihydrofuran warranted further investigation. With the kinetic data available it was thought that an appropriate treatment might provide kinetic data for the formation of 2,3-dihydrofuran from 2-vinyloxirane.

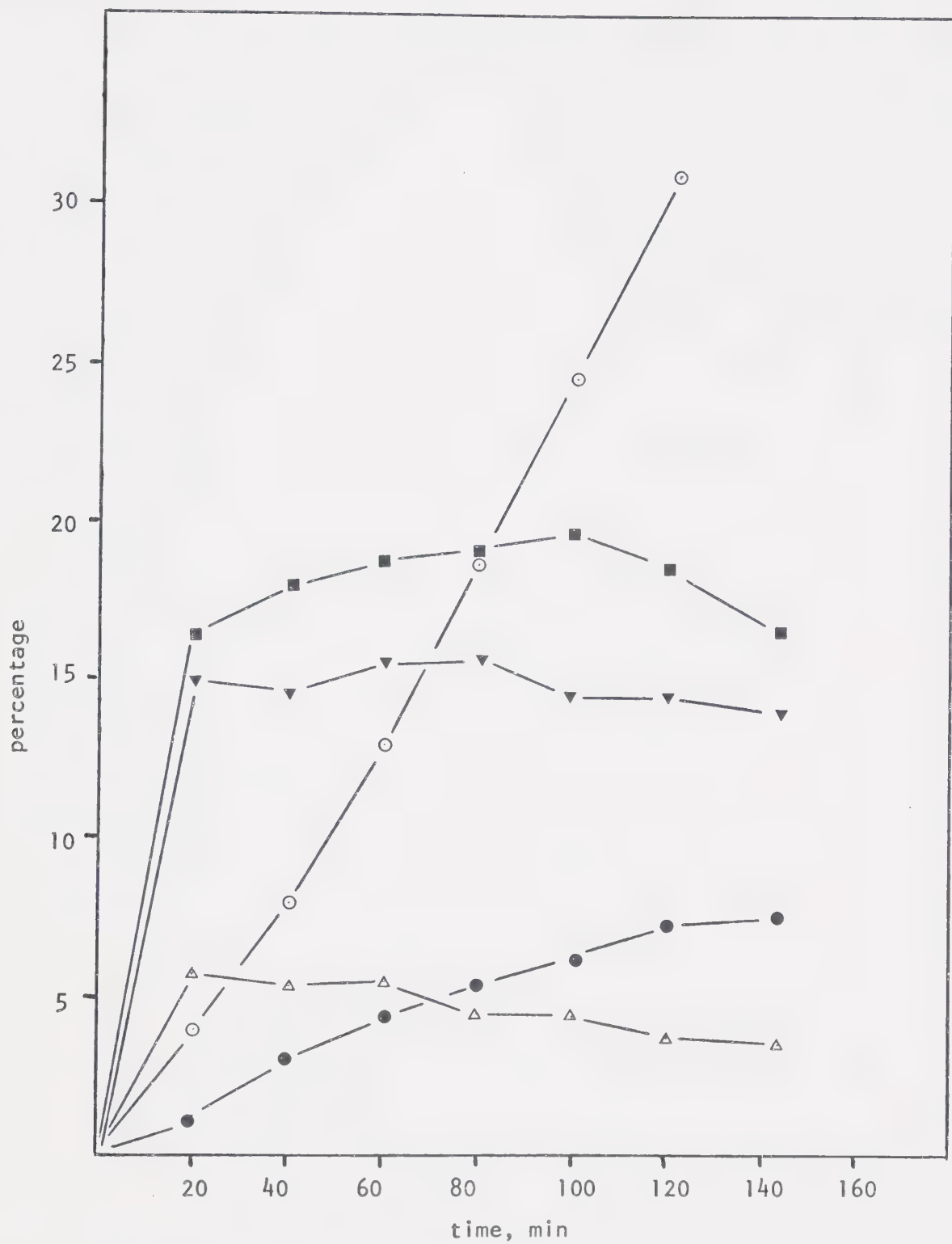


FIGURE 33. Product distribution for the thermolysis of 12 at 307.4°C with a trace of air in the system.

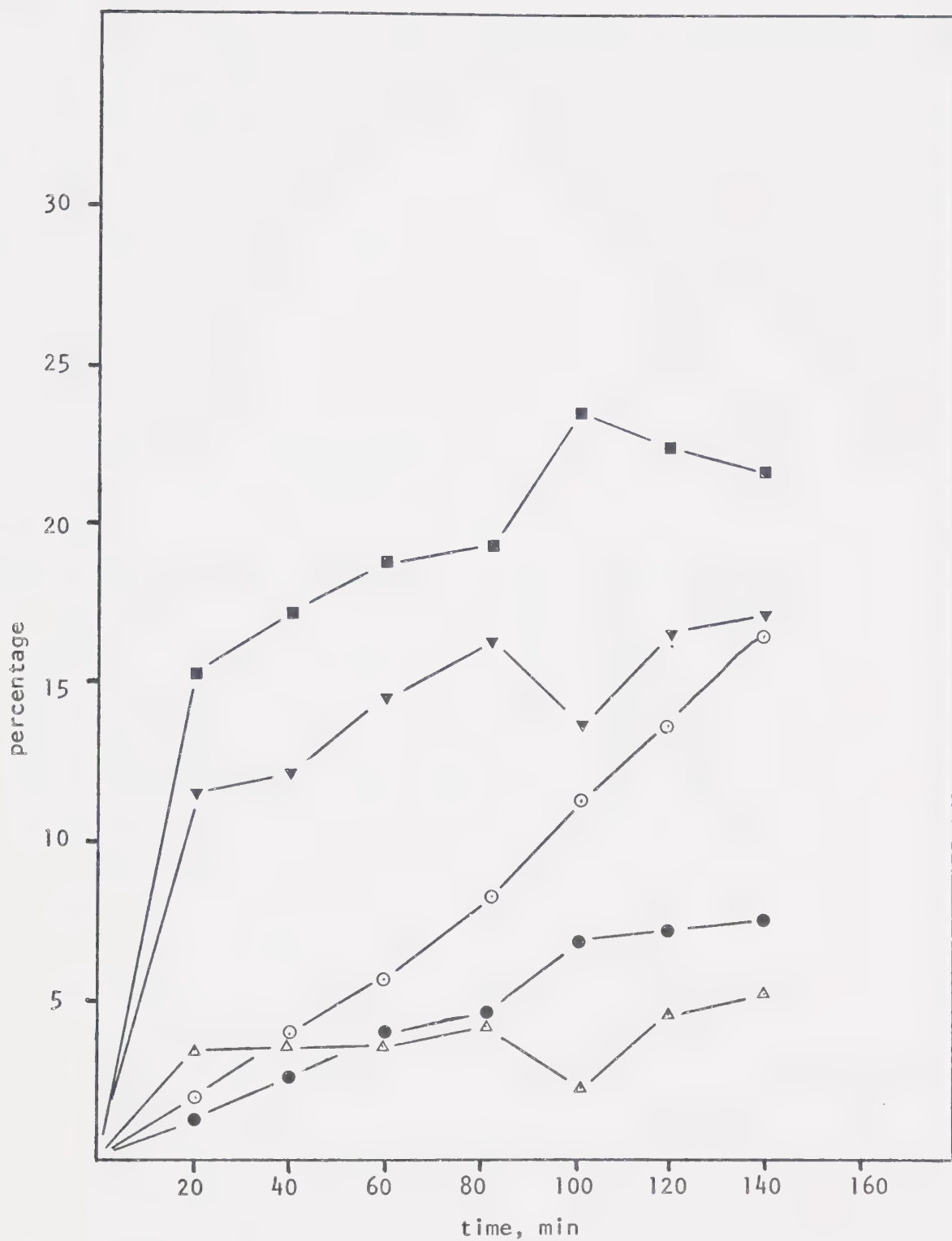


FIGURE 34. Product distribution for the thermolysis of 21 at 307.4°C with a trace of air in the system.

KEY FOR FIGURE 35

Total butenals	□	(good condition)
	■	(poor condition)
Propene + CO	○	(good condition)
	●	(poor condition)
2,3-Dihydrofuran	△	(good condition)
	▲	(poor condition)

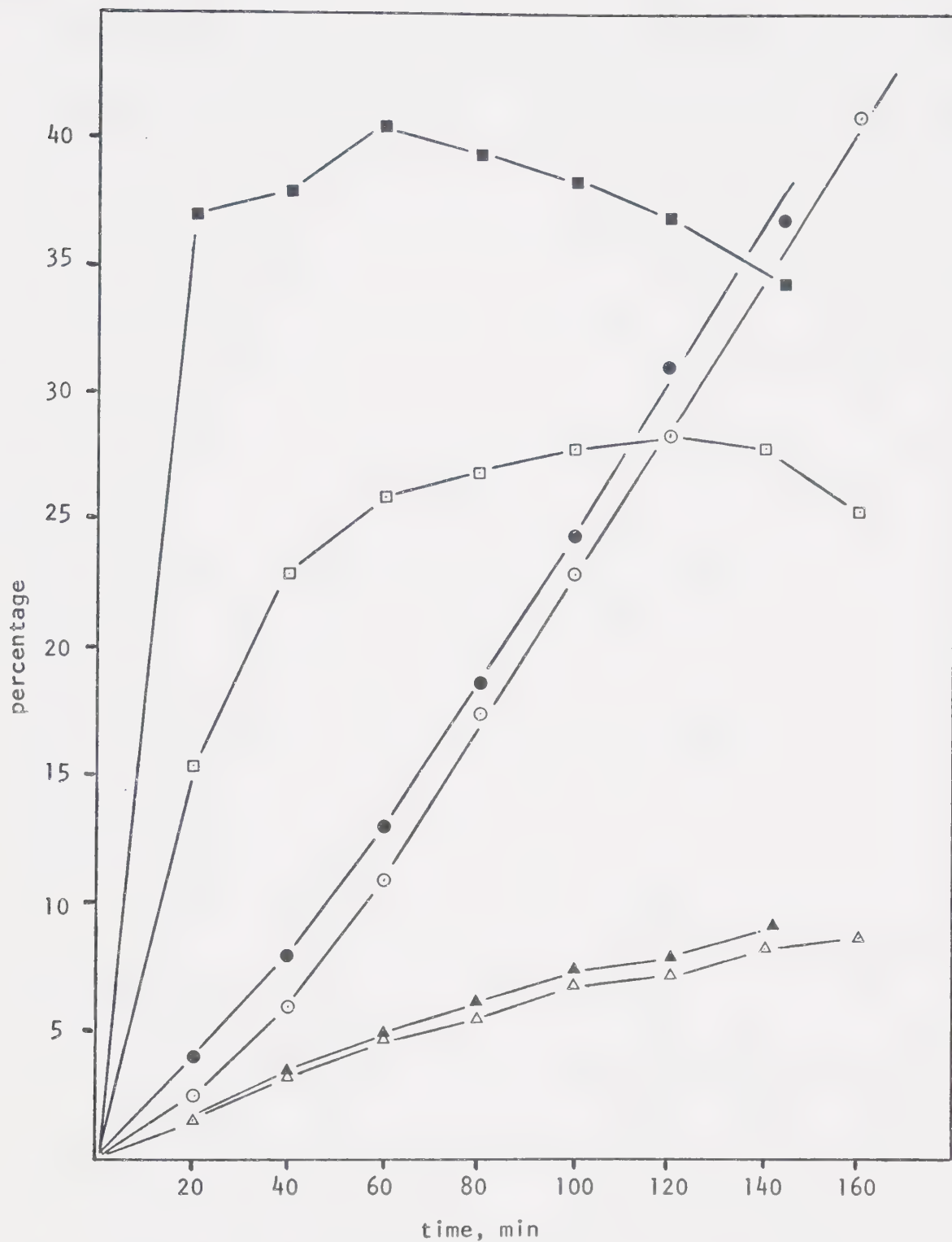
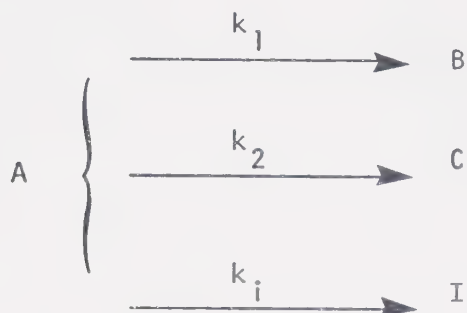


FIGURE 35. Comparison of product distributions for the thermolysis of 12 at 307.4°C with change in the condition of the reaction vessel.

For a compound decomposing to several products by simultaneous first order processes we can write:



And

$$\begin{aligned}
 -\frac{d[A]}{dt} &= k_1[A] + k_2[A] + \dots\dots\dots k_i[A] \\
 &= k_n[A] \text{ where } k_n = \sum_i k_i
 \end{aligned}$$

The overall kinetics are thus also first order.

We can write:

$$\frac{d[B]}{dt} = k_1[A] \quad ; \quad \frac{d[C]}{dt} = k_2[A] \quad \text{etc.}$$

and therefore

$$\frac{d[B]}{dt} \bigg/ -\frac{d[A]}{dt} = k_1[A]/k_n[A] = k_1/k_n$$

A plot of $[B]$ versus $[A]$ should therefore be linear and the slope given by k_1/k_n . Since an internal standard was present in the kinetic runs we can equally well construct a plot of

$$\frac{\text{Int. (Dihydrofuran)}}{\text{Int. (Standard)}} \quad \text{versus} \quad \frac{\text{Int. (Vinyloxirane)}}{\text{Int. (Standard)}}$$

where Int. = integrator output from the detector. This plot has the advantage that the absolute percentages are inconsequential to the rate study, and errors introduced by the integration of poorly-shaped peaks are eliminated. A typical plot obtained is shown in Figure 36. The slope was determined by the least squares analysis as previously described and the values of the rate constants for the formation of 2,3-dihydrofuran at various temperatures are given in Table VI. The complete kinetic data are detailed in the Appendix.

It should be noted that the reproducibility of the rate constants was not as good as that obtained for the rate constants for the overall decomposition.

The Arrhenius activation parameters were determined by a least squares analysis of a plot of $\log k$ versus $(1/T)$. The variation of the rate constant with temperature is shown graphically in Figure 37. The values of the activation parameters at the 90% confidence level were estimated as:

$$E_a = 50.6 \pm 2.5 \text{ Kcal.mole}^{-1}$$

$$\log A = 14.3 \pm 0.9$$

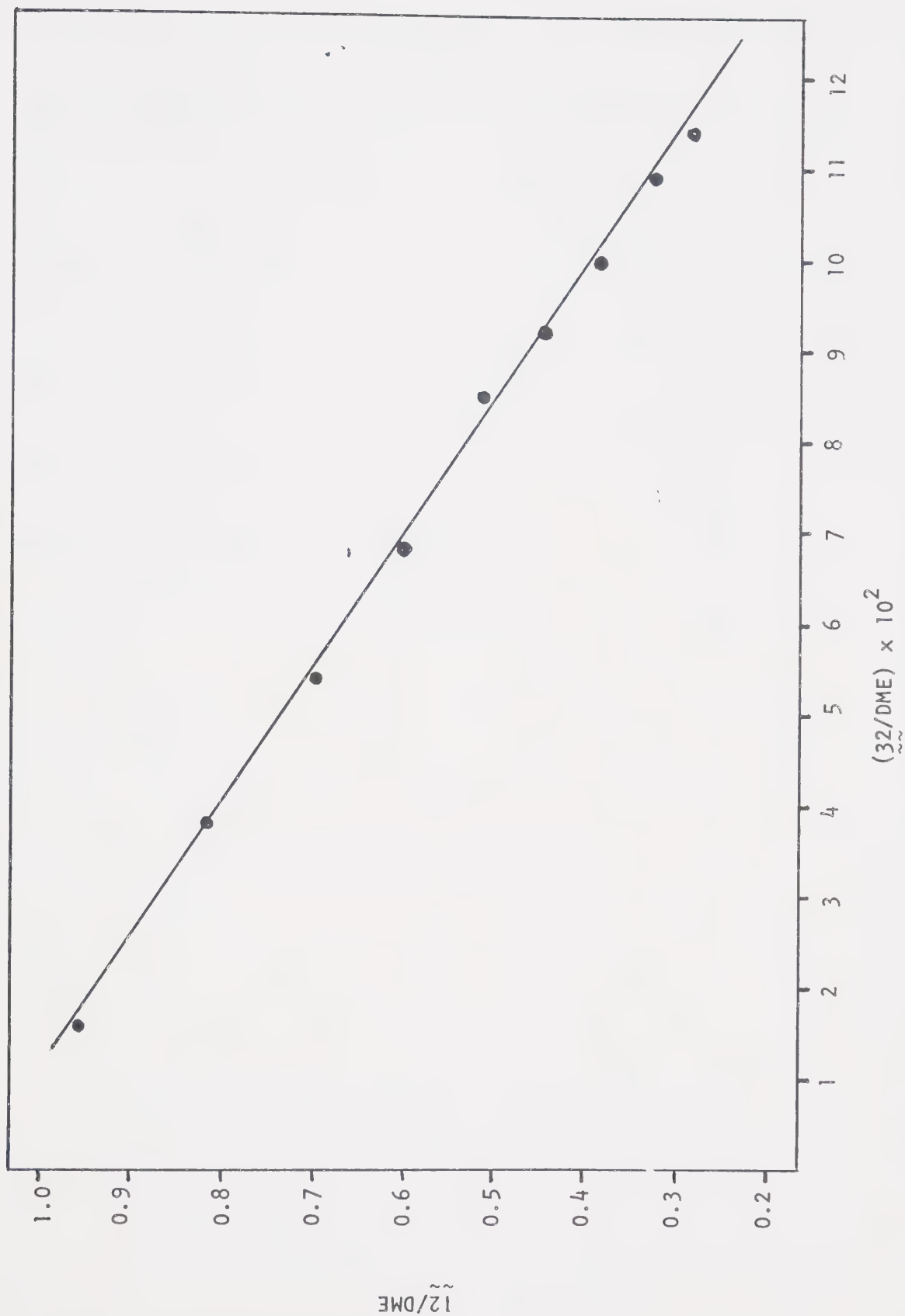


FIGURE 36. Plot of $(\frac{12}{DME})$ versus $(\frac{32}{DME}) \times 10^2$ for the thermolysis of 2-vinyloxirane at 307.4°C.

TABLE VI

Rate constants for the formation of 2,3-dihydrofuran

Temp. (°C)	Number of runs	$10^5 k \text{ (sec}^{-1}\text{)}$	
		<u>± probable error</u>	<u>at 90% confidence</u>
292.70	4	0.60 ± 0.03	± 0.04
297.52	5	0.95 ± 0.03	± 0.04
302.16	5	1.32 ± 0.10	± 0.14
307.40	5	1.88 ± 0.05	± 0.07
312.50	5	2.82 ± 0.12	± 0.17

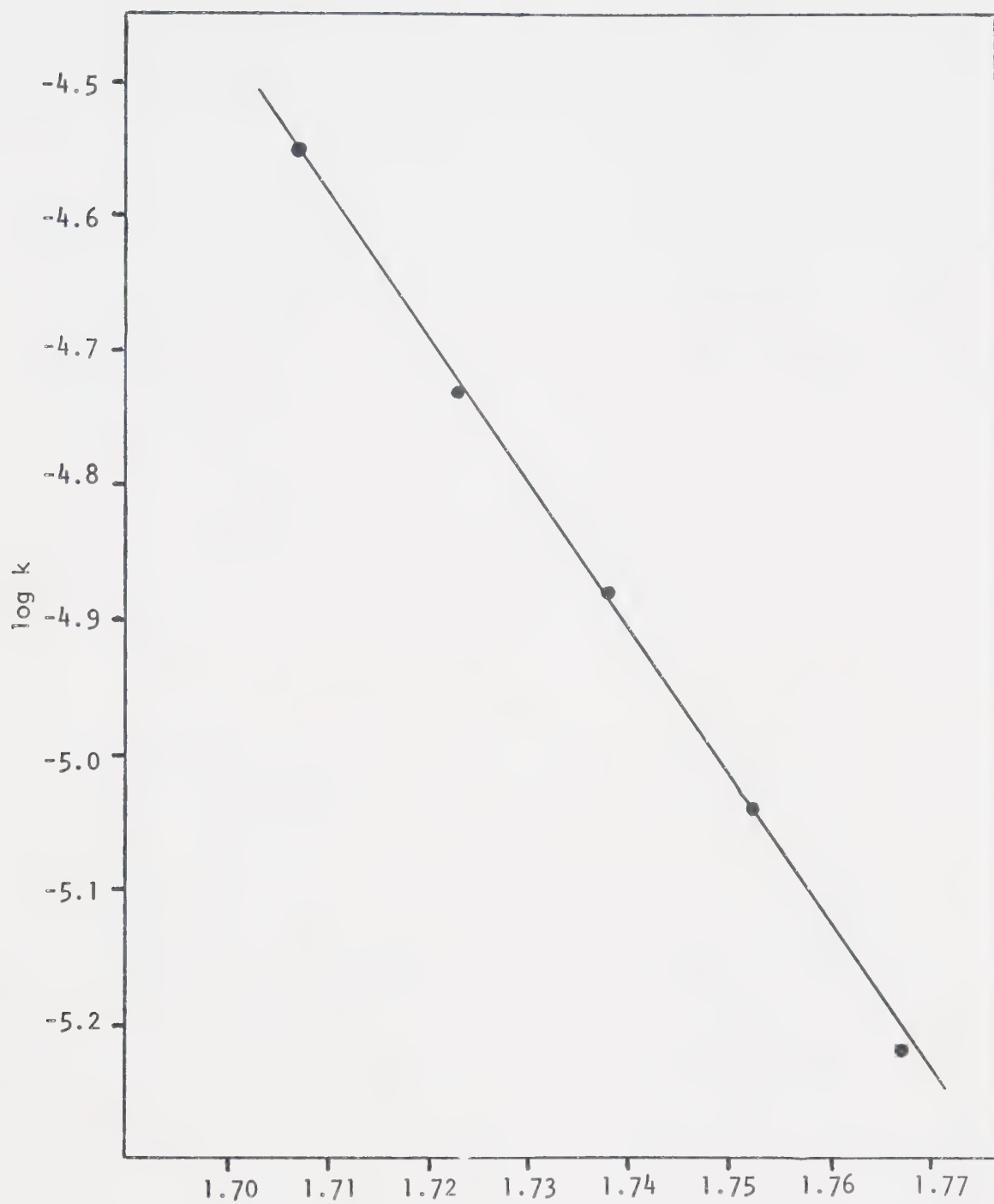


FIGURE 37. Plot of $\log k$ versus $1/T$ for the formation of 2,3-dihydrofuran.

An estimation of the deuterium isotope effect on the formation of 2,3-dihydrofuran was made from the kinetic data obtained at 307.4°C. The mean values of the rate constants together with their associated error limits are given in Table VII. The complete kinetic data are given in the Appendix. The observed isotope effects can thus be calculated and at the 90% confidence level were estimated as

<u>Compound</u>	<u>k_H/k_D</u>
13 ~~	1.19 ± 0.13
21 ~~	1.33 ± 0.12

The observed isotope effects were of similar magnitude to those obtained for the overall decomposition process, but the errors were considerably larger. It should be emphasized that it would be unwise to draw any mechanistic conclusions from the behaviour due to the unreliability of the measured isotope effects.

TABLE VII

Rate constants* for the formation of 2,3-dihydrofuran at
307.4°C

Compound	Number of runs	$10^5 k_1 (\text{sec}^{-1})$	
		\pm probable error	at 90% confidence
12 (d ₀) ~~	5	1.88 \pm 0.05	\pm 0.07
13 (<u>cis</u> d ₁) ~~	3	1.58 \pm 0.05	\pm 0.13
21 (d ₂) ~~	4	1.44 \pm 0.04	\pm 0.07

* No correction has been made for isotopic purity.

(v) Control experiment

It was noted earlier that the thermolysis of 2-vinyl-oxirane-3,3- d_2 produced 3-butenal with an unequal distribution of deuterium between C1 and C2. It was thought that the loss of deuterium at C2 could be the result of a surface-catalyzed exchange process.

A thermolysis of 2-vinylloxirane was carried out in the reaction vessel which had been repeatedly treated with D_2O . The 2-butenals were recovered and analyzed by high resolution mass spectrometry. Under very high resolution, the M+1 peak was resolved to show clearly the presence of a signal due to ^{12}CD , and thus the feasibility of a surface-catalyzed exchange was demonstrated.

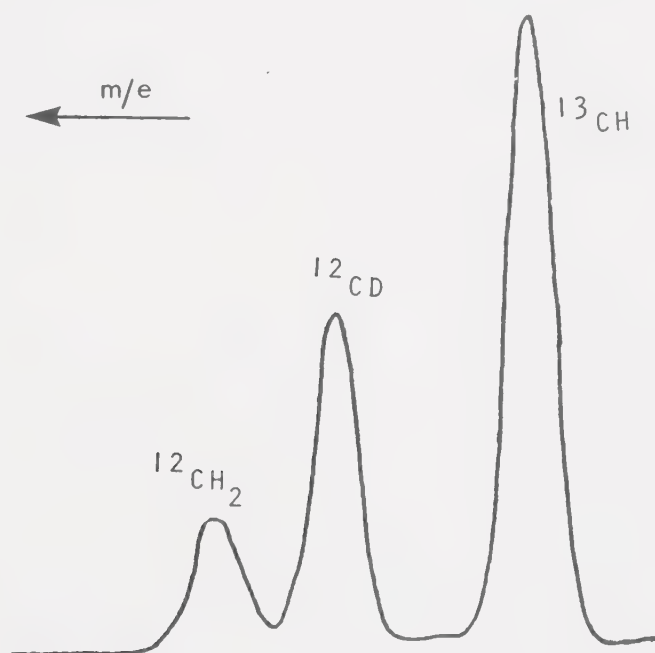


FIGURE 38. The very high resolution mass spectrum of the M+1 peak of the 2-butenals from the control experiment.

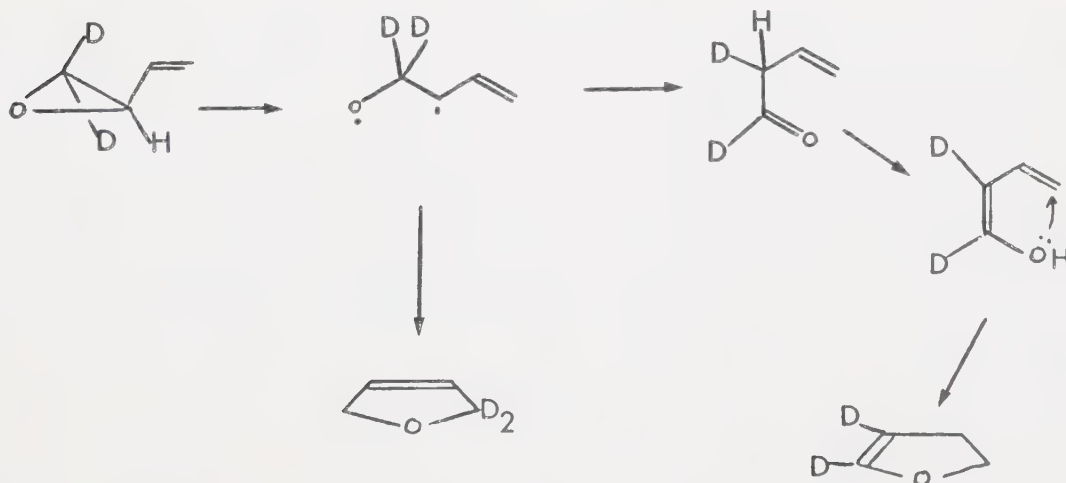
D I S C U S S I O N

A. Product Studies

The products identified from the gas phase thermolysis of 2-vinyloxirane were 2,3-dihydrofuran, 3-butenal, (E) and (Z)-2-butenal, propene and carbon monoxide. From an inspection of Figure 30 it can be seen that the butenals were initially the major decomposition products but soon gave way to a preponderance of carbon monoxide and propene. The thermal instability of the butenals under the reaction conditions was apparent from an analysis of the product composition after ten half-lives. Carbon monoxide, propene and 2,3-dihydrofuran were the only products present in appreciable amounts. 3-Butenal was almost totally absent and the isomeric 2-butenals were considerably reduced relative to 2,3-dihydrofuran. The condition of the reaction vessel was observed to have a considerable influence on both the rate of decomposition and the product distribution. The presence of a trace of air in the system caused a complete reversal of the relative proportions of butenals, as can be seen from a comparison of Figures 30 and 33. An inspection of Figure 35 shows that the initial rate of decomposition was increased together with a concomitant increase in the proportion of isomeric butenals relative to the amount of dihydrofuran.

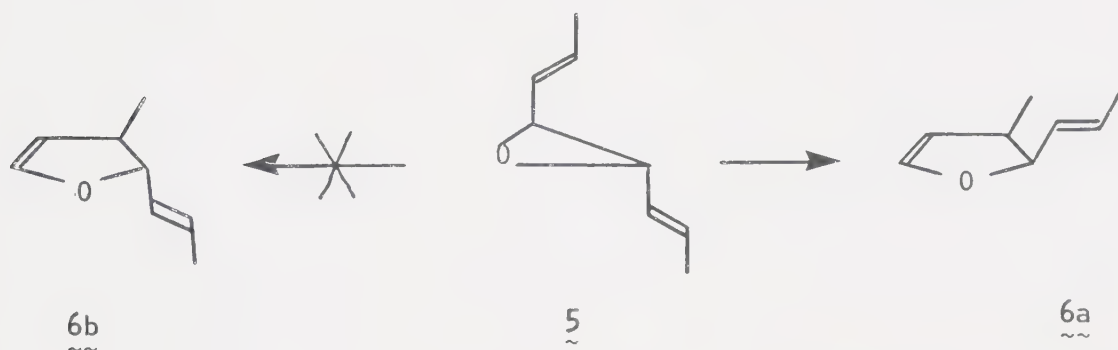
Certain mechanistic implications are apparent from a consideration of the deuterium distribution in the thermolysis products. An examination of the p.m.r. spectrum (Figure 13) of the 2,3-dihydrofuran produced from 2-vinyloxirane-3,3- d_2 shows that deuterium is located exclusively at the 2-position. The p.m.r. spectra of the 2,3-dihydrofuran produced from the cis and trans-mono-deuterated 2-vinyloxiranes (Figures 18 and 24 respectively) are also consistent with deuterium located only at the 2-position.

It is difficult to visualize how 2,3-dihydrofuran could arise directly as a result of an initial carbon-oxygen bond cleavage. If we consider the possibility of a surface-catalyzed isomerization of the enolic form of 3-butenal then we would expect to observe no deuterium at C2. We might also expect that some 2,5-dihydrofuran would be produced.

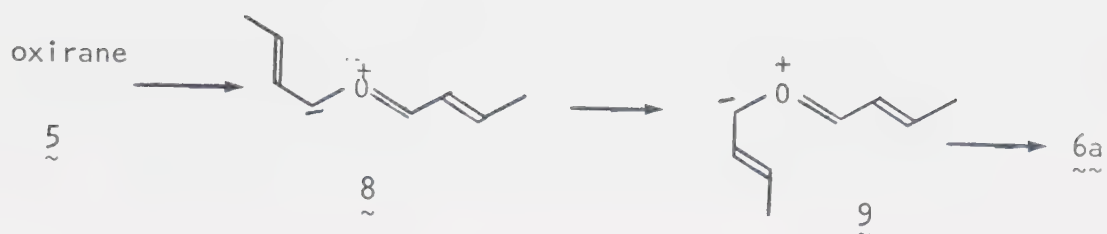


The observed deuterium location at C2 and the lack of 2,5-dihydrofuran allow us to reject this mechanism as a route to 2,3-dihydrofuran.

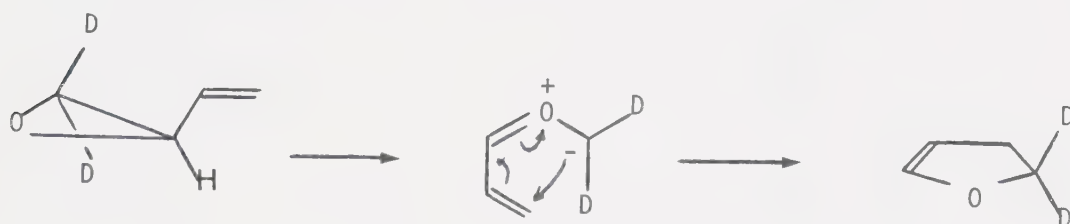
A possible pathway which would be consistent with the observed deuterium location is the operation of a concerted 1,3-sigmatropic migration. This has been ruled out in a study (25a) of the divinylloxirane system where it was observed that the 2-vinyl-2,3-dihydrofuran produced directly from chiral trans-2,3-divinylloxirane was racemic. The operation of a concerted process has been similarly ruled out on stereochemical grounds by Chuche (24) in a study of E,E-2,3-dipropenyloxirane.



The orbital symmetry allowed product is $\sim\sim$ 6b but the observed product, which would be forbidden by orbital symmetry, is the thermodynamically less stable $\sim\sim$ 6a. This has been rationalized in terms of an isomerization at an intermediate carbonyl-ylide stage.



The operation of this process in the 2-vinyloxirane system would result in exclusive deuterium location at C2, but a more detailed stereochemical test of the mechanism was not undertaken in this study.



The deuterium distribution in the 3-butenal produced from 2-vinyloxirane-3,3-d₂ (21), cis-3-deuterio-2-vinyloxirane (13) and trans-3-deuterio-2-vinyloxirane (20) are summarized in Table VIII.

The significant feature of the d.m.r. spectra is the observation of only two distinct signals indicative of the location of deuterium at only C1 and C2. It is of interest to note that some deuterium has been lost from the 2-position of the 3-butenal produced from 21, which may be the result of a surface-catalyzed exchange process occurring via the enol.

The feasibility of a surface catalyzed exchange

TABLE VIII

The deuterium distribution in the 3-butenal produced from
the thermolyses of 21, 13 and 20 at 307.4°C

3-Butenal	Figure #	Method	C1	C2	C3	C4
from <u>21</u>	16	(d.m.r.)	58	42	0	0
	14	(p.m.r.)	58	42	0	0
from <u>13</u>	21	(d.m.r.)	69	31	0	0
	19	(p.m.r.) ^a	78	22	0	0
from <u>20</u>	28	(d.m.r.) ^b	47	53	0	0
	25	(p.m.r.)	66	31	0	0

a. The integration of this spectrum was of poor quality

b. The ratio of aldehydic deuterium to methylene deuterium changed upon the addition of CDCl_3 . The ratio quoted is that after addition of CDCl_3 and is considered to be unreliable for this sample.

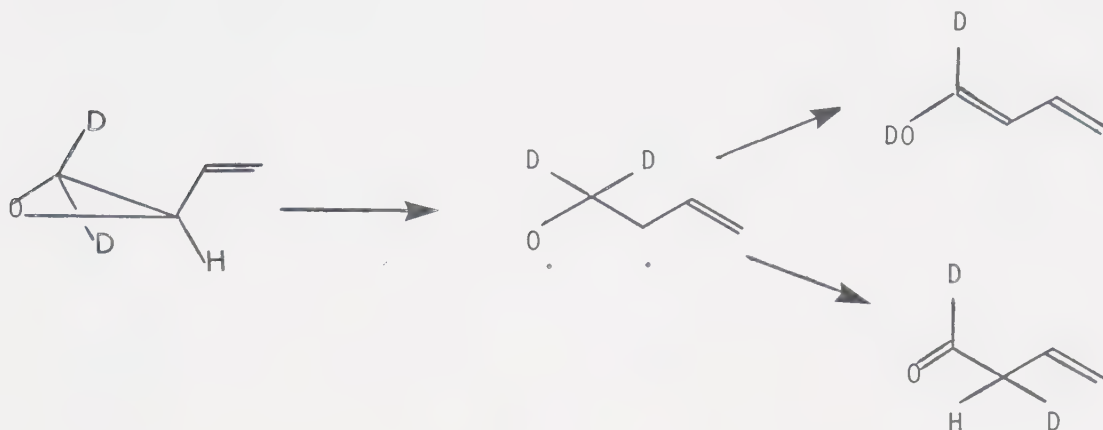
process was established by a control experiment. When 2-vinyloxirane was thermolyzed in the reaction vessel which had been pre-treated with D_2O , a small amount (1~2%) of deuterium was incorporated into the 2-butenals produced.

The similarity of the deuterium distribution in the 3-butenal produced from 13 and 20 indicates that there is no stereochemical preference for the mode of hydrogen migration, which suggests that the 3-butenal is produced from a random biradical intermediate rather than by a concerted process. It is likely that the observed deuterium distribution is not an exact reflection of that produced kinetically. If we consider the possibility of an intramolecular decomposition of 3-butenal to propene and carbon monoxide



then we might expect a difference in the relative rates of decomposition due to the presence of a deuterium isotope effect. Such a reaction may be expected to cause the butenals to be enriched with deuterium at the aldehydic position and depleted with respect to the methylenic deuterium, thus preventing us from placing a precise interpretation on the migration ratios. The location of

deuterium at only C1 and C2 has certain mechanistic implications. If we consider the possibility of a 1,2-hydrogen shift either to carbon or oxygen, then we would expect 3-butenal and/or the dienol to be produced as initial products.



The observed deuterium distribution could be accommodated by such a scheme, but we can rule out the reversible decomposition of an intermediate because otherwise we would have expected to observe some hydrogen incorporation into the aldehyde group of the 3-butenal produced from 21.

The deuterium distributions in the 2-butenals produced from the thermolyses of 21, 13 and 20 are summarized in Table IX. A quantitative determination of the deuterium distribution could not be obtained from the p.m.r. spectra due to overlapping signals for the (E) and (Z) isomers. The facility of the isomerization of (Z)-2-butenal to (E)-2-butenal is apparent from the observation that two samples originally containing both isomers had isomerized

TABLE IX

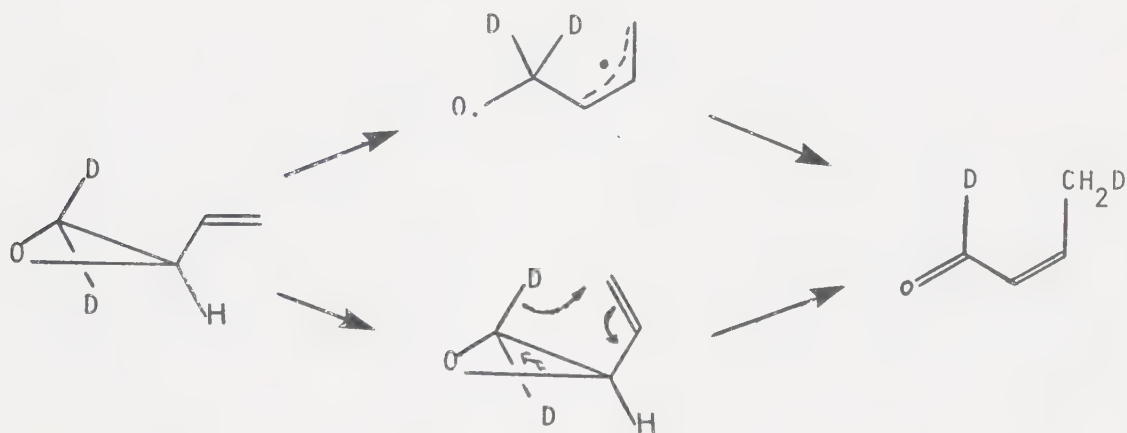
The deuterium distribution in the 2-butenals produced from
the thermolyses of $\underline{\underline{21}}$, $\underline{\underline{13}}$ and $\underline{\underline{20}}$ at 307.4°C, estimated
from the d.m.r. spectra

2-Butenals	Figure #	C1	C2	C3	C4
from $\underline{\underline{21}}$	17 (<u>E</u>)	52	27	0	21
	17 (<u>Z</u>)	51	26	0	23
from $\underline{\underline{13}}$	22 (<u>E</u>) ^a	83	10	0	7
from $\underline{\underline{20}}$	29 (<u>E</u>) ^a	68	18	0	14

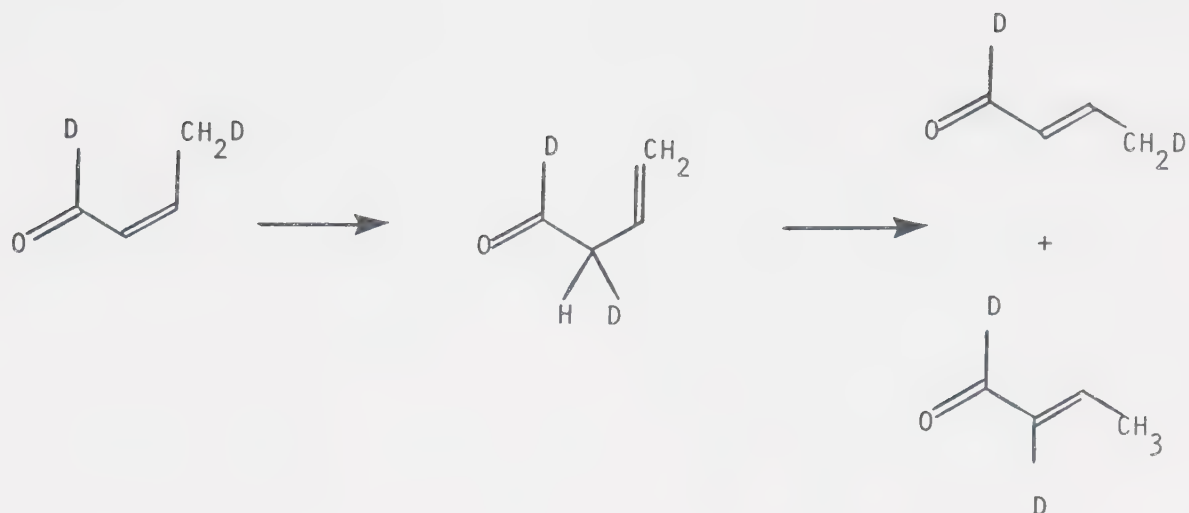
a. Signals for (Z)-2-butenal not detected.

to the more stable (E) isomer when the d.m.r. spectra were obtained. An inspection of the p.m.r. spectrum (Figure 15) of the 2-butenals produced from 21 indicates that only deuterium is present in the aldehyde group. The most notable feature of the d.m.r. spectra is that the deuterium is distributed between C1, C2 and C4 in the 2-butenals produced from each oxirane.

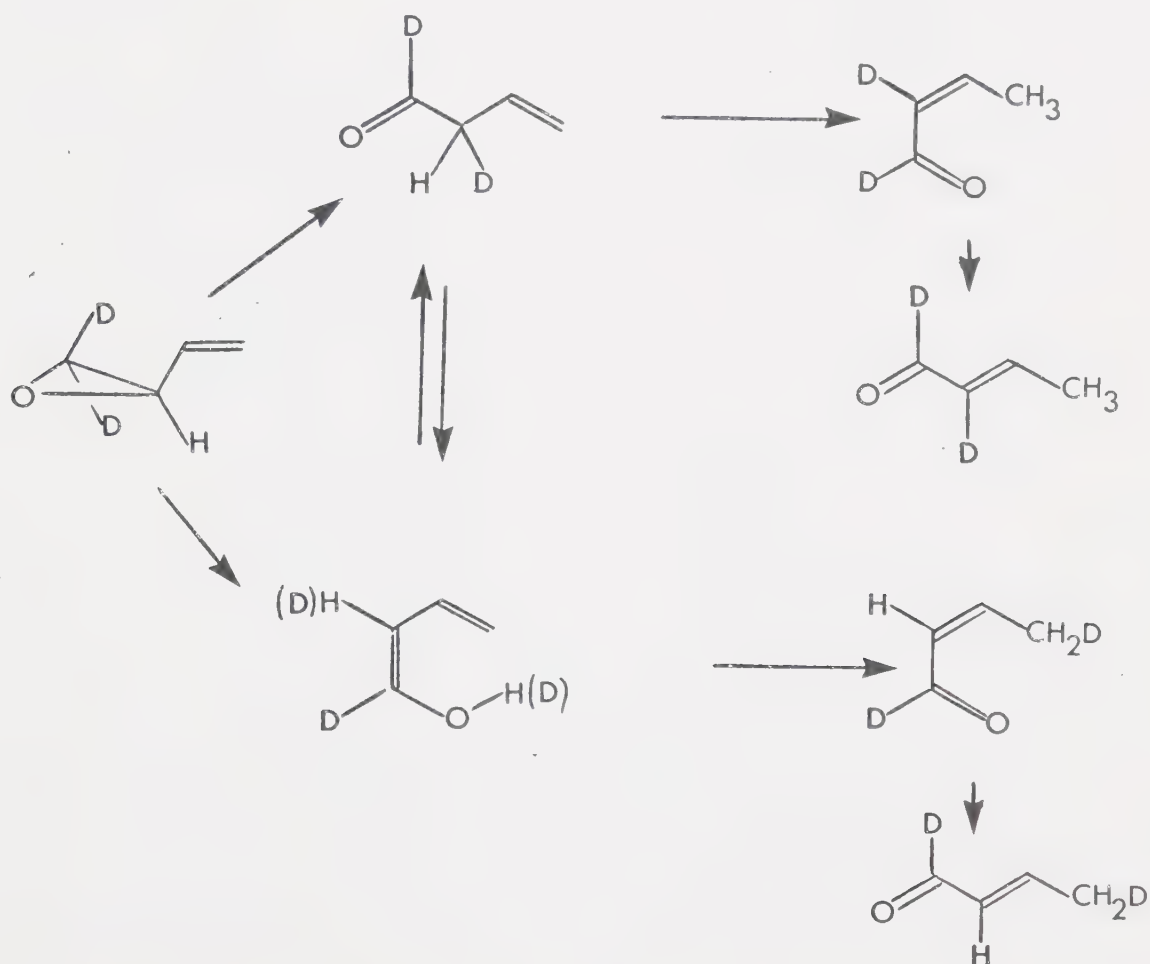
If we consider a 1,4-hydrogen shift as a possible direct route to the 2-butenals, then this would account for deuterium at C1 and C4 but would not predict deuterium at C2.



If we consider a mechanism whereby (Z) and (E)-2-butenal are interconverted via 3-butenal, then although this could result in a distribution to C2, it can be ruled out since it would require the presence of deuterium at C4 of the 3-butenal.



If, however, 3-butenal is an initial thermolysis product then we can consider a scheme whereby equilibration with the enol might provide a route to the 2-butenals.



In such an equilibration the distribution of deuterium between C1 and C2 of 3-butenal would be maintained. A thermally allowed 1,5 hydrogen shift ($\sigma^2_s + \pi^4_s$) in the enol could then produce (Z)-2-butenal with a deuterium distribution in accord with the experimental observations. The possibility of reversibility of the 1,5 shift can be ruled out since it would require the incorporation of deuterium at C4 of the 3-butenal.

This scheme implies that the thermodynamically favoured (E)-2-butenal arises via an equilibration with (Z)-2-butenal. It is known (36) that (Z)-2-butenal is thermally unstable and readily rearranges to the (E) isomer by a process that is accelerated by the presence of traces of acid. This scheme also implies that the 2-butenals are secondary reaction products and therefore might be expected to exhibit an induction period for their formation. If, however, the isomerization of 3-butenal was very fast then it would make the detection of such an induction period very difficult.

A preliminary study (38) of the thermal treatment of a mixture of isomeric butenals (containing mainly 3-butenal) at 260° showed a rapid loss of 3-butenal together with an increase in the proportions of the 2-butenals, along with the formation of carbon monoxide and propene. This observation lends support to a scheme

wherein the 2-butenals are produced from 2-vinyloxirane as a result of secondary processes.

Since the thermodynamically unstable 3-butenal is observed throughout the course of the reaction, in greater than its thermodynamic proportions, it cannot be the species which is rapidly isomerizing to the 2-butenals and thus the dienol tautomer is suspected as being one of the primary products.

B. Kinetic Studies

Over the temperature range 292-312°C the gas phase thermal decomposition of 2-vinyloxirane was observed to proceed by overall first-order kinetics. The formation of 2,3-dihydrofuran was observed to follow first-order kinetics, but due to the thermal interconversion of the butenals produced it was not possible to determine the kinetic parameters for their formation. The occurrence of a fast competitive racemization process was detected when chiral 2-vinyloxirane was subjected to gas phase thermolysis over the temperature range 255-275°C.

The Arrhenius activation parameters were determined for these processes and are presented in Table X.

The occurrence of a slow, competitive cis-trans isomerization process was observed during the thermolysis of cis and trans-3-deuterio-2-vinyloxirane. It is of

TABLE X

Arrhenius activation parameters for the thermolysis of
2-vinyloxirane

Reaction	E_a (kcal mole ⁻¹)	log A	Ref.
Overall decomposition	47.8 ± 0.3	14.1 ± 0.1	Table I
Dihydrofuran formation	50.6 ± 0.7	14.3 ± 0.3	Table VI
Racemization	44.2 ± 0.7	13.5 ± 1.6	Table II

TABLE XI

Rate constants and relative rates for the reactions of
2-vinyloxirane at 307.4°C

Reaction	$10^5 k(\text{sec}^{-1})$	Relative Rate
Overall decomposition	12.4	6.89
Dihydrofuran formation	1.88	1.04
Racemization (k^{α}_{obs})	72.4 ^a	40.2
<u>cis</u> \rightleftharpoons <u>trans</u> interconversion	1.80	1.0

a Extrapolated from lower temperature using the data from
 Table V.

TABLE XII

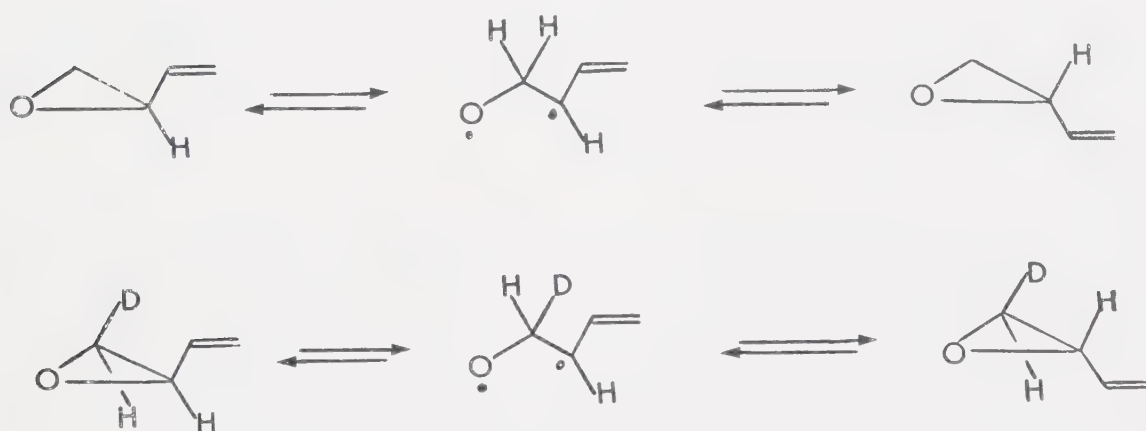
Deuterium isotope effects on the thermal reactions of
2-vinyloxirane

Reaction	$\delta\Delta G^\ddagger/n$ (cal.mole ⁻¹)	Ref.
Overall decomposition	140-220	Table IV
Dihydrofuran formation	165-200	Table VII
Racemization	≈0	Table V

interest to compare the relative magnitudes of the rate constants for the thermal reactions of the 2-vinyloxirane system, which are illustrated in Table XI. From an inspection of Table XI it is apparent that the most facile thermal process is a racemization. The cis-trans isomerization and dihydrofuran formation proceed at comparable rates and are both slow relative to the overall rate of decomposition.

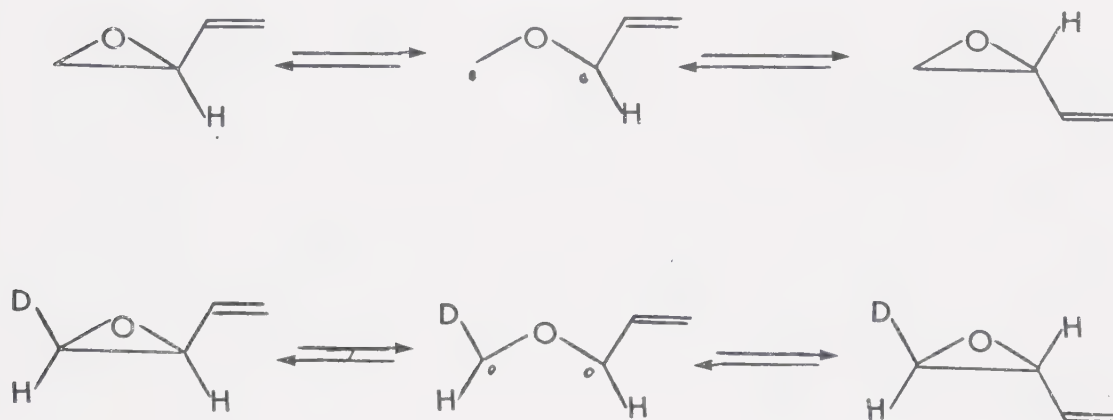
The kinetic isotope effects for the thermal reactions of 2-vinyloxirane in terms of the free energy change per deuterium $\delta\Delta G^\ddagger/n$ are given in Table XII.

If we consider an initial carbon-oxygen bond cleavage as a possible mechanism for the racemization, then a subsequent rotation and recyclization would result in an enantiomerization of 2-vinyloxirane.



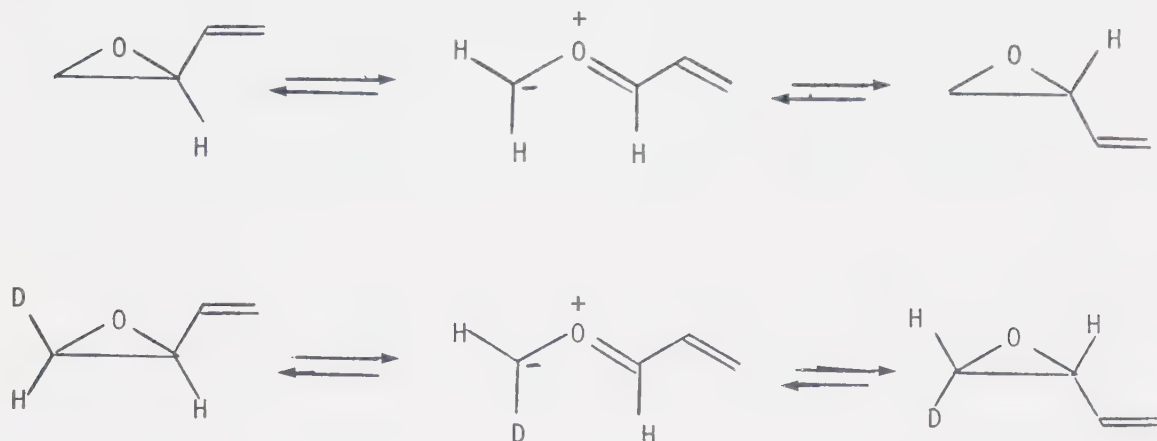
This sequence of operations when applied to 3-deuterio-2-vinyloxirane would result in cis-trans isomerization,

Since no kinetic isotope effect was detected for the racemization then this mechanism would predict that racemization and cis-trans isomerization would proceed at comparable rates. The forty-fold difference in the rates of these processes (Table XI) allows us to rule out this mechanism as a common route for the stereoisomerizations. By the same argument we can rule out a similar route wherein a single rotation and recyclization are preceded by an initial carbon-carbon bond cleavage.

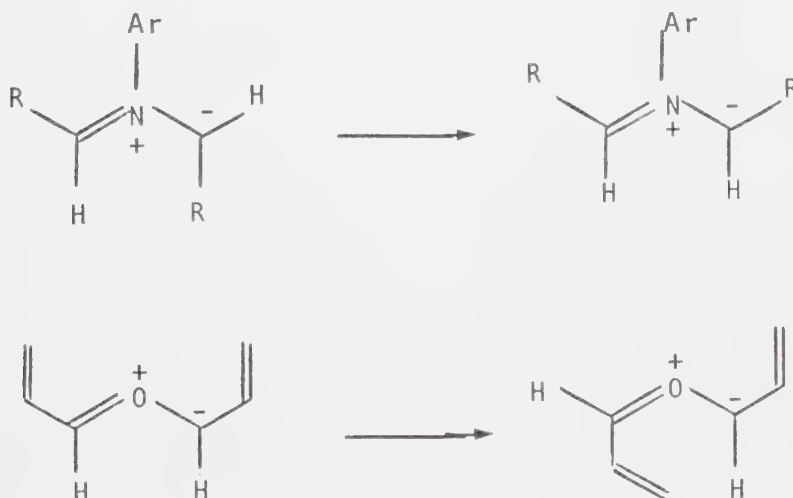


A synchronous conrotatory carbon-carbon bond cleavage to a planar carbonyl-ylide has been suggested (25) as the most probable mechanism to account for the facile gas-phase racemization of trans-2,3-divinyloxirane. If we consider this mechanism as a reasonable candidate for the racemization of 2-vinyloxirane it

would, however, preclude the possibility of cis-trans isomerization.



The question arises as to how this mechanism can be reconciled with the observed cis-trans isomerization. The observation of cis-trans isomerization in both aziridines (17) and divinylloxirane (25) has been rationalized in terms of an external rotation in a planar azomethine-



ylide or carbonyl-ylide, and such a process could equally well be operable in the 2-vinyloxirane system.

The possibility of a slow reversible carbon-oxygen bond cleavage occurring competitively with the reversible carbonyl-ylide formation, and being responsible for the slow rate of cis-trans isomerization, cannot readily be dismissed.

If we consider that the rate of formation of butenals is given by subtracting the rate of dihydrofuran formation from the overall rate of decomposition of the 2-vinyloxirane, then the rates of formation of butenals will be as in Table XIII.

The observed deuterium kinetic isotope effects on the formation of butenals from the deuterated vinyloxiranes are small when considered in terms of the traditional primary deuterium kinetic isotope effects wherein a C-H stretching mode is part of the reaction co-ordinate (39). It has been suggested (40) that a reduced value of the isotope effect would be expected for a reaction proceeding via a non-linear activated complex, such as that for hydrogen migration in a pinacol rearrangement. The free energy change for the 2-vinyloxirane-butenal interconversion is given in Table XIV along with those of other processes wherein an isotope effect has been observed for a reaction which is principally a hydrogen migration.

TABLE XIII

Calculated rates of formation of butenals in the 2-vinyl-
oxirane system^a

Oxirane	Butenal formation $10^5 k(\text{sec}^{-1})$	k_H/k_D
12 ~~	10.52	-----
13 ~~	9.02	1.17
21 ~~	8.26	1.27

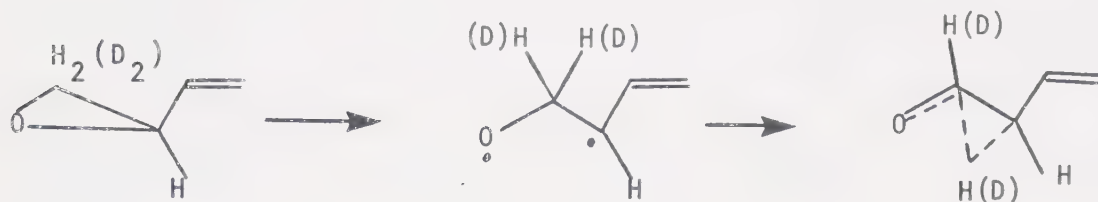
a. Calculated from the data of Tables III and VII

TABLE XIV

Isotope effects for reactions having non-linear activated complexes

Reaction	k_H/k_D	$T^\circ C$	$\delta\Delta G^\ddagger$ (cal mole ⁻¹)	Ref.
$Ph_2C-CH(D)Ph \longrightarrow Ph_2CH(D)-C(=O)Ph$	3.3	43.3	750	41
$(CH_3)_2C(OH)-CH(D)CH_3 \longrightarrow (CH_3)_2CH(D)COCH_3$	1.68	60	340	42
$(CH_3)_2CH-CH(D)CH_3 \longrightarrow (CH_3)_2C(OC(=O)CH_3)-CH_2CH_3$	2.1	25	440	43
	1.27	307	278	this work

In an attempt to predict the magnitude of the kinetic isotope effect for the formation of butenals let us consider a scheme wherein the carbon-oxygen bond of the oxirane is cleaved to give a biradical intermediate which then undergoes a hydrogen migration, in the product determining step, involving mainly a C-H twisting mode as the reaction coordinate (44).



In order to calculate the secondary deuterium isotope effect on the ring opening we have chosen the methylene group of oxirane (C_2H_4O) as a model for 2-vinyloxirane and the methylene group of hexamethylene tetramine ($C_6H_{12}N_4$) as a model for the methylene group of the biradical. The infra-red vibrational frequencies of these two compounds have recently been assigned (45,46), together with the frequencies of C_2D_4O (47) and $C_6D_{12}N_4$ (46). The pertinent frequencies are given in Table XV.

It has been suggested (48) that secondary deuterium isotope effects are the result of the creation of new, isotopically sensitive vibrational frequencies during the course of a reaction. If we now make a summation over the vibrational levels of our four models, the sum $\delta\Delta\omega$ is given by (49):

TABLE XV

Infrared frequencies used to calculate the secondary
deuterium kinetic isotope effect for oxirane ring opening
via carbon-oxygen cleavage

Mode	C_2H_4O	C_2D_4O	$C_6H_{12}N_4$	$C_6D_{12}N_4$
CH stretch (A)	3079	2317	2955	2288
CH stretch (S)	3019	2174	2880	2110
CH ₂ Def.	1490	1013	1455	1120
F ₂ Wag	1120	970	1370	1075
E Twist	1143	896	1325	1000
F ₂ Rock	821	577	850	670
	<u>Σ10672</u>	<u>7947</u>	<u>10835</u>	<u>8203</u>

$$\delta\Delta\omega = \left[\sum \omega(\text{C}_2\text{H}_4\text{O}) - \sum \omega(\text{C}_2\text{D}_4\text{O}) \right] - \left[\sum \omega(\text{C}_6\text{H}_{12}\text{N}_4) - \sum \omega(\text{C}_6\text{D}_{12}\text{N}_4) \right]$$

and using the data of Table XV we obtain $\delta\Delta\omega = 93 \text{ cm}^{-1}$.

Since $E_0 = hc\omega/2$ then this is an energy difference ($\delta\Delta G^\ddagger$) of $133 \text{ cal. mole}^{-1}$ which gives a calculated value of $k_{\text{H}}/k_{\text{D}} = 1.12$ for the ring opening at 307° .

In order to calculate the isotope effect for the hydrogen migration in the rate determining step we neglect one twisting mode in the transition state and thus obtain $\delta\Delta\omega = 325 \text{ cm}^{-1}$. This would give a free-energy difference ($\Delta\delta G^\ddagger$) of $465 \text{ cal. mole}^{-1}$ which would then result in a value of $k_{\text{H}}/k_{\text{D}} = 1.50$ for butenal formation at 307° .

The mechanism for butenal formation must fit the observed constraints that:

- (a) cis-trans isomerization of the deuterated oxiranes is slower than butenal formation,
- (b) a kinetic deuterium isotope effect is observed on the formation of butenals,
- (c) that both cis and trans-3-deuterio-2-vinyloxirane give rise to comparable deuterium labelling patterns in the butenal products such as to imply the stereochemical equivalence of the methylene hydrogens (deuteriums) along the reaction coordinate.

The data can be accommodated by a reaction scheme such that a C-O biradical is a post-transition state intermediate on the reaction coordinate as depicted in Figure 39.

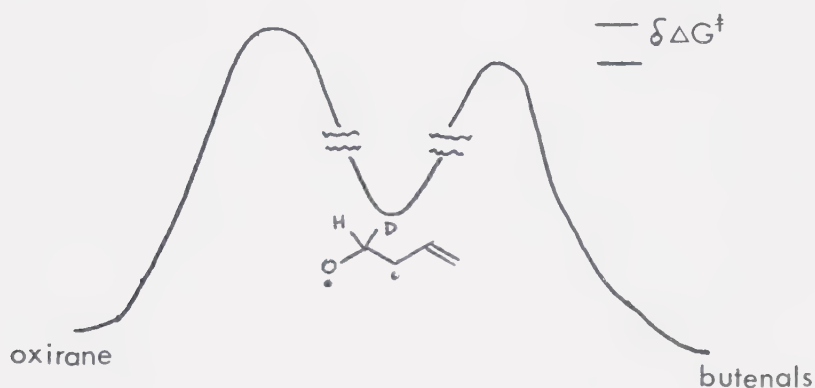


FIGURE 39. Reaction coordinate wherein the biradical is a post-transition state intermediate.

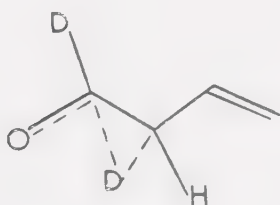
It can be shown that a deuterium isotope effect in the second step of the reaction would be observed in the overall kinetics. If we consider the data for the thermolysis of cis-3-deuterio-2-vinyloxirane (13) then we can obtain an estimate of the difference in height of the free-energy barriers ($\delta\Delta G^\ddagger$, Figure 39) for the forward and reverse processes. Combining the value for the rate of cis-trans isomerization ($k = 1.80 \times 10^{-5} \text{ sec}^{-1}$, Table XI) with the value for the rate of butenal formation ($K = 9.02 \times 10^{-5} \text{ sec}^{-1}$, Table XIII) allows us to calculate that the reverse process has a free-energy barrier

some $1.06 \text{ kcal.mole}^{-1}$ higher than that for butenal formation.

$$\delta\Delta G^\ddagger = Rt \ln (9.02/2 \times 1.8) = 1.06 \text{ kcal.mole}^{-1}$$

The factor of 2 is included since the molecules returning to the oxirane would have an equal chance of becoming cis or trans.

This implies that for 1000 molecules arriving at the biradical intermediate, per unit of time, 716 would go on to products and 284 would return to the oxirane. Upon going to 2-vinyloxirane-3,3-d₂ (21) we might expect little or no perturbation of the first energy barrier, but a deuterium migration in the second step should increase the height of the energy barrier in a transition state approximated by



If we consider the difference in the rates of butenal formation for 13 and 21 to be a manifestation of a kinetic isotope effect on the second step of the reaction, $[k(21)/k(13) = 1.09]$, then of our 1000 molecules at the

intermediate stage 656 will go on to butenals (716/1.09) and 344 will return to oxirane.

If we now consider the non-deuterated case (12) we would require that 836 molecules would go forward (716 x 1.17) and 164 would go back. This data are summarized in Table XVI.

The small change in the molecules per unit time arriving at the intermediate, from a consideration of an isotope effect on the ring opening, would cause a minimal perturbation of the model. Since the overall rate of decomposition of the oxirane is influenced by the partitioning of the intermediate between the forward and reverse reactions, it can thus be seen that the small difference in the free-energy barriers for these two processes would allow an isotope effect on the second step to be observed kinetically.

The data presented is best interpreted in terms of a carbon-oxygen biradical intermediate, but the cis-trans isomerization of the 3-deuterio-2-vinyloxiranes could equally well be occurring from a carbonyl-ylide intermediate that is not upon the reaction coordinate to butenal formation. If such is the case then the rate-determining transition state would be the same as suggested in our reaction model, but it is difficult to understand why cis-trans isomerization is not faster than

TABLE XVI

The partitioning of the biradical intermediate A (including) and B (neglecting) a secondary deuterium isotope on the ring opening

Oxirane	Intermediate		Product
	A	B	
21 ~~	946	1000	656
13 ~~	1000	1000	716
12 ~~	1060	1000	838

observed. For these reasons we prefer the biradical intermediate mechanism of the preceding paragraph.

E X P E R I M E N T A L

All boiling points are uncorrected.

Purifications by preparative gas chromatography (GC) were carried out on a Nester Faust Model 850 "Prep-kromatic". The columns used were 6 ft biwall tubing packed with 20% β,β' -oxydipropionitrile (ODPN) or 20% Carbowax 1500 on Chromosorb S 30-60 mesh. The carrier gas was helium at a flow rate of 500 ml min⁻¹. The purity of materials was checked using a Varian Model 1200 Gas Chromatograph with 6 ft columns of 1/8" i.d. packed with 10% ODPN or 10% Carbowax 1500 on high performance Chromosorb WAW/DMCS 80-100 mesh.

The nuclear magnetic resonance (n.m.r.) spectra were obtained using a Varian A60 or HA100 spectrometer. The proton decoupled deuterium magnetic resonance spectra were obtained using a Bruker HFX 100 spectrometer.

GC/Mass Spectrum analysis was performed on a Varian 1200 gas chromatograph coupled to an A.E.I. MS 9.

The optical rotations were determined on a Perkin Elmer Model 241 polarimeter.

Microanalyses were performed by the Microanalytical Laboratory of the Department of Chemistry, University of Alberta.

A. Air Bath System

Quantitative rate experiments were conducted in the static Pyrex vacuum system constructed as shown in the schematic diagram in Figure 40. The system was equipped throughout with Hoke stainless steel diaphragm and bellows valves. The reaction vessel was a Pyrex flask (1000 ml) situated in a well-insulated air bath with a fast air circulation provided by a high-speed fan located at the bottom of the bath. Main heaters controlled by a Variac were used to bring the temperature to about 20° below the desired temperature, and secondary heaters controlled by a Melabs Model CTC1A proportional temperature controller were used to maintain the desired oven temperature. The temperature was measured by a five-junction iron/constantan thermocouple which had been calibrated against a Hewlett-Packard (HP) Model 2801A quartz thermometer. The temperature stability of the system was monitored by coupling the output of the HP Model 3420B digital voltmeter to a HP Model 7100BM strip chart recorder. The longterm stability was better than $\pm 0.1^\circ$ and was typically $\pm 0.06^\circ$.

The Hoke Model 4213Q6Y high temperature valves (V1,V2) attached to the reaction vessel were located inside the oven to eliminate any dead-space effects during the sampling procedure. The vacuum manifold

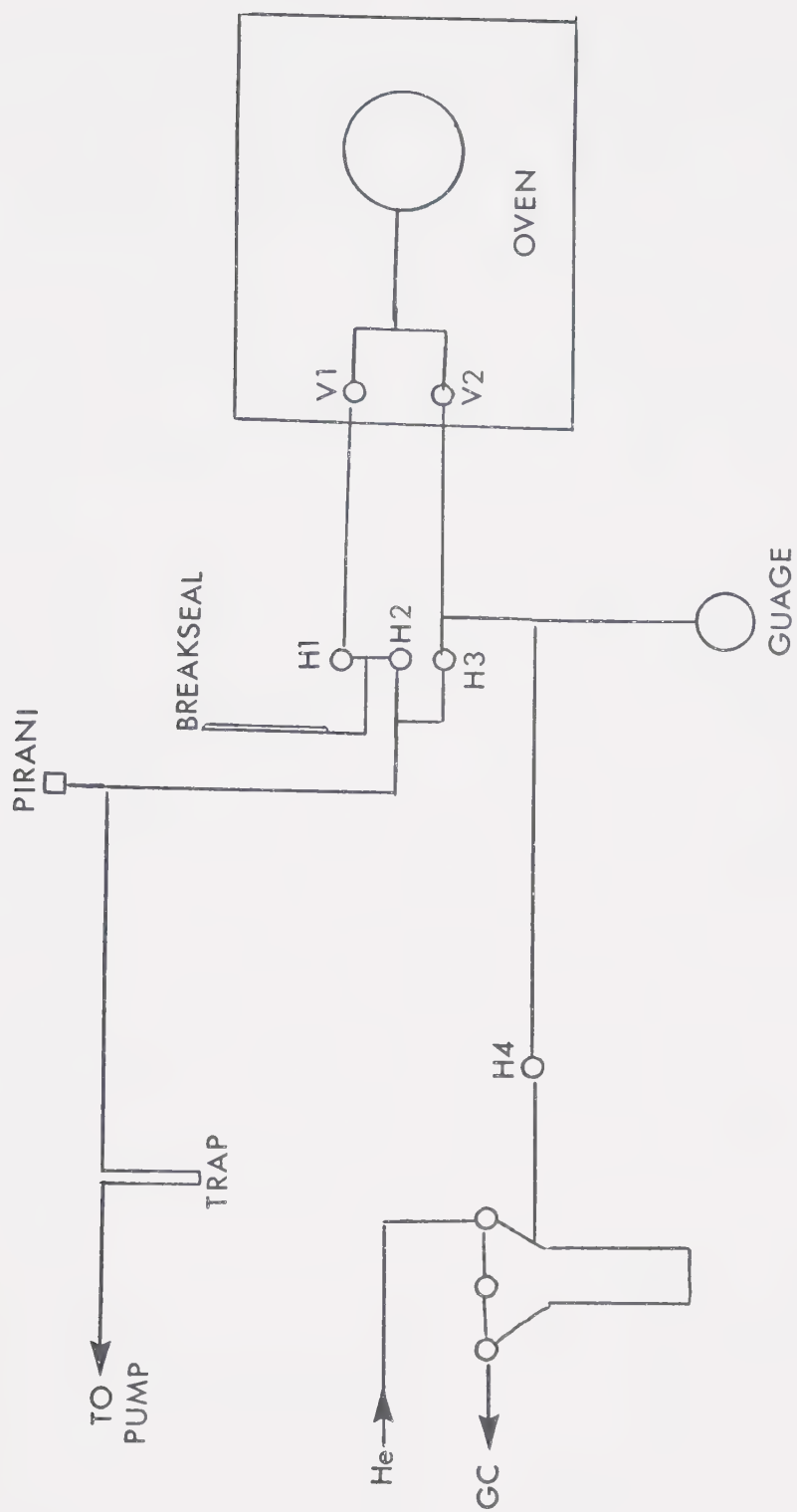


FIGURE 40. Schematic diagram of the apparatus used for the thermolyses.

valves (H1, H2, H3, H4) were Hoke Model 4251N6Y stainless-steel bellows valves. The valves utilized for the GC sample injection system were quick-action Hoke Model C415K knife-edge stainless-steel bellows valves. Heating tape was applied to the oven inlet system from H3 to V1 and maintained at 100°. Heating tape was applied to the oven outlet system and GC injector system and maintained at 75°.

Sample analysis was performed on a 6 ft column (1/8" i.d.) of 10% ODPN on high-performance 80-100 mesh Chromosorb WAS/DMCS with a helium gas flow rate of 25 ml min⁻¹ coupled to a Gowmac Model TR11B thermal conductivity detector. GC integration was performed with a HP Model 3370A electronic integrator.

All samples for the kinetic runs were prepared from materials dried by distillation from calcium hydride, and were degassed and transferred to break-seals by standard procedures.

B. Oil Bath System

The k_H/k_D study of the racemization of 2-vinyl-oxirane was conducted in breakseals of approximately 75 ml volume placed in a well insulated oil bath. The temperature was controlled by a Melabs Model CTC1A proportional temperature controller, and measured by an HP Model 2801A quartz thermometer calibrated by the National Bureau of Standards. The temperature stability of the oil bath was monitored by recording the analogue output of an HP Model 2802A platinum resistance thermometer with an HP Model 3420B digital voltmeter coupled to a strip chart recorder. The long term stability of the system was better than $\pm 0.1^\circ$.

(C) Preparations

2-Vinyloxirane (12).

The procedure was essentially that of Bottini (50). N-Bromosuccinimide (178 g, 1 mol) was added over 2 h to a well-stirred mixture of butadiene (108 g, 2 mol), distilled water (500 ml), glacial acetic acid (5 ml) and ether (500 ml). The reaction mixture was stirred overnight and the excess butadiene was allowed to evaporate. The ether layer was separated and the aqueous layer extracted with additional ether (2 x 300 ml). The combined ether extracts were washed with saturated sodium chloride solution and the ether evaporated to give 129 g (85%) of crude 1-bromo-3-buten-2-ol. This crude product was added dropwise to a hot solution of potassium hydroxide (290 g) in water (430 ml), and the 2-vinyloxirane distilled as an azeotrope bp 63-65°. The water was separated and the product dried over sodium sulfate and distilled to give 34 g (59%) bp 63-64/705 torr (lit. (50) 65-65.8/739 torr). The 2-vinyloxirane was further purified by preparative GC on ODPN at 40°. The n.m.r. spectrum δ TMS (CDCl_3) : 2.63 (quartet, 1H), 2.95 (quartet, 1H), 3.35 (multiplet, 1H) and 5.2-5.8 (multiplet, 3H).

3-Butyn-1-ol (14).

The procedure was essentially that of Schulte and Reiss (26). A suspension of sodium amide in liquid

ammonia was prepared by adding, over a period of 1 h, freshly cut sodium metal (46 g, 2.0 g. atom) to liquid ammonia (1250 ml) containing a crystal of ferric nitrate. Acetylene (purified by passage through concentrated sulfuric acid then potassium hydroxide pellets) was then bubbled into the stirred suspension. After 5 h a black suspension of sodium acetylide saturated with acetylene was produced. Ethylene oxide (128 g, 2.9 mol) was distilled into the reaction mixture over a period of 1.5 h. The passage of acetylene was continued to maintain saturation. The reaction mixture was stirred overnight during the evaporation of the ammonia. Next day solid ammonium chloride (120 g) was added followed by methylene chloride (1000 ml). Water (200 ml) was then added and the reaction mixture was stirred to produce two clear layers. The methylene chloride layer was separated, the aqueous layer saturated with more ammonium chloride and extracted with methylene chloride (3 x 300 ml). The combined extracts were dried over potassium carbonate, and the solvent removed by distillation through a Vigreux column. The residual liquid was fractionated at atmospheric pressure to give 77 g (55%) bp 121-125° (Lit. 127-129°/760 torr). The n.m.r. spectrum δ TMS (CDCl_3) showed: 2.05 (triplet, 1H), 2.42 (multiplet, 2H), 3.72 (triplet, 2H) and 3.00 (singlet, 1H).

4-Chloro-1-butyne (15).

The procedure was essentially that of Roberts (27). Thionyl chloride (130 g, 1.09 mol) was added dropwise to a mixture of 3-butyne-1-ol (67 g, 0.96 mol) and pyridine (2.5 ml) at a rate such that the exothermic reaction mixture was maintained below 10°. When about 20 ml of thionyl chloride had been added a brisk evolution of hydrogen chloride commenced and the reaction temperature began to fall. During the remainder of the addition the cooling bath was periodically removed so that the reaction temperature was maintained at 3-5°. After stirring for 1 h the reaction mixture was gradually heated to reflux and refluxed 0.5 h. The mixture was added to ice-cold water (500 ml) and potassium carbonate added to neutralize the hydrogen chloride. The upper oily layer was separated, washed twice with saturated sodium chloride solution and dried over 4 Å molecular sieves. Distillation at atmospheric pressure gave 67 g (79%) bp 83-84° (lit 86-87°/762 torr). The n.m.r. spectrum δ TMS (CDCl_3) showed: 2.00 (triplet, 1H), 2.61 (multiplet, 2H) and 3.57 (triplet, 2H).

4-Chloro-1-butyne-1-d (16).

4-Chloro-1-butyne (60 g) was dissolved in methylene chloride (200 ml), and repeated exchanges with deuterium oxide (50 ml) and barium oxide (50 mg) effected by vigorous magnetic stirring for 24 h. Deuterium incorporation

was monitored by n.m.r. integration of an aliquot from the methylene chloride layer. After five exchanges the alkyne proton was no longer observable in the n.m.r. spectrum. The methylene chloride layer was dried over 4 Å molecular sieves and the solvent removed by spinning-band distillation. Distillation of the residual liquid gave 52.7 g (87.8%). The n.m.r. spectrum δ TMS (CDCl_3) showed: 2.67 (triplet, 2H), 3.62 (triplet, 2H) and the absence of the alkyne proton resonance.

(Z)-4-Chloro-1-butene-1-d (17)

The procedure was an adaption of that of Brown (28). Diglyme and boron trifluoride etherate were freshly purified before use. A mixture of diglyme (150 ml), sodium borohydride (6.8 g, 0.18 mol) and 2-methyl-2-butene (33.6 g, 0.48 mol) was stirred and cooled below 5° in an ice/salt bath. Boron trifluoride etherate (34.1 g, 0.24 mol) was added over a period of 2 h at a rate such that the reaction temperature was maintained below 10°. The reaction mixture initially became homogeneous, and then a thick white precipitate of the organoborane was produced. After stirring for an additional 3.5 h the mixture was cooled to 0°. A solution of 4-chloro-1-butyne-1-d (17.7 g, 0.2 mol) in diglyme (20 ml) was added as rapidly as possible while controlling the reaction temperature below 5°. The

reaction mixture was stirred overnight and allowed to warm to room temperature. Next day, glacial acetic acid (100 ml) was added at a rate such that the reaction mixture was maintained below 5°. After stirring an additional 5 h at room temperature the mixture was added to ice-cold water (1500 ml) and extracted with methylene chloride (4 x 200 ml). The combined extracts were washed with cold sodium hydroxide solution then with saturated sodium chloride solution until neutral and dried over calcium sulfate. The methylene chloride was removed by spinning-band distillation and the residual liquid fractionated to give 6.7 g (36.6%) bp 69-70°/700 torr. The n.m.r. spectrum δ TMS (CDCl_3) showed: 2.5 (quartet, 2H), 3.56 (triplet, 2H), 6.0 (multiplet, 1H) and 5.05 (doublet, 1H).

cis-2- β -Chloroethyl-3-deuterio-oxirane (18).

(Z)-4-Chloro-1-butene-1-d (6.3 g, 0.069 mol) was dissolved in methylene chloride (180 ml) and meta-chloroperbenzoic acid (22 g, 0.127 mol) was added in portions over a period of 0.5 h at room temperature. After stirring overnight the mixture was filtered to remove the precipitated meta-chlorobenzoic acid and then distilled at room temperature under reduced pressure. The distillate was fractionated through a Vigreux column to remove the bulk of the methylene chloride and the res-

idual liquid fractionated to give 6.14 g (89.5%) bp 56-58°/28 torr. The n.m.r. spectrum δ TMS (CDCl_3) showed: 1.82 (quartet, 2H), 2.58 (doublet, 1H), 2.88 (quartet, 1H) and 3.57 (triplet, 2H).

cis-3-Deuterio-2-vinyloxirane (13).

The procedure was essentially that of Reppe (29). A mixture of cis-2- β -chloroethyl-3-deuterio-oxirane (2.13 g, 0.02 mol) and finely powdered potassium hydroxide (5.6 g, 0.1 mol) was gradually heated to 100° and the distillate collected in a cooled receiver, 1.49 g (100%). Final purification was accomplished by preparative gas chromatography (G.C.) on 20% β,β' -oxydipropionitrile (ODPN) on Chromosorb W at 40°. The n.m.r. spectrum δ TMS (CDCl_3) showed: 2.81 (doublet, 1H), 3.20 (quartet, 1H) and the vinyl group resonance as a multiplet 5.05-5.7 (3H).

1,2,5,6-Diisopropylidene-D-mannitol (26).

The procedure was essentially that of Tipson (31). Freshly fused anhydrous zinc chloride (141 g, 1.05 mol) was stirred with dry acetone (704 ml) until dissolved and the solution filtered. D-Mannitol (72.8 g, 0.42 mol, Fisher Chem. Co.) was added and the white suspension stirred vigorously at 20-25° for 0.5 h, then warmed to 45°. After 1 h the solution was virtually complete and it was then allowed to cool to 25-30°. The solution

was poured slowly into a vigorously stirred cold solution of potassium carbonate (176 g, 1.27 mol) in water (176 ml). The mixture was filtered and the precipitate extracted with chloroform (2 x 500 ml). The chloroform extracts were added to the filtrate, the mixture shaken vigorously and the chloroform layer separated. The aqueous layer was extracted with a further portion of chloroform (500 ml). The combined chloroform extracts were washed with saturated sodium chloride solution (200 ml), dried over sodium sulfate and evaporated under vacuum to give a white solid (84 g). This impure product was recrystallized from a mixture of chloroform (120 ml) and n-pentane (1500 ml) to give 55 g (52.5%), mp 121-123° (Lit. 120-121°).

Isopropylidene-D-glyceraldehyde (27).

The procedure was essentially that of Baer (32). Lead tetra-acetate (Arapaho Chemical Co.) was recrystallized from a mixture of glacial acetic acid and acetic anhydride, and dried overnight in a vacuum dessicator protected from light over potassium hydroxide pellets. It was assayed by the procedure of Fieser (51) and the activity found to be 89.6%. A suspension of di-isopropylidene D-mannitol (31.2 g, 0.119 mol) in anhydrous benzene (1000 ml) was stirred vigorously at room temperature and lead tetra-acetate (58.9 g, 0.119 mol at

89.6%) was added in small portions over a period of 0.5 h. After a further 0.5 h, a starch iodide test showed the presence of excess oxidant. A further portion of di-isopropylidene D-mannitol (1 g) was added, and after 5 min a starch iodide test showed complete consumption of the lead tetra-acetate. The reaction mixture was filtered and the precipitate washed with additional benzene (200 ml). The filtrate was distilled through a Vigreux column at 75-80°/700 torr from an oil bath maintained at 105-110°. The residual viscous oil was distilled under reduced pressure to give 18.3 g (59%) bp 30-40°/1-2 torr. The product was stored under nitrogen at 0°.

Methylene triphenylphosphorane

The procedure was essentially that of Schlosser (33). A suspension of sodium amide in liquid ammonia was prepared from freshly cut sodium metal (8.0 g, 0.348 mol) and liquid ammonia (1000 ml). Methyltriphenylphosphonium bromide (96 g, 0.26 mol) was added and the reaction mixture stirred overnight during the evaporation of the ammonia. Anhydrous benzene (1000 ml) was added and the reaction mixture stirred and refluxed for 1 h to dissolve the ylid. The mixture was cooled, and filtered under nitrogen through a 25-50 μ sinter to remove the precipitated salts. The clear, yellow solution of the ylide thus prepared was used directly for the next step.

(+)-(S)-Isopropylidene-3-buten-1,2-diol (28).

The freshly prepared ylide solution was stirred under a nitrogen atmosphere and cooled in an ice bath. A solution of isopropylidene D-glyceraldehyde (18.3 g, 0.14 mol) in benzene (50 ml) was added dropwise over 1 h, and the reaction temperature held below 10° by external cooling. After a further 1 h the excess ylid was destroyed by the addition of a solution of acetone in benzene until the reaction mixture was essentially colourless. The reaction mixture was filtered and the benzene removed by distillation through a Vigreux column. The residual oil was diluted with hexane (1000 ml), stirred vigorously, and then filtered to remove the precipitated triphenylphosphine oxide. The filtrate was washed with water and dried over 4 Å molecular sieves. The solution was distilled through a Vigreux column to remove benzene and hexane and the residue distilled under reduced pressure to give 10.5 g (59.5%) bp 50-52°/50 torr. An analytical sample was purified by preparative GC on ODPN.

Anal. calcd. for $C_7H_{12}O_2$: C, 65.57%; H, 9.44%.

Found: C, 65.39%; H, 9.67%.

$[\alpha]_{589}^{24} + 30.96$; $[\alpha]_{365}^{24} + 105.7$; (9.8 g/100 ml, 2-propanol).

The n.m.r. spectrum δ TMS ($CDCl_3$) showed: 1.57 (singlet, 3H), 1.60 (singlet, 2H), 3.58 (triplet, 1H), 4.1 (quartet, 1H), 4.5 (quartet, 1H), 5.1 - 6.2 (multiplet, 3H).

(-)-(S)-3-Buten-1,2-diol (29)

The procedure was essentially that of Meric and Vigneron (52). Dilute hydrochloric acid (3N, 25 ml) was added to a solution of isopropylidene-3-buten-1,2-diol (10.0 g) in 98% ethanol (115 ml), and the mixture refluxed for 1 h. It was then cooled and the excess acid neutralized by careful addition of solid sodium bicarbonate. The mixture was filtered and the precipitate washed with fresh ethanol (200 ml). The filtrate was evaporated under reduced pressure to give a viscous oil together with some inorganic salts. This product was dissolved in methanol (50 ml), and ether (250 ml) gradually added with vigorous stirring. The mixture was filtered to remove the precipitated inorganic salts and the filtrate was evaporated to give a clear, pale yellow oil. Residual water was removed by azeotropic distillation with benzene. The combined yield of diol from four of the above runs was 21 g. Distillation under reduced pressure gave 20.4 g, bp 58-60°/2 torr.

$[\alpha]_{589}^{22} = 43.6$; $[\alpha]_{365}^{22} = 152.8$; (4.62 g/100 ml, 2-propanol).

To check for any racemization during the cleavage of the isopropylidene group, a sample of the diol was converted back to the isopropylidene derivative by treatment with 2,2-dimethoxypropane in the presence of a catalytic quantity of *p*-toluenesulfonic acid. The product was purified by preparative GC on ODPN and the rotation

measured:

$[\alpha]_{589}^{22} + 29.65$; $[\alpha]_{365}^{22} + 100.80$; (6.32 g/100 ml, 2-propanol):

It was thus concluded that less than 5% racemization had occurred during the cleavage of the isopropylidene group.

(+)-(S)-2-Vinyloxirane (30).

A solution of (S)-3-buten-1,2-diol (2.20 g, 0.025 mol, $[\alpha]_{589}^{22} - 43.6$) in dry pyridine (25 ml) was stirred and cooled below 5°. Freshly recrystallized *p*-toluenesulfonyl chloride (5.25 g, 0.028 mol) was added over 10 min and the mixture stirred 18 h at 5°. The reaction mixture was poured into ice-cold water (125 ml) and extracted with several portions of ether. The combined ether extracts were washed with ice-cold hydrochloric acid (3N) until the washes remained acidic. The ether extracts were then washed with saturated sodium bicarbonate solution, followed by a saturated sodium chloride solution and dried over anhydrous sodium sulfate. Evaporation of the ether at room temperature gave a colourless oil 5.72 g (96%), which rapidly crystallized. To the monotosylate thus prepared was added finely powdered potassium hydroxide (8 g), and the mixture gradually warmed in an oil bath to 100-110°. The distillate was collected in a cooled receiver. From several runs, the yield averaged 1-1.5 g of 2-vinyloxir-

ane containing a small amount of ether and water. The 2-vinyloxirane was further purified by preparative GC on ODPN at 40°.

$[\alpha]_{589}^{25} + 8.306$; $[\alpha]_{365}^{25} + 45.883$; (6.959 g/100 ml, 2-propanol).

1-Acetoxy-1-cyano-2-propene (22).

The procedure was essentially that of Chedron (30). Acetic anhydride (79 g, 0.77 mol) was added dropwise over 20 min to a solution of freshly distilled acrolein (43.3 g, 0.77 mol) in benzene (150 ml) at -10°. A solution of sodium cyanide (55 g, 1.12 mol) in water (280 ml) was added to the reaction mixture over 1.5 h at -5° to -10°. Efficient cooling was necessary to control the temperature of this exothermic reaction. The reaction mixture was stirred a further 1 h and then allowed to warm to 5° resulting in two clear layers being produced. The benzene layer was separated and the aqueous layer extracted with additional benzene (2 x 100 ml). The combined benzene extracts were washed with dilute acetic acid (2 x 100 ml), saturated sodium bicarbonate (3 x 100 ml), water (2 x 50 ml) and dried over sodium sulfate. The benzene was evaporated and the residual oil distilled under reduced pressure to give 80 g (83%) bp 58-60°/6-7 torr (lit. 63-65/10 torr).

Methyl 2-hydroxy-3-butenate (23)

A solution of 1-acetoxy-1-cyano-2-propene (100 g, 0.80 mol) in anhydrous methanol (100 ml) was heated to reflux, and a mixture of methanol saturated with dry hydrogen chloride (86 ml) and concentrated hydrochloric acid (22 ml) was added dropwise. The rate of addition was such that the reaction mixture was maintained at reflux. The mixture was refluxed an additional 2.5 h and then filtered to remove the precipitated ammonium chloride. The filtrate was evaporated to give a residual oil together with ammonium chloride. This was diluted with ether (500 ml) and added to a vigorously stirred saturated solution of sodium bicarbonate. The ether layer was separated, washed with water (2 x 100 ml) and dried over sodium sulfate. The ether was evaporated and the residual oil distilled under reduced pressure to give 52.4 g (56%) bp 58-60°/12 torr (lit. 60°/13 torr).

3-Buten-1,2-diol-1,1-d₂ (24)

Lithium aluminum deuteride (5.0 g, 0.12 mol, Ventron 98.5%) was added to freshly dried ether (350 ml) under a nitrogen atmosphere, and the mixture cooled in ice. A solution of methyl 2-hydroxy-3-butenate (17.5 g, 0.15 mol) in dry ether (50 ml) was added dropwise over 1 h, and the reaction mixture stirred an

additional 40 h at room temperature. Ether (100 ml, saturated with water) was then added dropwise, followed by a saturated solution of sodium potassium tartrate in water. The ether layer was separated and the aqueous layer subjected to continuous extraction with ether for 3 days. The combined ether extracts were evaporated and the residual oil azeotroped with benzene to remove any residual water. The residual oil was then distilled under reduced pressure to give 9.9 g (73%) bp 65-68°/2 torr.

2-Vinyloxirane-3,3-d₂ (21)

The procedure was that previously described for the conversion of (-)-(S)-3-buten-1,2-diol to (+)-(S)-2-vinyloxirane. The n.m.r. spectrum δ TMS (CDCl₃): 3.35 (triplet, 1H),; 5.2 - 5.8 (multiplet, 3H). The deuterium incorporation was estimated to be 98.5%.

(E)-4-Chloro-1-butene-1-d (19)

The procedure was essentially that previously described for the conversion of 4-chloro-1-butyne-1-d to (Z)-4-chloro-1-butene-1-d. 4-Chloro-1-butyne was treated with disiamylborane followed by protonolysis with deuterioacetic acid. The deuterioacetic acid was prepared by treatment of acetic anhydride with deuterium oxide

according to the procedure of Roberts (27). The product was purified by spinning-band distillation to give a 47.5% yield of (E)-4-chloro-1-butene-1-d. The n.m.r. spectrum δ TMS (CDCl_3) showed: 2.5 (quartet, 2H), 3.56 (triplet, 2H), 5.5 - 6.2 (multiplet, 1H) and 5.1 (doublet, 1H).

trans-2- β -Chloroethyl-3-deuterio-oxirane

The procedure was that previously described for the epoxidation of (Z)-4-chloro-1-butene-1-d. The product was distilled under reduced pressure to give a 58% yield of trans-2- β -chloroethyl-3-deuterio-oxirane. The n.m.r. spectrum δ TMS (CDCl_3) showed: 2.0 (quartet, 2H), 3.65 (triplet, 2H), 2.53 (doublet, 1H) and 3.05 (multiplet, 1H).

trans-3-Deuterio-2-vinyloxirane (20)

The procedure was that previously described for the conversion of cis-2- β -chloroethyl-3-deuterio-oxirane to cis-3-deuterio-2-vinyloxirane. The product (91%) was purified by preparative GC on ODPN at 40°. The n.m.r. spectrum TMS (CDCl_3) showed: 2.50 (doublet with fine splitting, 1H), 3.20 (multiplet, 1H), and the vinyl group resonance as a multiplet 5.05 - 5.7 (3H). The quartet centred δ 2.81 was attributed to the presence

of undeuterated 2-vinyloxirane. Careful integration of the n.m.r. spectrum indicated that the product was a mixture of trans-3-deuterio-2-vinyloxirane (81.4%) and non-deuterated 2-vinyloxirane (18.6%).

(-)-(R)-2-Vinyloxirane

This was prepared by partial asymmetric destruction of 2-vinyloxirane with di-3-pinanylborane by adaption of the procedure of Brown (34). A mixture of sodium borohydride (0.165 g, 0.0044 mol), (+)- α -pinene (1.36 g, 0.01 mol; Aldrich, $\alpha_D + 43.5^\circ$, neat) and diglyme (10 ml) was stirred and cooled under a nitrogen atmosphere in an ice bath. Boron trifluoride etherate (0.71 g, 0.005 mol) was added dropwise over 0.5 h at such a rate that the reaction temperature was maintained below 5° . After stirring for 4 h (below -5°) the resulting white suspension was cooled to -30° and vinyloxirane (0.70, 0.01 mol) was added rapidly. The mixture was maintained at -10° for 1.5 h and then water (0.5 ml) added to quench the reaction. It was then distilled at 0° under reduced pressure into a cooled receiver (acetone/ CO_2), and the water layer separated from the distillate. The product was purified by preparative GC on a 6 ft Carbowax 1500 column at 40° to give 0.246 g (34%) of (-)-(R)-2-vinyloxirane:

$[\alpha]_{589}^{25} = 0.675$, $[\alpha]_{365}^{25} = 5.040$ (4.444 g/100 ml, 2-propanol).

The optical purity was estimated to be about 9% based on the (+)-(S)-2-vinyloxirane obtained by synthesis from D-mannitol.

(-)-R-2-Vinyloxirane-3,3-d₂ (31)

This was prepared by partial asymmetric destruction of 2-vinyloxirane-3,3-d₂ by the procedure previously described for the non-deuterated 2-vinyloxirane. Purification by preparative GC on Carbowax 1500 at 40° gave 0.313 g (43.5%) of (-)-(R)-2-vinyloxirane-3,3-d₂:

$[\alpha]_{589}^{25} = 0.977$, $[\alpha]_{365}^{25} = 5.752$ (3.686 g/100 ml, 2-propanol).

The following vinyloxiranes were prepared and their thermolyses await our further investigation.

2-Methyl-2-vinyloxirane (36)

The procedure was essentially that previously described for the conversion of 1,3-butadiene to 2-vinyloxirane, utilizing 2-methyl-1,3-butadiene as the starting material. 2-Methyl-2-vinyloxirane (33%) bp 76-78°/705 torr (lit. 81°/735 torr (53)) was purified by preparative GC on ODPN. The n.m.r. spectrum δ TMS (CDCl₃) showed: 1.43 (singlet, 3H), 2.74 (quartet, 2H) and 5.08-5.97

(multiplet, 3H). This oxirane has previously been prepared by epoxidation of isoprene with peracetic acid in ether (54), and by base catalyzed cyclization of 1-chloro-2-methyl-3-buten-2-ol (55).

3,3-Dimethyl-2-vinyloxirane (37)

This was prepared by epoxidation of 4-methyl-1,3-pentadiene with meta-chloroperbenzoic acid following the procedure previously described for the epoxidation of (Z)-4-chloro-1-butene-1-d. The procedure was modified slightly in that only a 10% excess of meta-chloroperbenzoic acid was employed and the reaction mixture maintained at 0°. The product bp 94°/705 torr was purified by preparative GC on ODPN at 40° and eluted from the column as a single peak. The n.m.r. spectrum indicated that the product was the oxirane produced by epoxidation of the more highly substituted double bond. The n.m.r. spectrum δ TMS (CDCl_3) showed: 1.31 (doublet, 6H), 3.18 (doublet, 1H) and 5.17-6.07 (multiplet, 3H). Stogryn (56) gave bp 97 - 98°, but no additional data for the oxirane obtained by treatment of 4-methyl-1,3-pentadiene with meta-chloroperbenzoic acid.

cis-3-Methyl-2-vinyloxirane (38)

The epoxidation of (Z)-1,3-pentadiene with meta-chloroperbenzoic acid by the previously described pro-

cedure gave an approximately 4:1 mixture of two components. Preparative GC on ODPN at 70° cleanly separated the two components in a combined yield of 55%. The n.m.r. spectrum of the major component indicated that this was cis-3-methyl-2-vinyloxirane, δ TMS (CDCl_3): 1.28 (doublet, 3H), 3.02 - 3.48 (doublet, 2H) and 5.17 - 6.07 (multiplet, 3H). The n.m.r. spectrum of the minor component indicated that this was (Z)-2-propenyloxirane (39), δ TMS (CDCl_3): 1.79 (doublet with fine splitting, 3H), 2.60 (quartet, 1H), 2.95 (triplet, 1H), 3.58 (multiplet, 1H), 5.03 (triplet with fine splitting, 1H) and 5.53 - 6.07 (multiplet, 1H). These two oxiranes have previously been prepared by epoxidation of (Z)-1,3-pentadiene with peracetic acid in ether (54).

trans-3-Methyl-2-vinyloxirane (40)

The epoxidation of (E)-1,3-pentadiene gave an approximately 4:1 mixture of two components, which were cleanly separated by preparative GC on ODPN at 70°. The n.m.r. spectrum of the major component indicated that this was trans-3-methyl-2-vinyloxirane, δ TMS (CDCl_3): 1.31 (doublet, 3H), 2.70 - 3.12 (multiplet, 2H) and 5.07 - 5.67 (multiplet, 3H). The n.m.r. spectrum of the minor component indicated that this was (E)-3-propenyloxirane (41), δ TMS (CDCl_3): 1.87 (doublet with

fine splitting, 3H), 2.60 (quartet, 1H), 2.93 (triplet, 1H), 3.17 - 3.48 (multiplet, 1H), 5.16 (quartet with fine splitting, 1H) and 5.70 - 6.12 (multiplet, 1H). These two oxiranes have previously been prepared by epoxidation of (E)-1,3-pentadiene with peracetic acid in ether (54).

trans-3-Methyl-(E)-2-propenyloxirane (42)

The epoxidation of (E,E)-2,4-hexadiene with meta-chloroperbenzoic acid gave a single product (73%) which was purified by preparative GC on Carbowax 1500 at 60°. The n.m.r. spectrum δ TMS (CDCl_3) showed: 1.31 (doublet, 3H), 1.72 (doublet with fine splitting, 3H), 2.73 - 3.12 (multiplet, 2H), 5.18 (quartet with fine splitting, 1H) and 5.60 - 6.23 (multiplet, 1H). This n.m.r. spectrum is in close agreement with that recently published (57) for trans-3-methyl-(E)-2-propenyloxirane.

cis-3-Methyl-(Z)-2-propenyloxirane (43)

The epoxidation of (Z,Z)-2,4-hexadiene with meta-chloroperbenzoic acid gave a single product (65.5%) which was purified by preparative GC on Carbowax 1500 at 70°. The n.m.r. spectrum δ TMS (CDCl_3) showed: 1.27 (doublet, 3H), 1.78 (doublet with fine splitting 3H), 3.20 (quintet, 1H), 3.62 (quartet, 1H), 5.20 (triplet with fine splitting, 1H) and 5.57 - 6.12 (multiplet, 1H). This

n.m.r. spectrum is in close agreement with that recently published (57) of cis-3-methyl-(Z)-2-propenyloxirane.

3,3-Dimethyl-2-β-methylpropenyloxirane (44)

The epoxidation of 2,5-dimethyl-2,4-hexadiene with meta-chloroperbenzoic acid gave a single product which was purified by preparative GC on Carbowax 1500 at 80°. The n.m.r. spectrum appeared satisfactory for the expected product and showed δ TMS (CDCl_3): 1.32 (doublet, 6H), 1.78 (doublet, 6H), 3.35 (doublet, 1H) and 4.88 - 5.33 (multiplet, 1H). This oxirane has previously been prepared by the epoxidation of 2,5-dimethyl-2,4-hexadiene (58) and the n.m.r. spectrum is in agreement with that previously published (59).

Chiral 2-methyl-2-vinyloxirane

A partial asymmetric hydroboration of 2-methyl-2-vinyloxirane was carried out as previously described for 2-vinyloxirane. The conditions were modified slightly in that the reaction mixture was maintained at -10° for 3.25 h instead of 1.5 h. After purification by preparative GC on Carbowax 1500 at 50° a 29% recovery of 2-methyl-2-vinyloxirane was obtained:

$$[\alpha]_{589}^{22} = 5.65, [\alpha]_{365}^{22} = 18.39, (10.00 \text{ g/100 ml, 2-propanol})$$

The partial asymmetric hydroboration was repeated under identical reaction conditions using di-3-pinanylborane prepared from (-)- α -pinene $[\alpha]_D^{22} - 45^\circ$, neat). The recovered 2-methyl-2-vinyloxirane showed :

$$[\alpha]_{589}^{22} + 5.73, [\alpha]_{365}^{22} + 18.70 \text{ (9.64 g/100 ml, 2-propanol)}.$$

Chiral *trans*-3-methyl-2-(*E*)-propenyloxirane

A partial asymmetric hydroboration was performed on the racemic oxirane as previously described for 2-methyl-2-vinyloxirane. The specific rotation of the partially resolved oxirane thus obtained was:

$$[\alpha]_{589}^{22} + 9.16, [\alpha]_{365}^{22} + 26.10 \text{ (3.92 g/100 ml, 2-propanol)}.$$

REFERENCES

1. T. S. Chambers and G. B. Kistiakowsky, J. Amer. Chem. Soc., 56, 399 (1934).
2. S. W. Benson and H. E. O'Neal, "Kinetic Data on Gas Phase Unimolecular Reactions", U. S. Dept. of Commerce, National Bureau of Standards, (1970).
3. R. J. Crawford and A. Mishra, J. Amer. Chem. Soc., 87, 3768 (1965).
4. R. Hoffman, J. Amer. Chem. Soc., 90, 1475 (1968).
5. J. A. Berson and L. D. Pedersen, J. Amer. Chem. Soc., 97, 238 (1975).
6. J. A. Berson, L. D. Pedersen and B. K. Carpenter, J. Amer. Chem. Soc., 97, 240 (1975).
7. (a) C. G. Overberger and A. E. Borchert, J. Amer. Chem. Soc., 82, 1007 (1960).
(b) R. J. Ellis and H. M. Frey, J. Chem. Soc., 959 (1964).
(c) K. W. Eger, D. M. Golden and S. W. Benson, J. Amer. Chem. Soc., 86, 5420 (1964).
8. R. J. Ellis and H. M. Frey, J. Chem. Soc. Phys. Sect., 553 (1966).
9. M. R. Willcott and V. H. Cargle, J. Amer. Chem. Soc., 89, 723 (1967).
10. M. R. Willcott and V. H. Cargle, J. Amer. Chem. Soc., 91, 4310 (1969).

11. M. Arai and R. J. Crawford, Can. J. Chem., 50, 2158 (1972).
12. J. E. Baldwin and C. Ullenius, J. Amer. Chem. Soc., 96, 1542 (1974).
13. M. C. Flowers, R. M. Parker and M. A. Voisey, J. Chem. Soc. (B), 239 (1970).
14. M. C. Flowers and R. M. Parker, J. Chem. Soc. (B), 1980 (1971).
15. E. F. Hayes and A. K. Q. Siu, J. Amer. Chem. Soc., 93, 2090 (1971).
16. R. B. Woodward and M. R. Hoffman, Angew. Chem. Int. Ed. 8, 1475 (1969).
17. (a) R. Huisgen, H. Mader and H. Hermann, J. Amer. Chem. Soc., 93, 1779 (1971).
(b) J. H. Hall and R. Huisgen, Chem. Commun., 1187 (1971).
(c) R. Huisgen, J. H. Hall, C. H. Ross and W. Scheer, Chem. Commun., 1188 (1971).
18. E. Ullman and F. Milks, J. Amer. Chem. Soc., 84, 1315 (1962).
19. D. R. Arnold and L. A. Karnischky, J. Amer. Chem. Soc., 92, 1404 (1970).
20. T. Do-Minh, A. M. Trozzolo and G. W. Griffin, J. Amer. Chem. Soc. 92, 1402 (1970).
21. (a) H. Hamberger and R. Huisgen, Chem. Commun., 1190 (1970).

21. (b) A. Dahmen, H. Hamberger, R. Huisgen and V. Markowski, Chem. Commun., 1192 (1971).
22. H. H. J. MacDonald and R. J. Crawford, Can. J. Chem., 50, 428 (1972).
23. E. Vogel and H. Gunter, Angew. Chem. Int. Ed. 6, 395 (1967).
24. J. C. Pommelett, N. Manisse and J. Chuche, Tetrahedron 28, 3929 (1972).
25. (a) R. J. Crawford, V. Vukov and H. Tokunaga, Can. J. Chem., 51, 3718 (1973).
(b) V. Vukov and R. J. Crawford, Can. J. Chem., 53, 1367 (1975).
26. K. E. Schulte and K. P. Reiss, Chem. Ber. 86, 277 (1953).
27. J. D. Roberts and R. H. Mazur, J. Amer. Chem. Soc., 73, 2509 (1951).
28. (a) G. Zweifel and H. C. Brown, Org. React. 13, 1 (1963).
(b) R. W. Murray and G. J. Williams, J. Org. Chem., 34, 1896 (1969).
29. R. Reppe, Liebigs. Ann. Chem. 596, 80 (1955).
30. R. Palm, H. Ohse and H. Cherdron, Angew. Chemie. Int. Ed. 5, 994 (1966).
31. R. S. Tipson and A. Cohen, Carbohydrate Res., 7, 232 (1968).
32. E. Baer and H. O. L. Fischer, J. Biol. Chem. 128, 463 (1939).

33. (a) M. Schlosser, G. Muller and K. F. Christmann, Angew. Chem. Int. Ed. 5, 667 (1968).
(b) H. J. Bestmann, ibid. 4, 587 (1965).
(c) H. O. House and D. G. Mellilo, J. Org. Chem., 38, 1398 (1973).
34. H. C. Brown and G. Zweifel, J. Amer. Chem. Soc., 83, 486 (1961).
35. R. J. Abraham, K. Parry and W. A. Thomas, J. Chem. Soc. B., 446 (1971).
36. D. E. McGreer and B. D. Page, Can. J. Chem., 47, 866 (1969).
37. E. S. Swinbourne, "Analysis of Kinetic Data", Thomas Nelson and Sons (Canada) Ltd. 1971.
38. R. D. Cockroft, unpublished work (1971) from our laboratory.
39. K. B. Wiberg, Chem. Rev., 55, 713 (1955).
40. K. B. Wiberg, "Physical Organic Chemistry", John Wiley and Sons, Inc., New York, (1964).
41. C. J. Collins, W. T. Rainey, W. B. Smith and I. A. Kaye, J. Amer. Chem. Soc., 81, 460 (1959).
42. W. B. Smith, R. E. Bowman and T. J. Kmet, J. Amer. Chem. Soc., 81, 997 (1959).
43. S. Winstein and J. Takahashi, Tetrahedron 2, 316 (1956).
44. M. F. Hawthorne and E. S. Lewis, J. Amer. Chem. Soc., 80, 4296 (1958).

45. J. E. Bertie and D. A. Othen, Can. J. Chem., 51, 1155 (1973).
46. J. E. Bertie and M. Solinas, J. Chem. Phys. 61, 1666 (1974).
47. R. C. Lord and B. Nolin, J. Chem. Phys. 24, 656 (1956).
48. I. Safarik and O. P. Strausz, J. Phys. Chem., 76, 3613 (1972).
49. E. A. Halevi in "Progress in Physical Organic Chemistry", Vol. 1, Interscience Publishers, Inc., New York, (1963) p.109.
50. A. T. Bottini and V. Dev, J. Org. Chem., 27, 968 (1962).
51. L. F. Fieser, "Reagents for Organic Synthesis", John Wiley and Sons, Inc., New York (1967), p.135.
52. R. Meric and J.-P. Vigneron, Bull Soc. Chim. Fr., 327 (1973).
53. R. Pummerer and W. Reindel, Chem. Ber. 66, 355 (1933).
54. A. N. Pudovik and B. E. Ivanov, Zhur. Obshchei. Khim. 26, 2771 (1956).
55. K. Murata and A. Terada, Bull. Chem. Soc. Japan, 41, 495 (1968).
56. E. L. Stogryn and M. H. Gianni, Tetrahedron Lett. 34, 3025 (1970).
57. K.-N Chen, R. M. Moriarty, B. G. DeBoer, M. V. Churchill, J. Amer. Chem. Soc. 97, 5602 (1975).
58. J. K. Crandall, J. Org. Chem. 33, 423 (1968).
59. A.C. Day and M.C. Whiting, J. Chem. Soc. C, 1719 (1966).

VITA

The author was born in Oxford, England on December 19, 1946. He entered the Grammar School, Witney, Oxfordshire in 1958, and in 1965 was accepted by Brunel University, London England.

Upon graduation in 1969, with an Upper Second Class degree in Chemistry, he emigrated to Canada and entered the Faculty of Graduate Studies, University of Alberta.

He served as a Graduate Teaching Assistant in the Department of Chemistry while completing his Ph.D. program.

APPENDIX A.

Kinetic data for the thermolyses of the 2-vinyloxiranes.

1. Rate constants and activation parameters for the overall decomposition of 2-vinyloxirane and the formation of 2,3-dihydrofuran were obtained from the data of Runs #1 to #33.
2. Rate constants and activation parameters for the racemization of 2-vinyloxirane were obtained from the data of Runs #43 to #46.
3. The kinetic deuterium isotope effects on the overall decomposition of 2-vinyloxirane and on the formation of 2,3-dihydrofuran were obtained from the data of Runs #26 to #42.
4. The kinetic deuterium isotope effect on the rate of racemization of 2-vinyloxirane was obtained from the data of pages 187 and 188.
5. The product proportions from the thermolyses were obtained from the data of Runs #26 to #42.

It should be noted that, with the exception of Run #17, Runs #1 to #24 have no integration values included for the 2-butenals. This is a consequence of the small analytical sample withdrawn and the higher column temperature (50°) used, which precluded a reliable integration of the 2-butenal peaks in the chromatogram.

Run #1

Thermolysis of 12 at 292.70°C

Time (Min)	+ CO	32 ~	12 ~	33 ~	DME	34 ~	35 ~	$\log_{10}(12/DME)$
30	486	211	31650	1146	31620			0.00041
69	895	635	28810	2252	29930			0.02725
90	1599	766	27140	3188	30520			-0.05097
120	2568	983	25500	3785	32680			-0.10774
150	3704	1498	23970	3939	32010			-0.12562
180	4729	1840	21550	4877	30720			-0.15397
210	5947	1956	19440	4850	31210			-0.20560
240	6999	1992	18630	5246	29790			-0.20386
270	7877	2330	16700	5003	28120			-0.22630
300	9648	2523	16230	5516	30840			-0.27880
330	10390	2759	13480	5298	29250			-0.33644
360	11590	2957	12500	5122	29450			-0.37218
390	13160	2716	12140	5576	29480			-0.38531
420	12850	2811	10250	4388	27250			-0.42464
450	12160	4163	3706	11470	5603			-0.48227
480	15890	3304	9252	4255	29510			-0.50373
510	17040	3297	9054	4014	29380			-0.51121

Least squares analysis gives: $k = 4.7244 \times 10^{-5} \text{ sec}^{-1}$
 standard error: $= 9.677 \times 10^{-7}$

Thermolysis of 12 at 292.70°C

Run #2

Time (min)	+ CO	32 ~~	12 ~~	33 ~~	DME	34 ~~	35 ~~	$\log_{10}(12/DME)$
30	358	347	33410	1282	33090			0.00418
60	1022	633	30690	2148	32940			-0.03073
90	1784	1068	31570	3576	36260			-0.06015
121	2600	1122	25320	3956	30550			-0.08155
151	3571	1485	24360	4208	31490			-0.11150
180	4722	1626	21550	5000	31960			-0.17116
210	5926	1902	20530	3762	30510			-0.17205
240	6391	1976	16000	4395	26470			-0.21863
270	8663	2471	17840	6276	30510			-0.23305
300	10000	2655	16920	5600	31630			-0.27170
330	10490	2547	14250	5615	29850			-0.32113
375	12190	2795	13120	5292	29390			-0.35027
390	12790	2710	12410	6085	28310			-0.35817
420	13790	2899	11490	5874	28890			-0.40043
450	16780	3471	12010	6306	31500			-0.41877
480	16450	3077	9960	5423	29930			-0.47785

Least squares analysis gives: $k = 3.9787 \times 10^{-5} \text{ sec}^{-1}$
 standard error: $= 7.357 \times 10^{-7}$

Run #3 Thermolysis of 12 at 292.70°C

Time (min)	+ CO	32 ~~	12 ~~	33 ~~	DME	34 ~~	35 ~~	$\log_{10}(12/DME)$
31	332	305	34450	1530	33460			0.01266
63	1086	733	31550	2653	35240			-0.04804
90	1742	1078	28760	3051	33880			-0.07115
120	2567	1373	24720	4287	32570			-0.11977
150	3798	1599	24740	4917	33730			-0.13462
180	4539	1551	21640	5132	30290			-0.14604
216	5754	1872	19370	5004	31990			-0.21788
243	6959	2205	17830	5246	30990			-0.24007
270	7780	2296	16840	5158	30440			-0.25710
300	9041	2398	15710	5363	30830			-0.29280
330.3	10070	2418	13990	5389	29260			-0.32046
361	11460	2608	12920	5584	28790			-0.34798
390	12130	2763	12150	5443	29090			-0.37917
421	13430	2634	10940	5524	28740			-0.41947
450	13420	2850	9745	4693	26850			-0.44016
482	17220	3319	10290	5833	32750			-0.50280

Least squares analysis gives: $k = 4.0716 \times 10^{-5} \text{ sec}^{-1}$
standard error: $= 8.375 \times 10^{-7}$

Thermolysis of 12 at 292.70°C

Time (min)	+ CO	32 ~~	12 ~~	33 ~~	DME	34 ~~	35 ~~	$\log_{10} (12/DME)$
60	909	834	32180	2931	31000			0.01622
90	1756	904	28150	3153	30200			-0.03053
120	2885	1321	29960	5249	33790			-0.05224
150	3674	1585	25390	4577	31330			-0.09130
180	4818	1794	20350	5051	30100			-0.11590
210	6011	2082	22020	6146	31270			-0.15231
240	5587	1410	25050	7914	41280			-0.21693
270	8244	2583	17820	5889	29300			-0.21596
300.2	9998	2591	16800	6845	30230			-0.25513
330	10000	2495	13830	6247	26300			-0.27913
360	11100	2605	13290	5056	27310			-0.31280
390	12510	2942	12200	5321	27320			-0.35012
425	13090	2765	11010	5658	28660			-0.41549
450	15170	3224	10610	5553	28600			-0.43065
480	14340	3033	8460	4443	25680			-0.48222

Least squares analysis gives: $k = 8.3246 \times 10^{-5} \text{ sec}^{-1}$
standard error: $= 9.548 \times 10^{-7}$

Run #5

Thermolysis of 12 at 297.52°C

Time (min)	+ CO	32 ~~	12 ~~	33 ~~	DME	34 ~~	35 ~~	$\log_{10}(12/DME)$
45	2025	562	27710	4211	31650			-0.05774
60	2523	980	25730	4478	32380			-0.09984
75	3157	1292	25460	4571	32800			-0.11002
90	3696	1270	22720	4992	29890			-0.11912
106	5723	1837	22630	5481	33120			-0.16531
135	6677	2156	20830	5895	33430			-0.20545
150	6582	1918	17610	5316	28520			-0.20939
169	9168	2441	18260	6879	33100			-0.25833
183	9435	2477	17010	6098	31360			-0.26567
198	10150	2320	15150	5992	29160			-0.28437
215	10530	2689	13450	5342	28050			-0.31921

Least squares analysis gives: $k = 5.7184 \times 10^{-5} \text{ sec}^{-1}$

standard error: $= 1.978 \times 10^{-6}$

Run #6

Thermolysis of 12 at 297.52°C

Time (min)	+ CO	32 ~~	12 ~~	33 ~~	DME	34 ~~	35 ~~	$\log_{10}(12/DME)$
45.4	1632	433	23890	4863	29210			-0.08732
60	2279	740	25110	5555	32730			-0.11510
75.6	2710	1142	22390	5462	30790			-0.13836
90	3599	1652	20650	5532	31790			-0.18737
105	4401	1635	20680	5804	32510			-0.19647
120	5260	1662	19860	6515	31290			-0.19743
135.1	5646	1787	17720	6322	29830			-0.22619
150	6220	1764	15610	5527	27670			-0.24861
165	7503	1931	15620	6452	29690			-0.27893
180	9334	2528	16430	6783	33260			-0.30628
196.3	9840	2500	14090	6471	31920			-0.35515
212	10590	2568	13400	6094	30640			-0.35918
225.3	11900	2883	12960	6636	32610			-0.40075
240	12050	2652	11660	6467	29190			-0.39854
260	12830	2640	10400	6316	28420			-0.43659
275	14900	2903	9688	5924	29470			-0.48315
305	14900	2869	8225	5134	27490			-0.52404
327	14250	2502	6173	4577	23650			-0.58333
350	15290	2653	5960	4719	23840			-0.60206
403	20190	3218	5548	4744	28520			-0.71101

Least squares analysis gives: $k = 6.5586 \times 10^{-5} \text{ sec}^{-1}$
 standard error = 1.166×10^{-6}

Run #7

Thermolysis of 12 at 297.52°C

Time (min)	+ CO	32 ~~	12 ~~	33 ~~	DME	34 ~~	35 ~~	$\log_{10}(12/\text{DME})$
22	739	238	36150	4365	36090			0.00072
34.3	1057	477	34120	4926	36060			-0.02402
46	1533	859	33140	4829	38160			-0.06126
60	2140	1071	31260	5629	37030			-0.07356
80	3211	1283	27190	5904	36650			-0.12966
100	4456	1581	25020	6432	36580			-0.16496
120	5643	1911	23580	6833	36330			-0.18772
140	1428	430	4368	1169	6997			-0.20463
160	8506	2663	19680	6905	36440			-0.26755
180	9826	2718	18890	7326	35420			-0.27302
200	11470	2829	17100	7670	35510			-0.31735
220	12920	3251	15640	6901	35710			-0.35855
240	14690	3610	15260	7515	36520			-0.37898
261	15490	3287	13130	6449	33990			-0.41309
280	16480	3405	11930	6541	33360			-0.44659
300	17630	3453	10750	6104	33780			-0.49725
320	18690	3582	9687	6259	32310			-0.52315
340	19880	3570	9155	5763	32360			-0.54835

Least squares analysis gives: $k = 6.572 \times 10^{-5} \text{ sec}^{-1}$
 standard error: $= 9.980 \times 10^{-7}$

Run #8

Thermolysis of 12 at 297.52°C

Time (min)	+ CO	32 ~~	12 ~~	33 ~~	DME	34 ~~	35 ~~	$\log_{10}(12/DME)$
30	1076	473	33390	4056	37050			-0.04517
60	2023	966	28880	5014	36430			-0.10086
80	3102	1365	27010	5254	35970			-0.12442
100	4258	1501	25950	6034	37100			-0.15524
120	5050	1909	22970	6356	35990			-0.19502
140	6645	2394	21060	6902	36510			-0.23776
160	8008	2557	20390	6241	36870			-0.25726
181	9462	2610	18220	6612	36630			-0.30329
200	10830	2925	17910	7190	36660			-0.31110
220	11400	2858	15430	6723	33990			-0.34299
240	13660	3262	14950	7063	36130			-0.38323
260	13720	3342	12520	6386	33360			-0.42562
280	13670	3101	10770	5299	30970			-0.45873
300	16420	3534	10690	5546	33190			-0.49203

Least squares analysis gives: $k = 6.262 \times 10^{-5} \text{ sec}^{-1}$ standard error: $= 1.001 \times 10^{-6}$

Run #9

Thermolysis of 12 at 297.52°C

Time (min)	+ CO	32 ~~	12 ~~	33 ~~	DME	34 ~~	35 ~~	$\log_{10}(12/DME)$
40	1386	791	34310	4166	39250			-0.05842
60	2041	1074	29900	4708	37540			-0.09882
81	3110	1471	28150	5253	37660			-0.12640
101	4236	1781	27450	5606	38030			-0.14158
122	5517	2199	25270	5877	37760			-0.17443
140	6024	2129	21890	5816	34220			-0.19403
160	7007	2275	19050	5971	34050			-0.25222
180	9306	2755	19600	6270	35830			-0.26199
206	10100	2734	15960	6054	33520			-0.32227
221	11990	3292	17030	6531	35960			-0.32461
240	12350	3149	14640	5990	32510			-0.34648
260	14400	3333	13780	6324	35180			-0.40725
280	14820	3044	12530	6155	33230			-0.42358
300	16700	3401	11820	6736	34460			-0.46470

Least squares analysis gives: $k = 5.8918 \times 10^{-5} \text{ sec}^{-1}$
standard error: $= 1.447 \times 10^{-6}$

Run #10

Thermolysis of 12 at 297.52°C

Time (min)	+ CO	32 ~~	12 ~~	33 ~~	DME	34 ~~	35 ~~	$\log_{10}(12/DME)$
40	1194	683	34430	3997	39260			-0.05701
60	1742	924	28700	1029	35090			-0.08730
81	2973	1477	27590	5153	37510			-0.13340
100	4107	1760	28260	6138	38880			-0.13855
120	5035	1904	23900	5872	37000			-0.18980
140	5439	1627	18980	5223	31570			-0.22098
160	3504	1037	9772	2595	17000			-0.24047
180	8870	2449	19390	6787	36860			-0.27898
200	9836	2726	17510	6104	35140			-0.30252
220	11320	2898	15940	6465	35400			-0.34651
240	12600	3042	14750	6478	35160			-0.37726
260	13810	3227	13900	6233	35020			-0.40130
280	14870	3409	12200	6296	34370			-0.44982
301	15540	3301	11320	5999	31620			-0.44612

Least squares analysis gives: $k = 5.9843 \times 10^{-5} \text{ sec}^{-1}$
 standard error: $= 1.282 \times 10^{-6}$

Run #11

Thermolysis of 12 at 297.52°C

Time (Min)	+ CO	32 ~~	12 ~~	33 ~~	DME	34 ~~	35 ~~	$\log_{10}(12/DME)$
40	1151	801	33690	4249	38590			-0.05897
60	2086	984	31450	4681	38480			-0.08748
80	2678	1143	26310	4692	34860			-0.12221
100.3	3751	1642	25760	5363	37380			-0.16169
120	4745	1810	23170	5239	35860			-0.18968
140	6255	2108	22490	5930	35470			-0.19784
160	7919	2836	22680	6429	39120			-0.23676
180	9150	2769	20520	7309	37340			-0.26000
200	9801	2640	17820	6637	35480			-0.29908
220	11320	2920	16420	6589	35400			-0.33363
240	12710	2928	15200	6664	34920			-0.36123
260	13720	3240	13500	5902	35190			-0.41609
280	14450	3262	12300	6250	33860			-0.43978
300	15110	3287	11270	6022	33210			-0.46934
320.1	16800	3537	11130	6411	32680			-0.46779
341.2	17280	3713	9193	5420	32810			-0.55255
366	17940	3404	7967	5809	31010			-0.59021

Least squares analysis gives: $k = 6.1210 \times 10^{-5} \text{ sec}^{-1}$
 standard error: $= 1.321 \times 10^{-6}$

Run #12

Thermolysis of 12 at 302.16°C

Time (min)	+ CO	32 ~~	12 ~~	33 ~~	DME	34 ~~	35 ~~	$\log_{10}(12/DME)$
32	1269	688	27440	3215	36850			-0.12805
60	3234	1604	25230	4583	38010			-0.17798
90	5224	1736	20510	5030	34700			-0.22836
120	7908	2438	17790	5246	35260			-0.29711
150	11070	3039	16690	6904	37040			-0.34621
181	12920	3094	12370	5510	33550			-0.43332
210	15330	3454	11200	5036	33580			-0.47686
240	16350	3209	8141	4724	29520			-0.56032
270	18270	3533	6907	4607	30200			-0.64072
300.2	20320	3735	6201	4101	30340			-0.68955

Least squares analysis gives: $k = 8.2301 \times 10^{-5} \text{ sec}^{-1}$
standard error: $= 1.842 \times 10^{-6}$

Run #13

Thermolysis of 12 at 302.16°C

Time (min)	+ CO	32 ~~	12 ~~	33 ~~	DME	34 ~~	35 ~~	$\log_{10}(12/DME)$
30	1189	476	27230	2643	41110			-0.17890
60	2695	1250	23080	3573	37260			-0.20801
90	5244	1759	21100	5212	40020			-0.27799
120	6609	1907	16110	5247	34180			-0.32668
150	8906	2281	13570	5505	33760			-0.39582
180	10530	2159	10840	4629	29040			-0.42797
210	12390	2643	9134	5223	33640			-0.56619

Least squares analysis gives: $k = 7.8577 \times 10^{-5} \text{ sec}^{-1}$

standard error: $= 6.668 \times 10^{-6}$

Run #14

Thermolysis of 12 at 302.16°C

Time (min)	+ CO	32 ~~	12 ~~	33 ~~	DME	34 ~~	35 ~~	$\log_{10}(12/DME)$
30	1118	743	29980	2832	33300			-0.04561
60	2866	1407	26540	4449	32430			-0.08705
90	5033	1589	22160	5966	30970			-0.14537
121	7537	2324	19210	7009	30560			-0.20163
150	9418	2541	15360	6435	28490			-0.26830
180	12040	2648	13080	6465	29090			-0.34714
210	14260	3044	11140	5828	29090			-0.41686
256	16420	3228	8046	5525	25310			-0.49771
270	17850	3491	7742	5089	27120			-0.54444
304	18530	3450	5990	4494	26110			-0.63938

Least squares analysis gives: $k = 8.3548 \times 10^{-5} \text{ sec}^{-1}$
 standard error: $= 2.106 \times 10^{-6}$

Run #15

Thermolysis of 12 at 302.16°C

Time (min)	+ CO	32 ~~	12 ~~	33 ~~	DME	34 ~~	35 ~~	$\log_{10}(12/\text{DME})$
30	1074	763	31310	2984	31290			-0.00028
60	2993	1301	29110	4831	32620			-0.04944
90	5255	1971	23910	6322	32250			-0.12995
120	7623	2432	20420	6914	32170			-0.19740
150.3	9345	2640	15330	6516	26180			-0.23243
180	12780	3199	14680	7553	30070			-0.31141
210	14710	3497	11350	6795	29140			-0.40949
240	17080	3577	10100	5793	29590			-0.46682
272	18360	3798	8224	6005	30500			-0.56922
300	19510	3600	6234	4744	26230			-0.62403

Least squares analysis gives: $k = 9.0155 \times 10^{-5} \text{ sec}^{-1}$
standard error: $= 2.458 \times 10^{-6}$

Run #16

Thermolysis of 12 at 302.16°C

Time (min)	+CO	32 ~~	12 ~~	33 ~~	DME	34 ~~	35 ~~	$\log_{10} (12/DME)$
30	1006	493	31290	3293	31290			-0.0000
60	3007	1436	28040	5243	33490			-0.07714
90	5021	1976	22740	5779	31830			-0.14605
120	7052	2073	17600	6674	29630			-0.22622
155	10440	2774	15670	68650	31490			-0.30310
180	12780	3135	14000	6900	30410			-0.33689
210	14860	3293	11640	5850	29670			-0.40636
240	16660	3287	9706	5927	27390			-0.45055
270	18630	3325	8005	5626	26730			-0.52364
301	20140	3452	6450	5316	26520			-0.61401

Least squares analysis gives: $k = 8.3329 \times 10^{-5} \text{ sec}^{-1}$
standard error: $= 1.896 \times 10^{-6}$

Thermolysis of 12 at 302.16°C

Run #17

Time (min)	+ CO	32 ~~	12 ~~	33 ~~	DME	34 ~~	35 ~~	$\log_{10}(12/DME)$
20	2113	1713	137300	3056	125600	11150	4473	-0.03868
40	5291	3630	117500	4175	126500	14670	6905	-0.03205
60	10680	5590	113500	6191	133000	16300	8792	-0.06886
80	16590	7385	105800	7368	136600	20240	11230	-0.11097
100	21830	7934	83750	8086	124600	17760	10060	-0.15426
120	26980	8797	76560	8571	120400	18450	11750	-0.19662
140	34000	9692	69200	9613	120500	18170	10220	-0.24088
160	38590	9466	57990	8423	111000	14460	7999	-0.28197
180	44260	10500	51620	10270	110300			-0.32976

Least squares analysis gives: $k = 8.4939 \times 10^{-5} \text{ sec}^{-1}$
 standard error: $= 1.843 \times 10^{-6}$

Run #18

Thermolysis of 12 at 312.50°C

Time (min)	+ CO	32 ~~	12 ~~	33 ~~	DME	34 ~~	35 ~~	$\log_{10}(12/DME)$
15.5	1334	752	31480	3222	33110			-0.02192
30	3087	1312	26670	5660	32090			-0.08035
46	6301	2063	23650	7226	35170			-0.17234
60	7562	2072	18160	6324	29730			-0.21408
75	10310	2740	14700	7017	30230			-0.31312
90	12630	2871	12530	7068	28770			-0.36099
105.1	15500	3144	10310	6682	30140			-0.465888
120	17440	3274	9029	6436	28190			-0.49446
135	18650	3479	6693	5617	28120			-0.62339
150	20630	3663	6309	5126	27320			-0.63652

Least squares analysis gives: $k = 1.8288 \times 10^{-4} \text{ sec}^{-1}$ standard error = 5.803×10^{-6}

Run #19

Thermolysis of 12 at 312.50°C

Time (min)	+ CO	32 ~~	12 ~~	33 ~~	DME	34 ~~	35 ~~	$\log_{10}(12/DME)$
15	1445	731	31800	3913	35640			-0.04951
30	3250	1352	25920	5415	34600			-0.12544
45	4873	1785	19310	5780	29630			-0.18595
60.4	8173	2638	20130	7844	34920			-0.23923
79	11860	8340	15580	7503	32670			-0.32158
90	13860	3435	13740	7544	30290			-0.34331
105	16750	3868	11090	7452	32720			-0.46988
135	18200	3485	6715	4965	26050			-0.58876
150	22240	3797	6203	6119	27200			-0.64197

Least squares analysis gives: $k = 1.6936 \times 10^{-4} \text{ sec}^{-1}$
standard error = 5.328×10^{-6}

Run #20

Thermolysis of 12 at 312.50°C

Time (min)	+ CO	32 ~	12 ~	33 ~	DME	34 ~	35 ~	log ₁₀ (12/DME)
15	1475	722	34620	4272	39640			-0.05881
30	3464	1546	28550	6483	37090			-0.11365
45	5595	2001	23090	8139	32780			-0.15219
60	9065	2768	20620	8814	35750			-0.23899
80.1	12370	4377	16880	8840	33100			-0.29246
90	14250	3748	14010	8694	35270			-0.40097
105	16130	3215	11360	7830	30520			-0.42921
120	18640	3549	9735	6584	31370			-0.50818
135	22010	4040	8051	6833	31600			-0.59384
150	23010	4103	6791	5376	30580			-0.65350

Least squares analysis gives: $k = 1.7322 \times 10^{-4} \text{ sec}^{-1}$
standard error = 5.962×10^{-6}

Run #21

Thermolysis of 12 at 312.50°C

Time (min)	+ CO	32 ~~	12 ~~	33 ~~	DME	34 ~~	35 ~~	log ₁₀ (12/DME) ~~
15	1947	685	28790	4349	35120			-0.08631
30	3804	1270	24260	6292	34860			-0.15744
45	5750	1987	19520	6145	33040			-0.22856
60	8019	2271	16670	6723	31560			-0.27720
90	13780	3079	11890	7740	30760			-0.41280
105	14970	2960	9346	6386	28950			-0.49102
120.2	18780	3559	8016	6660	31960			-0.60065
135	20030	3823	6743	5708	29260			-0.63742
150	21480	3563	5492	5407	28570			-0.71618

Least squares analysis gives: $k = 1.7955 \times 10^{-4} \text{ sec}^{-1}$
standard error = 4.270×10^{-6}

Run #22

Thermolysis of 12 at 312.50°C

Time (min)	+ C0	32 ~~	12 ~~	33 ~~	DME	34 ~~	35 ~~	$\log_{10}(12/DME)$
15	2125	641	29780	6194	37340			-0.09825
30	4227	1248	26120	8082	36700			-0.14769
45	6356	2060	21490	8629	36320			-0.22791
60	8451	2441	16630	8126	33680			-0.30648
75	12260	3161	15920	9710	37610			-0.37336
90	14930	3252	13220	8813	32510			-0.39079
105	15070	1289	9169	7713	29970			-0.51436
120	17460	3238	7950	6743	29250			-0.56576
135	19610	3518	6438	6302	28770			-0.65019
150	21480	3558	5405	5785	28120			-0.71622

Least squares analysis gives: $k = 1.7694 \times 10^{-4} \text{ sec}^{-1}$
standard error = 5.007×10^{-6}

Time (min)	+ C0	32 ~~	12 ~~	33 ~~	DME	34 ~~	35 ~~	log ₁₀ (12/DME)
15.6	1542	770	32160	4719	34620			-0.03201
30	3732	1572	27840	7411	33850			-0.08489
45	5451	1969	20170	7099	29200			-0.16068
60	6448	2703	18440	8367	30160			-0.21367
75	11030	2904	15770	8542	29080			-0.26576
91	14420	3447	12750	8482	29840			-0.36929
105	16270	3392	10480	8045	28260			-0.43081
120	16970	3280	8264	6231	25800			-0.49443
135	23510	4362	8225	7454	31150			-0.57832
150	22640	3926	6222	7046	26280			-0.62570

Least squares analysis gives: $k = 1.7422 \times 10^{-4} \text{ sec}^{-1}$
standard error = 3.360×10^{-6}

Run #24

Thermolysis of 12 at 312.50°C

Time (min)	+ CO	32 ~~	12 ~~	33 ~~	DME	34 ~~	35 ~~	$\log_{10}(12/DME)$
15.5	1633	678	32480	5896	31540			-0.01275
30	3892	1640	29110	8315	34740			-0.07679
46	5692	1907	20040	7247	28150			-0.14758
60	8820	2675	19810	9282	32300			-0.21232
75	12640	3201	17310	9936	31110			-0.25460
90	15340	3645	13890	9050	31280			-0.35256
105	16460	3381	11040	8255	27400			-0.39478
120	19660	3761	9304	7615	27860			-0.47631
135	22710	3916	8126	7674	28130			-0.53929
150	23350	4159	6081	6351	27710			-0.65866

Least squares analysis gives: $k = 1.8000 \times 10^{-4} \text{ sec}^{-1}$
standard error = 5.196×10^{-6}

Run #25

Thermolysis of 12 at 312.50°C

Time (min)	+ CO	32 ~~	12 ~~	33 ~~	DME	34 ~~	35 ~~	$\log_{10}(12/DME)$
21	6149	3601	112200	4734	122700	19620	7010	-0.03885
44	17450	7365	88680	6298	129100	26320	10720	-0.16310
60	27980	9552	73570	7729	123200	26200	11600	-0.22391
80.5	40680	10890	57740	7748	120400	25550	11390	-0.31915
100	49490	11530	43130	6136	109400	23130	11850	-0.40424
120.5	60550	12410	33800	6789	106900	20870	9766	-0.50006
144	74120	13940	26240	6325	110900	19930	9082	-0.62597
160	74530	13100	20120	5515	98110	16150	5143	-0.68809

Least squares analysis gives: $k = 1.7841 \times 10^{-4} \text{ sec}^{-1}$

standard error = 2.357×10^{-6}

Run #26

Thermolysis of 12 at 307.40°C

Time (min)	+ CO	32	12	33	DME	34	35	log ₁₀ (12/DME)
20	3611	2081	109600	3167	121100	12140	4379	-0.04333
*40	10120	5259	106800	6234	145000	21040	14360	-0.13280
60	15450	6277	79630	5035	116500	17670	12070	-0.16525
80	23050	8254	66630	6181	112700	20940	14930	-0.22825
100	28790	8722	51270	5411	102400	19440	11850	-0.30044
120	47650	12080	57120	8085	131700	24340	14510	-0.36280
140	44120	10290	36460	5703	96800	11790	12710	-0.42406
160	52020	11270	31240	6067	95980	16880	4498	-0.48747
185	66630	12770	29200	6055	107200	18320	11470	-0.56481

*Neglected in analysis

Least squares analysis gives:

$$k = 1.2222 \times 10^{-4} \text{ sec}^{-1}$$

$$\text{standard error} = 8.813 \times 10^{-7}$$

Time (Min)	+ C0	32 ~~	12 ~~	33 ~~	DME	34 ~~	35 ~~	$\log_{10}(12/DME)$
20	3763	2335	128400	5172	133800	12260	8842	-0.01789
40.3	8447	4937	95690	4722	112500	15972	9587	-0.07029
60	15440	6600	83690	5605	115400	18130	12900	-0.13953
80	28600	10170	83850	8899	133300	22330	16830	-0.20133
100	33990	10150	62080	8229	114800	18471	11970	-0.26699
120	38280	9895	47220	7137	100700	14160	11420	-0.32890
141	50580	11750	43300	2759	107400	18680	6075	-0.39452
160	49850	10720	31610	8671	90730	15430	9022	-0.45793
185	67920	21620	30170	7289	106000			-0.54573

Least squares analysis gives:

$$k = 1.2300 \times 10^{-4} \text{ sec}^{-1}$$

$$\text{standard error} = 1.114 \times 10^{-6}$$

Thermolysis of 12 at 307.40°C

Time (Min)	+ CO	32 ~~	12 ~~	33 ~~	DME	34 ~~	35 ~~	log ₁₀ (12/DME)
20	3325	2457	114200	3958	117500	14760	7910	-0.01237
40	8681	4565	95070	5699	112100	17410	8959	-0.07156
60	14980	6345	77700	5525	106600	19010	11340	-0.13734
80	24040	8278	69790	6905	110600	20980	11930	-0.19996
100	31040	9189	56180	6746	101500	19740	12250	-0.25688
120	39530	10610	47220	7200	101600	17600	11110	-0.33277
140	46550	10970	39290	6905	97160	17790	10770	-0.39343
160	59130	12840	36380	7942	107200	18290	10360	-0.46933
180	60850	12240	27970	6889	97770			-0.54351

Least squares analysis gives:

$$k = 1.2676 \times 10^{-4} \text{ sec}^{-1}$$

$$\text{standard error} = 1.843 \times 10^{-6}$$

Run #29

Thermolysis of 12 at 307.40°C

Time (Min)	+ CO	32 ~~	12 ~~	33 ~~	DME	34 ~~	35 ~~	$\log_{10}(12/DME)$
20	3949	2566	219800	5491	136000	13420	6715	-0.02026
40	8802	4321	97610	5202	117600	16560	7500	-0.08091
60	16410	6929	87420	6560	120600	20460	11590	-0.13974
80	27620	9547	81220	9351	131100	22470	10590	-0.20794
100	31980	9427	57440	8292	107200	18340	10500	-0.27098
120	42580	11200	52160	8678	112100	20790	13430	-0.33227
141	46920	10800	41110	8163	105400			-0.40889
160	59240	12610	38400	8248	111000	20860	11420	-0.46099
180	61300	12330	29200	7537	99630	18340	11750	-0.53301

Least squares analysis gives

$$k = 1.2307 \times 10^{-4}$$

$$\text{standard error} = 1.007 \times 10^{-6}$$

Run #30

Thermolysis of 12 at 307.40°C

Time (Min)	+ CO	32 ~~	12 ~~	33 ~~	DME	34 ~~	35 ~~	$\log_{10}(12/DME)$
20	3142	1821	108600	2469	113600	13820	4324	-0.01955
40	9637	5217	109800	5474	134700	19530	7356	-0.08877
60	17240	7119	92980	5453	132500	23830	9106	-0.15383
80	57540	7131	63490	4499	104700	21980	10730	-0.21724
100	30290	9102	55740	5672	106900	22460	8286	-0.28281
120	36170	9077	44770	5091	99050	20450	8666	-0.34487
140	45240	10100	39660	5350	101200	19650	8712	-0.40683
162	49390	10220	30950	4719	93540	19680	8908	-0.48034
180	60760	11690	29580	5434	102900	19450	9969	-0.54142

Least squares analysis gives

$$k = 1.2399 \times 10^{-4} \text{ sec}^{-1}$$

$$\text{standard error} = 5.643 \times 10^{-7}$$

Run #31

Thermolysis of 12 at 307.40°C

Time (Min)	+ CO	32 ~~	12 ~~	33 ~~	DME	34 ~~	35 ~~	$\log_{10}(12/DME)$
20	3637	2353	126200	6084	127600	7421	8022	-0.00479
40	7931	3998	92650	6471	110700	10100	11330	-0.07730
60	14460	6145	77520	8274	107700	11010	13530	-0.14280
80	23340	8351	71180	8942	114800	13140	14410	-0.20758
100	33460	10050	63360	10270	118400	15060	18860	-0.27154
120	44160	11650	56980	11330	124800	13190	17030	-0.34049
140	45870	10730	40850	9105	103700	12920	15540	-0.40459
160	57690	11940	37570	10200	110900	10210	12780	-0.47009
180	56220	10900	27430	7748	94270	9844	12900	-0.53615

Least squares analysis gives

$$k = 1.2668 \times 10^{-4}$$

$$\text{standard error} = 5.326 \times 10^{-7}$$

Time (Min)	+ CO	32 ~~	12 ~~	33 ~~	DME	34 ~~	35 ~~	$\log_{10}(12/DME)$
20	2653	2313	113500	3211	111000	7127	5448	-0.00967
40	7833	4357	99760	4422	109200	10310	4630	-0.03927
60	15060	6552	87190	5637	110400	14890	8680	-0.10250
80	26050	9450	84530	7878	125000	19500	13610	-0.16990
100.1	31020	9470	62070	7271	105700	14170	9663	-0.23119
*120	36450	8816	62120	67940	97900	14760	10340	-0.19755
140	46630	11740	44000	7809	100800	14080	11290	-0.36001
160	58520	13150	40110	9011	107100	15590	3869	-0.42654
180	59730	12350	31000	7300	95410	12840	71630	-0.48823

* Neglected in least squares analysis

Least squares analysis gives

$$k = 1.2141 \times 10^{-4}$$

$$\text{standard error} = 1.278 \times 10^{-6}$$

Run #33

Thermolysis of 12 at 307.40°C

Time (Min)	+ CO	32 ~~	12 ~~	33 ~~	DME	34 ~~	35 ~~	$\log_{10}(12/DME)$
*20	3374	2863	138100	3959	125400	11440	5410	-0.04190
40	9249	4893	114600	5304	130700	19020	8862	-0.05709
60	16000	6630	89620	6295	118500	20720	9708	-0.12131
81	26180	9389	80900	7964	126700	23470	10950	-0.19483
100	34890	10190	67310	8456	122500	21780	11110	-0.26006
120	40930	10630	53620	8664	112300	20550	11420	-0.32105
140.1	49320	11250	44690	7758	110000	18720	10310	-0.39118
160.5	58750	11020	36700	5393	106400	19150	12020	-0.46228
180	64030	12470	32090	7589	104300	16100	2292	-0.51191

*Neglected in least squares analysis.

Least squares analysis gives

$$k = 1.2657 \times 10^{-4}$$

$$\text{standard error} = 1.453 \times 10^{-6}$$

Thermolysis of 2l at 307.40°C

Run #34

Time (min)	+ CO	32 ~~	12 ~~	33 ~~	DME	34 ~~	35 ~~	$\log_{10}(12/DME)$
20	1385	2030	125200	4946	123600	5417	5294	-0.00559
40	3301	4150	107500	6351	121900	11290	7247	-0.05460
60	7186	7010	114600	9785	146800	14780	11640	-0.10754
80	9324	7234	80720	10210	113500	14910	13490	-0.14801
100	12450	8247	62940	9937	111900	17010	14330	-0.20847
120	17680	9515	64990	11540	117100	18160	15930	-0.25571
142	22010	10790	57250	12970	115900	17540	15040	-0.30631
160	24750	10780	48540	13590	109500			-0.35331

Least squares analysis gives: $k = 0.9917 \times 10^{-4} \text{ sec}^{-1}$
 standard error = 2.406×10^{-6}

Time (min)	+ CO	32 ~~	12 ~~	33 ~~	DME	34 ~~	35 ~~	$\log_{10}(12/DME)$
20	1576	1816	124800	3910	124400	10310	4318	-0.00139
40	3585	4138	111800	5536	127700	13320	6179	-0.05775
60	6736	6269	100100	7889	127700	18580	8773	-0.10576
80	10560	7490	88850	8464	127600	20710	10070	-0.15719
100	14820	9353	79600	10550	128000	24030	13620	-0.20630
120	28620	11340	75080	13130	135300	26620	15690	-0.25577
140	23060	10810	58530	12690	118300	24770	15030	-0.30561
160	28230	12400	53760	13990	122500	25600	16100	-0.35768
180	29270	11430	41590	12380	107100	20860		-0.41080

Least squares analysis gives: $k = 0.9746 \times 10^{-4} \text{ sec}^{-1}$
standard error = 6.520×10^{-7}

Run #36

Thermolysis of 21 at 307.40°C

Time (min)	+ C0	32 ~~	12 ~~	33 ~~	DME	34 ~~	35 ~~	log ₁₀ (12/DME)
20	1395	2256	141200	3535	138000	8321	3945	-0.00996
40	3688	4292	117200	5730	131200	13490	5815	-0.04901
60	7048	6343	109200	7523	136400	17100	10080	-0.09659
80	10170	7416	89310	9267	124400	19360	10110	-0.14392
100	13740	8383	75850	10640	118300	19710	10610	-0.19303
120	18420	10050	68900	12010	121500	18820	10210	-0.24636
140	22910	10860	60790	13250	119600	21290	14770	-0.29390
160	27140	11840	51940	14580	115500	17830	9274	-0.34708
180.5	32340	12700	46870	16520	117600	20170	14470	-0.39951

Least squares analysis gives: $k = 0.9673 \times 10^{-4} \text{ sec}^{-1}$

standard error = 6.958×10^{-7}

Run #37

Thermolysis of 13 at 307.40°C

Time (min)	+CO	32 ~~	12 ~~	33 ~~	DME	34 ~~	35 ~~	log ₁₀ (12/DME)
20	2343	2283	136900	4183	135900	10660	3820	-0.00318
40	5636	5033	113110	5868	132000	14830	6373	-0.06711
60	10470	7102	104100	6339	134900	21270	9623	-0.11256
80	15260	8314	83850	7841	122600	22350	10790	-0.16499
100	21190	9938	74810	8591	124100	23430	11030	-0.21981
120	26630	10920	62460	9326	118400	22970	11840	-0.27775
140	30820	11050	51930	8890	111800	23470	11950	-0.33302
160	37730	11960	46290	11520	112600	21120	8943	-0.38605
180	40980	12310	37260	10740	105200	19270	12070	-0.45077

Least squares analysis gives: $k = 1.0640 \times 10^{-4} \text{ sec}^{-1}$
standard error = 1.301×10^{-6}

Time (min)	+ CO	32 ~~	12 ~~	33 ~~	DME	34 ~~	35 ~~	$\log_{10}(12/DME)$
20	1866	2396	125300	2668	125900	7600	3485	-0.00207
40	5229	4493	110200	4824	124300	12400	6267	-0.05229
60	7987	6278	88730	5225	114000	17040	7235	-0.10883
80	15150	8263	84590	6965	124200	20600	10400	-0.16680
*100	18440	7844	67230	5145	107100	18250	3920	-0.20223
120	25250	10460	60280	8420	114400	22070	12330	-0.27825
140.5	29780	11020	49790	7945	109300	22260		-0.34148
160	37390	12300	45970	9409	112500	23820	15920	-0.38868
180	39190	11710	35620	8125	100900			

* neglected in least squares analysis.

Least squares analysis gives: $k = 1.0823 \times 10^{-4} \text{ sec}^{-1}$
standard error = $8,310 \times 10^{-6}$

Run # 39

Thermolysis of 13 at 307.40°C

Time (min)	+ CO	32 ~~	12 ~~	33 ~~	DME	34 ~~	35 ~~	$\log_{10}(12/DME)$
*20	1967	2408	131500	3257	117500	7462		-0.04889
40	5549	5130	119300	5660	131800	12750	6302	-0.04327
60	9530	6689	96110	6567	121400	14950	7560	-0.10145
80	14790	8112	84070	8072	120600	18250	10150	-0.15671
100.5	19560	9612	71970	8637	118000	19740	11110	-0.21473
120	25510	10400	61280	9610	113900	17480	9174	-0.26920
140	32080	11420	55190	11150	113300	23420	13430	-0.31237
160	36200	11790	47040	9741	110800	21140	12930	-0.37207
180	40950	12390	40450	10640	108600			

* Neglected in least squares analysis

Least squares analysis gives: $k = 1.0454 \times 10^{-4}$
standard error = 1.162×10^{-6}

Run #40

Thermolysis of 20 at 307.40°C

Time (min)	+ CO	32 ~~	12 ~~	33 ~~	DME	34 ~~	35 ~~	log ₁₀ (12/DME)
20	2272	1923	121100	2833	124400	10600		-0.01168
40	6055	4410	107200	5083	121100	13260	3247	-0.05295
60	11540	6498	95670	6688	122400	16440	8465	-0.10701
80	15240	6928	71630	6457	103900	16230	7857	-0.16152
100	22250	8582	65050	6384	108000	20300	9355	-0.22018
120	28130	9711	56460	7545	104600	18280	9546	-0.26779
140	33550	10330	47720	7878	102200	18320	10150	-0.33075
160	42020	11600	44290	9165	105900	20980	9611	-0.37859
180	46740	102020	36210	8442	103300	19960	9832	-0.45527

Least squares analysis gives: $k = 1.0558 \times 10^{-4} \text{ sec}^{-1}$

standard error: $= 2.104 \times 10^{-6}$

Thermolysis of 20 at 307.40°C

Time (min)	+ C0	32 ~~	12 ~~	33 ~~	DME	34 ~~	35 ~~	$\log_{10}(12/DME)$
20	2478	2352	124900	5427	124100	6664	6819	-0.00279
40	6054	4259	104600	5776	120600	13330	10070	-0.06182
60	12150	6229	97800	8495	127200	12380	11080	-0.11415
80	17530	7561	79530	8339	118100	13790	13820	-0.17172
100	23430	8965	66520	10080	109800	16130	16670	-0.21765
120	32290	10760	63010	10040	119300	15490	15430	-0.27723
140	40250	12050	55320	11480	120900	16860	3370	-0.33954
160	41720	11200	42390	10150	105900	14240	13790	-0.39763
180	52100	13150	40670	11710	113500	14720	4265	-0.44572

Least squares analysis gives: $k = 1.0740 \times 10^{-4} \text{ sec}^{-1}$

standard error: $= 1.156 \times 10^{-6}$

Time (min)	+ C0	32 ~	12 ~	33 ~	DME	34 ~	35 ~	log ₁₀ (12/DME)
20	2391	2032	126700	3852	123100	6824	4049	-0.01252
40	6436	4609	114100	5674	128700	13000	5646	-0.05229
60	12240	6911	102000	7240	130400	17520	8333	-0.10668
82	41250	8392	84260	7947	124300	20820	11000	-0.16885
100	25110	9451	73550	9576	119200	18240	10170	-0.20969
120	33350	11330	66580	10650	122700	20020	11550	-0.26550
140	37040	10850	52930	10100	111300	17000	10410	-0.32279
160	45400	12610	47480	11060	116700	17720	11550	-0.39056
180	50140	12350	40570	11250	111200	16020	10810	-0.43790

Least squares analysis gives: $k = 1.0707 \times 10^{-4} \text{ sec}^{-1}$

standard error: $= 1.273 \times 10^{-6}$

The racemization of 2-vinyloxirane at 265.0°C

Run #43

Time (min)	oxirane (%)	α_{obs}^{25}	$[\alpha]_{436}^{25}$	$\log_{10}([\alpha_t]/[\alpha_o])$
0	100	1.603	23.035	
90	97.2	1.241	18.358	-0.0986
120	96.4	1.187	17.028	-0.1312
150	96.1	1.118	15.755	-0.1650
*180	95.3	1.096	14.457	-0.2023
210	95.3	0.897	13.688	-0.2260
240	93.9	0.810	12.867	-0.2529

* neglected in least squares analysis

Least squares analysis gives: $k = 3.9603 \times 10^{-5} \text{ sec}^{-1}$

standard error: $= 7.38 \times 10^{-7}$

The racemization of 2-vinyloxirane at 275.0°C

Run #44

Time (min)	oxirane (%)	α_{obs}^{25} (436 nm)	$[\alpha]_{436}^{25}$	$\log_{10}([\alpha_t]/[\alpha_o])$
0	100	1.603	23.035	
30	97.9	1.406	19.008	-0.0835
60	96.2	1.262	16.202	-0.1528
90	94.8	0.977	14.170	-0.2110
*120	92.6	0.905	11.533	-0.3004
150	91.4	0.644	10.659	-0.3347
180	90.2	0.553	9.008	-0.4039
*210	88.9	0.372	8.092	-0.4543
240	87.1	0.387	6.697	-0.5365

* neglected in least squares analysis

Least squares analysis gives: $k = 8.2197 \times 10^{-5} \text{ sec}^{-1}$
 standard error: $= 9.29 \times 10^{-7}$

The racemization of 2-vinyloxirane at 255.0°C

Run #45

Time (min)	oxirane (%)	α_{obs}^{25} 436 nm	$[\alpha]_{436}^{25}$	$\log_{10}([\alpha_t]/[\alpha_o])$
0	100	1.603	23.035	
60	98.8	1.520	20.931	-0.0416
120	97.6	1.369	19.858	-0.0645
180	97.5	1.271	18.724	-0.0900
240	96.7	1.153	17.525	-0.1187
300	96.5	1.141	16.244	-0.1517
*360	95.3	1.121	14.891	-0.1895
422	94.9	0.952	14.359	-0.2053
482	93.4	0.895	13.481	-0.2327

* neglected in least squares analysis

Least squares analysis gives: $k = 1.7693 \times 10^{-5} \text{ sec}^{-1}$

standard error: $= 3.04 \times 10^{-7}$

The racemization of 2-vinyloxirane at 265.0°CRun #46

Time (min)	oxirane (%)	α_{obs}^{25}	$[\alpha]_{436}^{25}$	$\log_{10}[\alpha_t]/[\alpha_o]$
0	100	1.603	23.035	
90	97.4	1.193	18.385	-0.0979
120	96.9	1.116	16.997	-0.1320
150	96.2	1.126	15.578	-0.1699
180	95.4	0.979	14.636	-0.1970
210	95.0	0.898	13.681	-0.2263
240	94.5	0.834	12.704	-0.2584
270	93.1	0.781	11.895	-0.2838
300	92.6	0.663	11.211	-0.3127

Least squares analysis gives: $k = 3.9190 \times 10^{-5} \text{ sec}^{-1}$

standard error: $= 7.57 \times 10^{-7}$

The competitive racemization of $\underline{30}$ and $\underline{31}$ at 240.0°C

Sample #	Compound	Time	α_{obs}^{25} (365 nm)	$[\alpha]_{365}^{25}$	$[\alpha]_{365}^{25}$	$\log_{10}([\alpha]_{\text{t}}/[\alpha]_{\text{o}})$	10^6 k sec^{-1}
1	$\underline{30}$	2180.9	+0.735	27.503	45.883	-0.222	3.912
2	$\underline{30}$	2179	+1.102	26.775	"	-0.234	4.128
3	$\underline{30}$	2179.2	+1.027	26.479	"	-0.239	4.205
4	$\underline{30}$	2500.4	+0.701	26.612	"	-0.237	3.632
5	$\underline{30}$	2502.4	+1.283	24.327	"	-0.276	4.227
6	$\underline{30}$	2500.4	+1.258	24.491	"	-0.273	4.185
7	$\underline{31}$	2179	-0.232	-3.069	-5.230	-0.232	4.078
8	$\underline{31}$	2180	-0.261	-3.369	-5.752	-0.232	4.090
9	$\underline{31}$	2175.3	-0.242	-3.499	-5.752	-0.216	3.809

The competitive racemization of 30 and 31 at 240.0°C

Sample #	Compound	Time	α_{obs}^{25} (436 nm)	$[\alpha_t]_{436}^{25}$	$[\alpha_o]_{436}^{25}$	$\log_{10}([\alpha_t]/[\alpha_o])$	$10^6 \text{ k obs sec}^{-1}$
1	30	2180.9	+0.378	+14.144	+23.035	-0.212	3.728
2	30	2179	+0.561	+13.360	"	-0.237	4.021
3	30	2179.2	+0.522	+13.459	"	-0.233	4.111
4	30	2500.4	+0.360	+13.153	"	-0.243	3.736
5	30	2502.5	+0.648	+12.287	"	-0.273	4.187
6	30	2500.5	+0.636	+12.382	"	-0.270	4.139
7	31	2179	-0.115	-1.521	-2.615	-0.235	4.146
8	31	2180	-0.131	-1.691	-1.691	-0.235	4.132
9	31	2175.3	-0.124	-1.793	-1.793	-0.209	3.693

APPENDIX B.

Programs for the Hewlett-Packard Model #65 calculator.

The programs LSQ 1 and LSQ 2 are used to evaluate the best straight-line fit, and the associated error limits, according to the method of least-squares for an equation of the form $y = a + bx$. The computational procedure follows that of Swinbourne (37) outlined in the Results Section.

The program LSQ 1 allows input of the number of data points (n) and the values of the corresponding x, y pairs. The appropriate constants are included in the program such that:

- a. For the treatment of first-order kinetic data the entry of time, x (minutes), and the logarithmic function, y , gives the rate constant in sec^{-1} .
- b. For the evaluation of Arrhenius activation parameters the entry of $\log k$, y (sec^{-1}), and the reciprocal temperature, x ($^{\circ}\text{K}$), gives the value of E_a in cal.mole^{-1} .

The program LSQ 2 takes the data generated by LSQ 1 and evaluates the standard error of the slope and intercept. It should be noted that the term "standard error" defined by the treatment of Swinbourne is the same as the more generally used term "standard deviation".

SAMPLE USER INSTRUCTIONS.

<u>Step</u>	<u>Keys</u>	<u>Output</u>
1. Enter LSQ 1		
2. Initialize	RTN RS	
3. Enter n	RS	
4. Enter x	ENTER	
5. Enter y	RS	
6. Repeat steps 4 and 5 for each data pair.		
7. Compute Slope	A	Slope
8. Compute intercept	B	Intercept
9. Compute rate	C	Rate (sec^{-1})
10. Compute E_a	D	E_a (cal.mole^{-1})
11. Enter LSQ 2		
12. Compute error	A	S. e. intercept
13. Compute error	B	S. e. slope
14. Compute error	C	S. e. rate
15. Compute error	D	S. e. E_a

LSQ 1.

<u>CODE</u>	<u>KEYS</u>	<u>CODE</u>	<u>KEYS</u>	<u>CODE</u>	<u>KEYS</u>
21	DSP	09	9	09	9
04	4	23	LBL	34 08	RCL 8
84	RS	11	A	71	X
33 01	STO 1	34 02	RCL 2	51	-
23	LBL	34 01	RCL 1	24	RTN
09	9	81	-	23	LBL
84	RS	33 07	STO 7	13	C
33	STO	34 03	RCL 3	34	RCL
61	+	34 01	RCL 1	09	9
02	2	81	÷	42	CHS
35 07	g xoy	33 08	STO 8	02	2
33	STO	34 06	RCL 6	83	.
61	+	34 01	RCL 1	03	3
03	3	34 07	RCL 7	00	0
41	ENTER	34 08	RCL 8	03	3
41	ENTER	71	X	71	X
71	X	71	X	06	6
33	STO	51	-	00	0
61	+	34 08	RCL 8	81	÷
04	4	41	ENTER	24	RTN
35 08	g R↓	71	X	23	LBL
35 07	g xoy	34 01	RCL 1	14	D
41	ENTER	71	X	34	RCL
41	ENTER	34 04	RCL 4	09	9
71	X	35 07	g x y	42	CHS
33	STO	51	-	04	4
61	+	81	÷	83	.
05	5	33	STO	05	5
35 08	g R	09	9	07	7
71	X	24	RTN	06	6
33	STO	23	LBL	71	X
61	+	12	B	24	RTN
06	6	34 07	RCL 7		
22	GTO	34	RCL		

LSQ 2.

<u>CODE</u>	<u>KEYS</u>	<u>CODE</u>	<u>KEYS</u>	<u>CODE</u>	<u>KEYS</u>
23	LBL	04	1/x	02	2
11	A	34 08	RCL 8	83	.
34 05	RCL 5	41	ENTER	03	3
34 01	RCL 1	71	X	00	0
34 07	RCL 7	34 04	RCL 4	03	3
41	ENTER	81	\div	71	X
71	X	61	+	01	1
71	X	71	X	83	.
51	-	34 01	RCL 1	09	9
33 05	STO 5	02	2	08	8
34 04	RCL 4	51	-	07	7
34 01	RCL 1	81	\div	71	X
34 08	RCL 8	31	f	24	RTN
41	ENTER	09	$\sqrt{}$	23	LBL
71	X	24	RTN	14	D
71	X	23	LBL	02	2
51	-	12	B	83	.
33 04	STO 4	34 05	RCL 5		
34 06	RCL 6	34	RCL	03	3
34 01	RCL 1	09	9	00	0
34 07	RCL 7	34 06	RCL 6	03	3
34 08	RCL 8	71	X	71	X
71	X	51	-	06	6
71	X	34 04	RCL 4	00	0
51	-	34 01	RCL 1	81	\div
33 06	STO 6	02	2	24	RTN
34 05	RCL 5	51	-		
34	RCL	71	X		
9	9	81	\div		
34 06	RCL 6	31	f		
71	X	09	$\sqrt{}$		
51	-	24	RTN		
34 01	RCL 1	23	LBL		
35	g	13	C		

B30148